UNIVERSITA' DEGLI STUDI DI NAPOLI "FEDERICO II"

PhD thesis in Industrial products and process engineering

(XXIX cycle)

Photoresponsive azobenzene-based materials for smart cell culture applications

Chiara Fedele

Supervisor
Prof. Paolo A. Netti

Advisor
Dr. Silvia Cavalli

Coordinator
Prof. Giuseppe Mensitieri

March 2014 – March 2017

PHOTORESPONSIVE AZOBENZENE-BASED MATERIALS FOR SMART CELL CULTURE APPLICATIONS

A THESIS SUBMITTED IN PARTIAL FULFILLMENT OF THE REQUIREMENT FOR THE DEGREE OF DOCTOR OF PHILOSOPHY IN
INDUSTRIAL PRODUCTS AND PROCESS ENGINEERING

AUTHOR
Chiara Fedele

SUPERVISOR
Prof. Paolo A. Netti

ADVISOR
Dr. Silvia Cavalli

COORDINATOR
Prof. Giuseppe Mensitieri

Table of Contents

Chapter 1

Introduction*

Abstract. The realization of biomaterials whose properties are activated or inhibited on demand via light is interesting for fundamental biological studies as well as for the future development of new devices. One of the most widely used molecule in light-controlled systems is the azobenzene for its ability to isomerize in response to light. In this Chapter, the fascinating photomechanical effects, resulting from azobenzene-modified materials illumination and some of the photopatterning techniques will be reviewed, together with the emerging applications of azobenzene-based photoresponsive materials for cell culture studies.

*This Chapter is part of a review article in preparation: C. Fedele, S. Cavalli and P. A. Netti. "Azobenzene-based polymers and their emerging application as cell-instructive materials".

1.1 Next generation of cell-instructive materials (CIMs)

Tissue dynamics results from a complex spatial and temporal coordination of many different events that take place at the interface between cells and their surrounding environment. More specifically, either chemical cues or the physical characteristics of the extracellular matrix (ECM) (in terms of topography and mechanical properties) are able to regulate the biological response through cell membrane receptors (e.g. integrins) and intercellular signaling pathways.[1-2] For example, contact guidance is the phenomenon by which cell behavior is directed *in vivo* by the topography of the ECM fibrillar proteins.[3-4] In order to develop the so-called cell-instructive materials (CIMs), i.e. biomaterials able to elicit a specific cell response, such as cell alignment and directed migration, or, ultimately, cell phenotype determination, a complete understanding of the complex dynamic equilibrium between cells and the ECM is determinant.[5] Thus, dynamic biomimetic materials able to reproduce *in vitro* the time-dependent cell-material crosstalk will represent the next generation of CIMs.[6] Therefore, a growing interest in the development of stimuli-responsive biomaterials has been shown. One of the most important examples of systems exposing a changing topographic signal to cells are shape memory polymers (SMPs).[7] SMPs are a class of active materials that have the ability to memorize a permanent shape through crosslinking, be manipulated and then fixed to a temporary shape by an immobilizing transition and later recover the permanent shape by a triggering event. Despite the promising results obtained with these materials, this shape-memory activity is often not reversible, or not suitable for biological applications.[7-10] Among several external stimuli, light is one of the most promising, as it can be precisely localized over a substrate, programmed in time and remotely addressable. So far, the use of light-responsive platforms has constantly grown. For example, light-responsive molecular switches have recently gained more attention for their implementation in the construction of

molecular machines and motors, topic of the Nobel Prize in Chemistry 2016, awarded to Jean-Pierre Sauvage, Fraser Stoddart and Ben Feringa.[11] This achieved reward will most probably converge scientists' efforts in conceiving new functional applications, also in the biological field, embedding these molecular systems for producing, for example, macroscopic work.

Nowadays, one of the most widely used molecule in light-controlled systems is the azobenzene.[12] In fact, when illuminated with a specific type of light, the azobenzene molecule undergoes an isomerization, which involves a change in the geometry of the molecule from the more stable *trans* isomer to the less stable *cis* isomer, the former having a rod-like shape, while the latter a bent conformation.[13-14] This process is reversible with light or heat, but the most interesting properties of azobenzenes from a materials science perspective come out when they are incorporated into polymers and other materials, in particular a number of fascinating photomechanical effects may occur upon light illumination.[15]

1.2 Photomechanical phenomena in different types of azomaterials

Photoinduced motions in azobenzene-based systems range from chromophore reorientations to material displacement, resulting in anisotropic optical properties (e.g. birefringence), surface patterning, or even in macroscopic shape changes.[16] Similarly, we can attribute each of these phenomena to different classes of materials. For example, the photoinduced mass transport occurs in amorphous materials, while reorientational chromophore motions at the domain level take place in liquid crystalline or semicristalline materials. However, what these phenomena have in common is the azobenzene isomerization, which can be tailored in terms of stability of the *cis* isomer or in the absorption spectrum by changing substituents on the phenyl rings of the molecule. These two characteristics, in particular, strongly determine the final photomechanical

effects and, thus, the azobenzene choice in the material design acquires a great importance.

1.2.1 Types of azobenzene

The position of the maximum absorption peak and the *cis* half life of an azobenzene are dependent on the electron donating/accepting properties of azobenzene ring substituents.[17] Based on the absorption spectrum, azobenzenes can be classified into three spectroscopic classes (Figure 1): azobenzene-type molecules, aminoazobenzene-type molecules, and pseudo-stilbenes.[15]

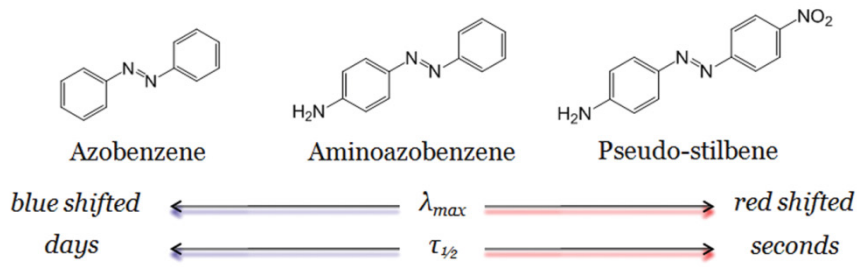

Figure 1. The three spectroscopic classes of azobenzene and their spectral characteristics: azobenzene-type, aminoazobenzene-type, pseudo-stilbene-type (or push-pull azobenzenes).[18]

Azobenzene-type molecules exhibit absorption characteristics similar to the unsubstituted azobenzene and a long half life of the *cis* isomer. The aminoazobenzene-type spectroscopic class, instead, includes azobenzenes with *ortho*- or *para*- substituents with an electron-donating group (e.g. $–NH_2$). This results in a red-shifted absorption peak and a shorter *cis* half life. Substitution of azobenzene at the 4 and 4' positions with an electron-donor and -acceptor (such as an amino and a nitro groups) leads to an asymmetric electron distribution, which characterizes the third spectroscopic class, the pseudo-stilbenes, or "push-pull" azobenzenes. These are significantly red-shifted and have the

shortest *cis* half lives. The choice of an azobenzene is strongly related to the properties that a material needs for a certain application.[16]

1.2.2 Amorphous azobenzene-based materials

As anticipated in section 1.2, azobenzene-based amorphous materials exhibit the unique appearance of surface patterns due to light-induced mass migration.[16] In this class of materials different kinds of polymer-dye systems can be listed. First of all we can classify them into linear polymers and molecular glasses. In the early stage of the research in this area, azobenzenes were blended in polymeric matrices, but, this weak interaction provided inefficient patterning ability.[19] The covalent attachment of azobenzenes to the polymeric backbone, instead, resulted in the possibility to form interesting nano- and micrometric surface structures.[20] Recently, supramolecular coupling between azobenzenes and polymer matrix is being implemented for surface patterning, from hydrogen bonded materials, to the newly explored field of halogen bonded supramolecular systems.[21-23] Another way of exploiting azobenzene-based photoinduced patterning ability is represented by grafting azopolymer brushes onto a substrate.[24-25] Polymer brushes are materials made up of polymeric chains chemically attached to a surface. Also here, both covalent coupling and supramolecular interactions between azobenzene moieties and polymer chains have been reported to produce surface patterns by means of light stimuli.[26-27]

Finally, small molecules with glass forming properties (the so-called molecular glasses) bound to azobenzenes have been demonstrated to be capable of mass transport in response to light.[28-29] In particular, in this last class of materials, since the system is monodisperse, the photomechanical behavior is highly reproducible.

1.2.3 Azobenzene-containing liquid crystalline elastomers (LCE) and hydrogels

Liquid crystals (LCs) represent a fascinating intermediate phase of matter, coupling the mobility of liquids with the ordered packing existing inside crystalline solids. Moreover, the combination between the entropic elasticity of polymeric elastomers with the LCs leads to intriguing materials, the so-called liquid crystalline elastomers (LCEs), which are extensively implemented as actuators and sensors.[30-31] In fact, they can change their shape in response to an external stimulus, mainly attributable to the disruption of the liquid crystalline order inside the material associated with local changes in volume. When paired, for instance, with azobenzenes, photocontrollable LC and LCE systems can be obtained, where light can be used to trigger the order/disorder transition inside the material itself. Although in the azobenezene context mentioning this class of materials is deserved, a review of the photomechanical phenomena associated with these materials is beyond the scope of this thesis, but the reader is addressed to the remarkable and comprehensive reviews available on the topic.[31-33]

Another class of materials which has been engineered with azobenzenes is represented by hydrogels.[34] The latter are polymeric materials formed by a 3D entangled network of hydrophilic chains connected through chemical or physical crosslinks.[35] Therefore, once hydrogels are immersed in aqueous media, they swell due to water absorption. This class of materials is widely employed in biomedical applications because they present tunable mechanical properties comparable with those of several tissues.[36-37] Hydrogels may be of synthetic origin or may exist already in nature. While natural hydrogels are biocompatible, biodegradable and generally encourage cell adhesion, on the other hand synthetic hydrogels can be easily engineered, thus offering the chance to independently tune their physiochemical properties. When

azobenzenes are included in crosslinked hydrogel matrices, the light-induced isomerization can change the mesh size and/or the swelling properties of the material.[38] For example, the supramolecular complex between cyclodestrin and azobenzene-containing polymers was found to provoke a reversible gelation upon UV light illumination due to the *trans*-*cis* photoisomerization of the azobenzene unit in different polymeric systems.[39-40]

1.3 Azopolymer photopatterning

1.3.1 Interference lithography

In 1995 two independent research groups (Nathanson/Rochon and Tripaty/Kumar) contemporarily reported for the first time a mass transport at the surface of a spin coated amorphous azopolymer thin film in response to an interference pattern of laser light.[41-42] Unexpectedly, this sinusoidal surface modulation (called surface relief grating, SRG) of the material appeared as the replica of the sinusoidal light interference pattern projected on it. SRGs are stable below T_g for a very long time (~years), but they can be erased at will using light or heat. Since then, this behavior has been largely investigated with a great number of experimental evidences and theoretical studies, but a comprehensive explanation of the phenomenon, which takes into account the structure-property relation of all the materials that show this behavior is still missing.[43-45] What seems to be for sure at the basis of this surface mass transport is the continuous azobenzene isomerization typically observed in push-pull azobenzenes, where the *trans* and the *cis* absorption bands overlap consistently and the *cis* half life is really short. Consequently, a certain wavelength can excite both *trans*-to-*cis* and *cis*-to-*trans* isomerization processes, leading to a continuous cycle. This molecular mobility extends also to the polymer chain level, leading to the fascinating anisotropic photoinduced mass migration, which characterizes these materials.[15] The light-induced

patterns are not permanent; in fact, heat, circular polarized light or an incoherent light source can revert the surface to its initial flat profile by a randomization of the azobenzenes. The formation of a pattern can be checked by monitoring the diffraction efficiency of a non absorbed laser (usually 633 nm).[20] Each polarization state has different efficiency in modulating the pattern, since it is able to orient chromophores in a different way (re-orientational theory) and/or confines the material motion in a specific direction (anisotropic photofluidization theory).[43] In a two-beam interference pattern there are alternating bright and dark areas and recent experimental setups coupling AFM onto an interference lithography system confirmed that the material tends to accumulate in the dark regions, probably in order to relax the stress, which accumulates from the isomerization movements.[46] Following these theoretical and phenomenological observations, it is possible to inscribe many different surface topographies by varying interference polarization and intensity.

The interference lithography described above can be obtained in two different configurations: in two-beam interference setup and in Lloyd's mirror configuration (Figure 2).[47]

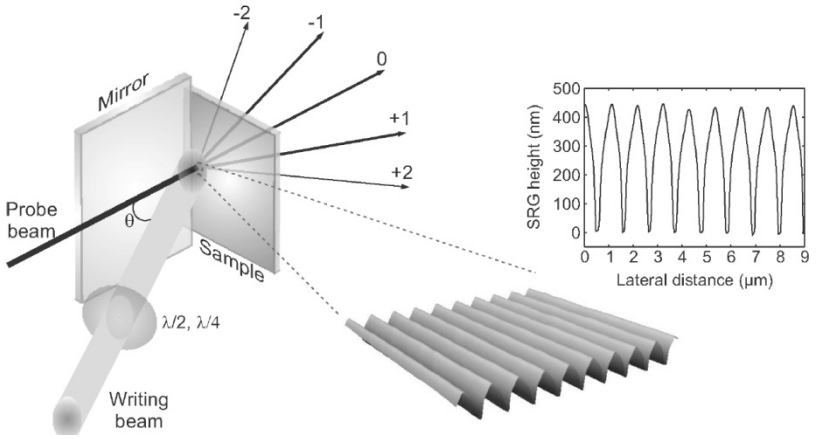

Figure 2. Graphical representation of Lloyd's mirror configuration for interference lithography and relative 3D model and cross section of the resulting surface modulation.[48]

In the former, a laser source is splitted into two beams, which are guided on the optical table (with their travel distance after splitting being less than the coherence length of the laser) in order to interfere at the surface of the material. In particular, in this configuration it is possible to change the polarization state of the two beams independently, leading to many different types of combinations.[49] In the latter, instead, the sample is fixed orthogonally at the edge of a mirror and one beam is projected at the intersection. In this way the laser is reflected by the mirror on the surface of the material, leading to the formation of interference fringes. Since the first discoveries, a growing effort has been put in the realization of more complex patterns for the broadening of azobenzene-based materials applications. For example, a three-beam interference setup has been used for the formation of hexagonally arranged ridges or troughs.[50] Even unusual polarization states have been implemented in SRG inscription in order to provide hierarchical structures. For instance, Kim et al. used elliptically polarized two-beam lithography in order to generate spontaneous superhelix-like arrangement in SRG.[51]

1.3.2 Focused laser beam

It is known that also a single focused laser beam can affect the surface modulation of an azomaterial producing different structures depending on the intensity level.[52-53] In particular, in low power regimes (intensities of tens-hundreds of $mWcm^{-2}$) a focused beam is able to make a hole in correspondence to the center of the laser spot with two lobes that pile up away from high intensity area along the polarization direction, while, when the power density switches to high power regimes (reaching hundreds of Wcm^{-2}), a protrusion instead of a cavity piles up in the center (Figure 3).

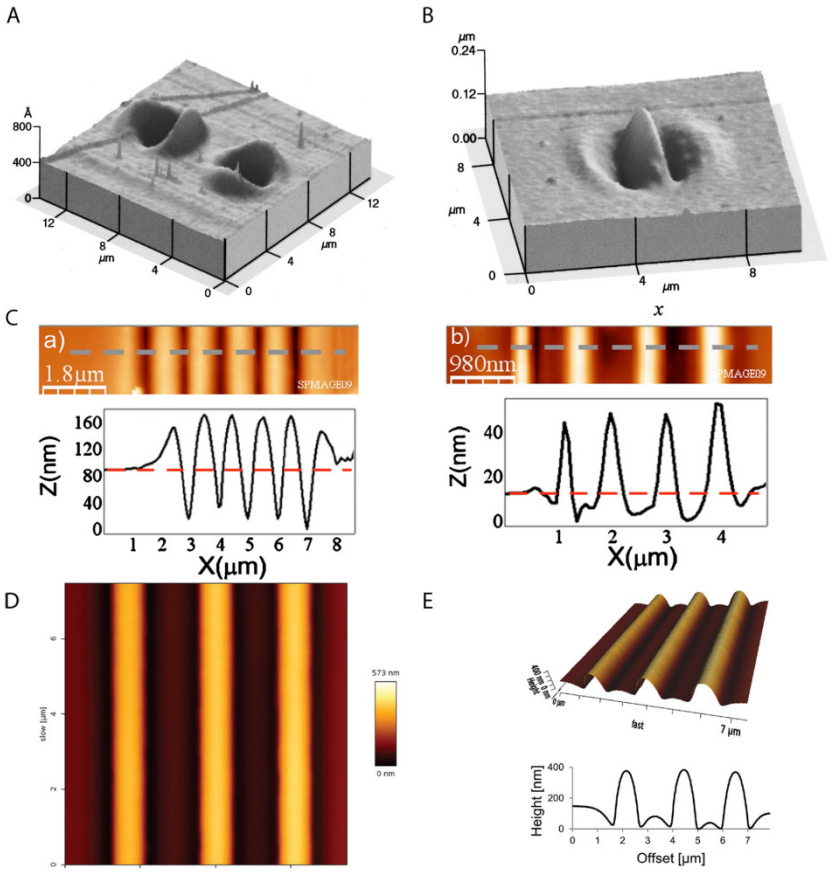

Figure 3. Linearly polarized focused laser beam inscriptions on azopolymer films. A) Low-intensity regime at orthogonal polarization directions and B) high-intensity regime.[53] C) Inscription of different stripes moving the sample a) orthogonally and b) along the polarization direction.[54] D) AFM image of a typical pattern inscribed by scanning the focused laser beam of a confocal microscope and E) its 3D projection and cross section.[55]

A relative movement between the material and the laser allows for the accumulation of the material in certain regions of the sample dictated by the laser scanning, either with galvanometric mirrors, or moving the sample by means of a motorized stage.

Ambrosio and co-workers, for example, demonstrated that it is possible to inscribe different structures if the sample is moved along the polarization direction or perpendicularly to it in low power regime.[54] When the sample was moved perpendicularly to the light polarization direction, it was observed the

formation of a channel 480 nm wide, with the material amassed at the edges. Instead, the movement of the sample along the polarization direction resulted in the opposite structures, consisting in ridges spaced by 1 μm, whose lateral size was comparable to the diameter of the focused laser spot (about 200 nm) (Figure 3C). Tuma et al. reported on the inscription of structures similar to sinusoidal SRG by coupling the scanning of the laser of the confocal microscope with the simultaneous sample movement in the perpendicular direction.[56] In a work previously published by our group, instead, the focused beam of a confocal microscope was directly used in order to write complex topographical patterns on the surface of a well-known azopolymer (Figure 3D and E).[55] Here, the mass transport induced by the azobenzene cyclical isomerization was activated only inside drawn regions-of-interest (ROIs) in which the focused laser beam was scanned by means of galvanometric mirrors.

1.3.3 Spontaneous patterning

In 2002, Hubert et al. reported for the first time about a new interesting mass transport phenomenon in azopolymers.[57] A spontaneous self-organization of the flat surface of a thin film into ordered hexagonal bumps was observed, just by a one-beam irradiation. As we have seen in the previous section, in interference lithography the material tends to accumulate in dark regions. In the absence of any dark region, as in the case of a single laser spot, the material creates a diffraction structure in order to optimize the light dissipation. Spontaneous patterns can be found in many other situations in nature, such as, for example, in the morphogenesis of patterns on animal fur (e.g. the stripes of a tiger), whose investigations were pioneered by Alan M. Turing.[58-59] In azobenzene-based materials not only the abovementioned hexagonal cells form, but also parallel stripes, or turbulent structures by changing irradiation conditions (Figure 5).

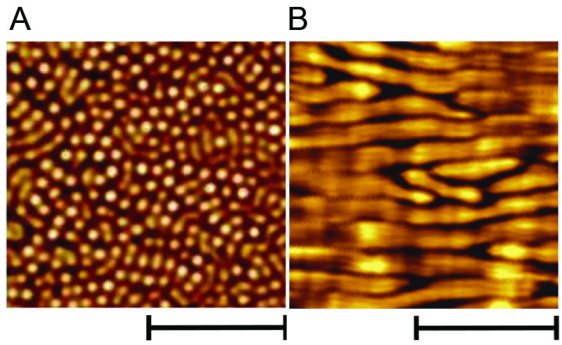

Figure 5. Spontaneous pattern formation in an azopolymer by A) unpolarized and B) linearly polarized light. Scale bars are, respectively, 10 and 5 μm.[59]

The recent work of Galinski and co-workers explained this characteristic behavior entirely by the principle of phase separation in the polymer.[59] In general, if a metastable system is subjected to a perturbation, it becomes readily unstable, tending to equilibrate again by the formation of two immiscible phases, which undergo a spatial reorganization. In the case of azopolymers, the perturbation of the system is represented by the light irradiation. In certain conditions one-beam irradiation triggers the formation of a lamellar surface pattern instead of an array of hexagonally packed microdomains. This pattern is called in many ways, as, among others, "willow structures" for their resemblance to the tangled structure of a willow basket. The microscopic features of these patterns in azomaterials can be manipulated by controlling the thickness of the deposited polymer or the temperature at which the material is written.[60] However, the precise underlying mechanism of such structural developments is still puzzling the scientific community.

1.3.4 Soft lithography plus reshaping

Another method to obtain peculiar patterns on azopolymers is the possibility of coupling soft lithographic methods and light-induced mass migration through reshaping effects. This combination could provide a new route to expand the potential applications of azopolymers in the microfabrication field. The name

"soft lithography" can be extended to a group of patterning techniques which share some characteristics, such as the implementation of elastomeric stamps in printing, molding, and embossing (e.g. replica molding, microcontact printing, solvent assisted micromolding, hot embossing).[61] An example of the coupling of these techniques to light-induced surface reshaping was given by Kang et al. using a microscale line array instead of a flat film (Figure 6A).[62] The irradiation of these structures with an interference pattern of light with many different polarization combinations allows for more complex geometries to be obtained through the so-called photofluidization of the material. Another example was given by Lee and co-workers who first produced a set of pillars using a PDMS negative master.[63] Then, the profile of the outer surface of the pillars was reshaped using polarized light with or without a capping layer (made up of PDMS) obtaining, for example, a set of elongated pillars in the polarization direction (Figure 6C and D). The work of Pirani and co-workers, instead, exploited the photofluidization phenomenon of an azopolymer adding a poly(methylmethacrylate) as stiffening element in pillar arrays.[64] The latter material prevented the polymer flow outside the pillar volume, guaranteeing a reversible bulk pillar elongation in the polarization direction (Figure 6E). Finally, the use of "photoreconfigurable" azo-material particles rather than conventional silica and thermoplastic polymers in nanosphere lithography might diversify the structural motifs that can be obtained.[65]

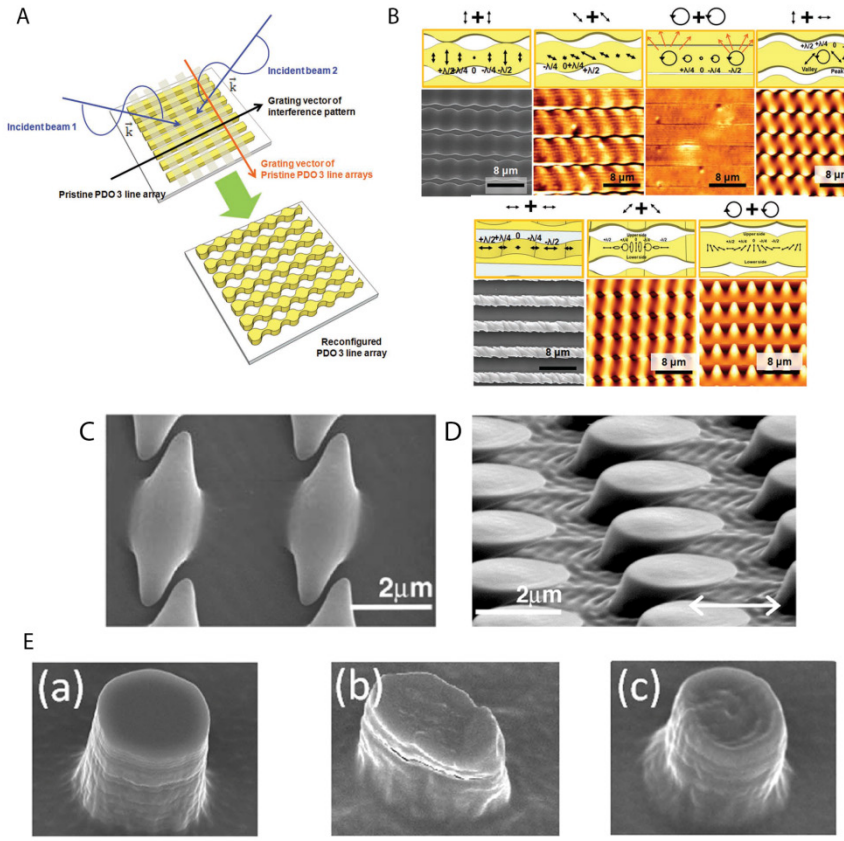

Figure 6. A) Graphical representation of a surface reshaping from an azopolymer line array and B) SEM and AFM images of reshaped patterns using different combinations of polarized light.[62] Pillars reshaping C) without and D) with a PDMS capping layer.[63] E) Reversible pillars elongation in the polarization direction.[64]

1.3.5 Non conventional methods

In addition to all the previous examples from the literature on how azopolymers can be patterned using light, a series of other less investigated methods can be listed as well. Combining the classical concept of mask-aided photolithography with azopolymers, Lambeth et al. inscribed a variety of different patterns on the surface of thin azopolymer films using a PDMS phase mask (proximity field nanopatterning).[66] For this purpose, a series of azopolymers of varying molecular weight were prepared via ring opening methatesis polymerization (ROMP). The light projected on the material surface was modulated, thus

diffracting light to form 3D interference intensity distributions on the film. As expected, the material migrated towards regions of low intensity exhibiting features sizes in the range of 40-225 nm.

Holographic patterning can be performed also by means of biphotonic processes in azobenzenes not belonging to the push-pull class (with a *cis* half life of the order of hours).[67] In these works a blue incoherent light was used to sensitize azobenzenes in the red region, provoking the azobenzene isomerization from *trans* to *cis* state, while the recording was performed with an interference pattern of a red laser. In fact, before irradiation with blue light, all the molecules were in the *trans* state, which is more stable, and no effect from the red light was observed. The red laser, responsible for inducing mass transport, provoked also the back-isomerization of the *cis* isomers to the *trans* state, in a cyclic manner, thus resembling the behavior of a push-pull azobenzene.

The azopolymer surface can be topographically manipulated not only in far field, but also in near field regime. The latter, in particular, can be achieved exploiting the configuration of a scanning near-field optical microscope (SNOM). The field-enhancement of the metallic tip can be used for drawing topographical structures at the surface of azobenzene-containing materials, overcoming the optical diffraction limit.[68] SNOM can be used also to monitor in real-time the formation of the inscribed structures.[69]

1.3.6 3D lithography using two-photon polymerization

Another way to obtain a pattern with a crosslinkable azomaterial is by using 3D photolithography.[70-71] One major example of the technique used is direct laser writing by means of two-photon polymerization (2PP), which allows for the fabrication of 3D micro- and nanostructures in photopolymerizable mixtures (photoresists). This technique is based on multiphoton polymerization, a

nonlinear optical phenomenon. The used laser is in the infrared region, so that the photoresist is perfectly transparent to it. By using an ultrashort pulsed laser, the intensity is sufficiently high to allow a multiphoton absorption within the focal volume (a "voxel") causing a photopolymerization. This approach can be applied to a great variety of materials and still the possibility to use functional customized materials is widely open. Recently, the miniaturization of actuators for various technological applications has been performed using 2PP and azobenzene-based LCE. This approach demonstrated to be successful because it allowed the maintenance of the liquid crystalline order inside the polymerized structures, scaling down to the microscale the photoinduced shape changes of azobenzene-containing LCEs (Figure 7).[70] This motions were successfully used in microrobot design (Figure 7B).[72-73]

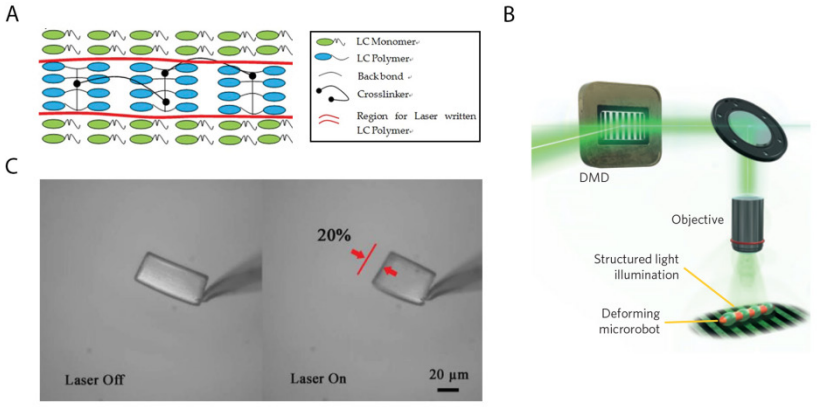

Figure 7. A) Graphical representation of aligned LCE mixture polymerized with 2PP.[70] B) Graphical representation of the motion mechanism of an azobenzene-based LCE microswimmer.[72] C) Actuation of this polymer mixture with light stimulus.[73]

1.4 Azopolymers as Cell-Instructive Materials (CIMs)

After reviewing the azobenzene photochemical properties and the photopatterning techniques employed on different materials, in this section an overview of the applications of azopolymers as light-responsive cell-instructive materials (CIMs) is given. To date, azobenzenes have been used in many

biological applications, such as in the realization of photosensitive micelles for smart drug delivery systems, or even for the *in vivo* control of protein conformation as molecular photoswitches (e.g. photopharmacology).[18, 74-78] However, works in which azopolymers are used for cell culture applications, even though really promising, are still very few and, to our knowledge, they have never been reviewed and critically discussed. In particular, the formation of linear topographies, made up of sinusoidal grooves (i.e. SRGs), over the surface of an azopolymer with an easy fabrication method, seemed to be an interesting way to probe *in vitro* the so-called contact guidance, the mechanism through which the micro- and sub-micrometer scale structures of the ECM proteins influence cell–matrix signaling in cell growth, orientation and migration processes. The difference with respect to more traditionally used biomaterials is that these materials possess dynamic properties that can potentially be powerful in biological application. In fact, the natural environment of a cell is rather dynamic, meaning that the chemical and physical properties of the extracellular matrix (ECM) are continuously changing around the cell, playing a fundamental role in the cell-ECM signaling and in the cell life cycle. With the development of novel light-responsive biomaterials exploiting the reversible activity of azobenzene molecules, it will be possible to get a deeper insight into the processes involved in the dynamic cell-material interaction.

1.4.1 Surface relief gratings

The first attempt to use azopolymers as CIMs has been carried out in 2004 by Baac and co-workers.[79] SRGs were imprinted on a glass slide spin coated with an azobenzene copolymer (Poly[(methylmethacrylate)-co-(Disperse Red 1 acrylate)]) (Figure 8A) and then primary human astrocytes (HAs) were cultured on it. First cell growth on this photoresponsive azobenzene copolymer substrate

was checked and then cell attachment and orientation on holographically formed SRG features were evaluated. Cells elongated in the pattern direction, and an application in the nerve regeneration after injury was then proposed.

Barillé et al. showed that pheochromocytoma (PC12) cells seeded on photopatterned azopolymer films aligned along the grooves and arranged orderly in a large area, while neurites were elongated along the pattern direction.[80] The main drawback of the described films is related to the low stability in cell culture conditions. For this reason, complex chemical functionalization of the solid support was necessary in order to prevent azopolymer film detachment in aqueous media.

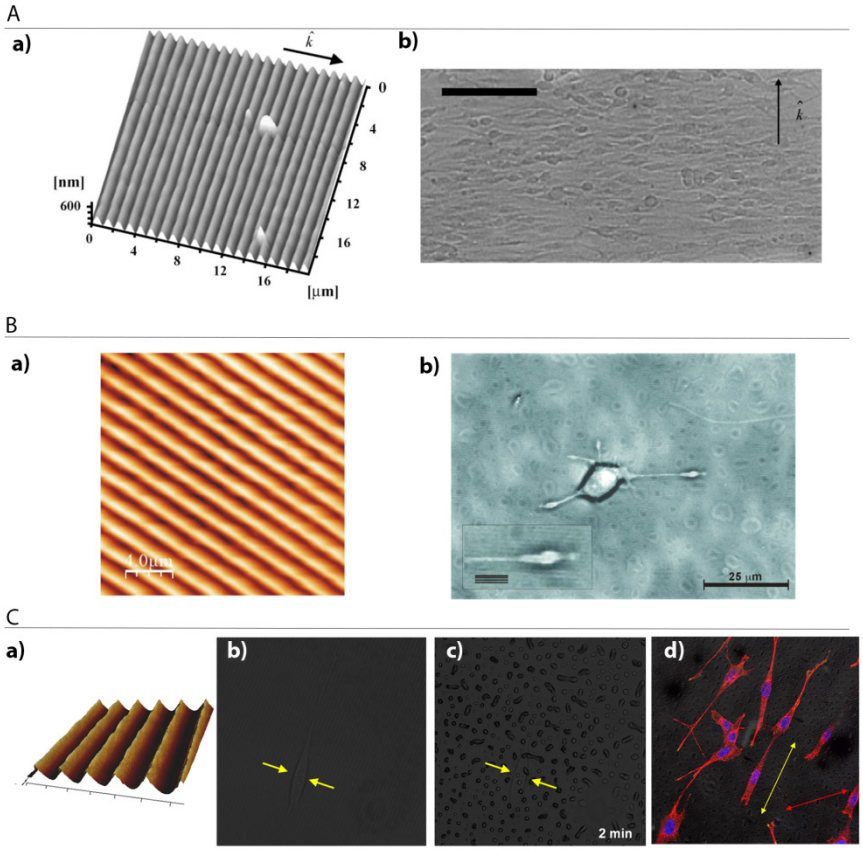

Figure 8. A) First application of azopolymer SRG to cell culture. a) AFM 3D projection and b) human astrocyte alignment (scale bar is 100 µm).[79] B) Second attempt of using SRG pattern for cell alignment. a) AFM analysis and b) PC12 cells neurites elongation.[80] C) Use of the

reversible behavior of azopolymer patterning in cell culture applications. a) AFM 3D projection of realized SRG, b) NIH-3T3 alignment, c) pattern erasure with living cells and d) cell fluorescence imaging on the side topography formed upon optical pattern erasure.[81]

Another example of the use of azomaterials as cell culture supports for future dynamic applications came from Rocha et al., where a siloxane polymer backbone functionalized in side chain with azobenzenes and other chemical groups was used for this purpose.[74] In particular, by changing the substitution degree and the type of substituents in the side chain of the polymer, the T_g could be tuned near the physiological temperature (37 °C). SRG inscription on these different materials has been carried out in order to probe the relationship between the chemical structure of the polymer, the material T_g and the efficiency and stability of the SRG over time. Moreover, the low stability of the photoinscribed topographies enabled the production of surfaces whose properties changed dynamically during cell culture, providing a tool for cell culture applications analogous to shape memory polymers, materials capable of recovering from a 'fixed' temporary shape to a 'memorized' permanent shape upon exposure to an external stimulus.[82] Finally a human hepatoma-derived cell line (HepaRG) was used to investigate the cell adhesion on these different substrates. In particular, they found that the incorporation of adenine nucleobase into the azo-polysiloxane chains improved the affinity of the polymer for cells as evidenced by the increased number of cells attached and by the formation of thick actin fibers as it also happened on the glass control sample. Even in this case, there was no effective reversibility of the topography, but the use of the synthesized substrates as dynamic cell culture supports is proposed as an interesting future perspective.

A work recently published by our group, showed the use of SRG on a glassy azopolymer for cell culture application, trying to exploit the reversibility of azopolymer photopatterning by using an incoherent light source.[81] In fact, these

topographic features were used to study the response of NIH-3T3 murine fibroblasts to the dynamic topographic changes of the substrate (Figure 8C). Patterns with different pitches were prepared by varying the angle between the laser beam and the mirror in Lloyd's interference lithography configuration. In terms of cell adhesion (length and orientation of focal complexes) and shape, cells polarized and elongated along the direction of the linear patterns, while assumed a roundish shape on the grids (two SRG superposed at 90°). Moreover, cells were aligned in the same direction of the underlying grating, while they were randomly oriented on the grid as well as on flat polymer in line with other *in vitro* studies conducted on different materials with similar pattern features. Finally, this work presented the pattern erasure using an incoherent light source, which produced some ordered bumped structures at the surface, resulting in the cell alignment to this new topographical cue.

In most of the examples reviewed in this section the use of SRG topographies in cell culture has been approached, leaving to the future perspectives a real biological study fully exploiting the dynamic and reversible features of these azobenzene-containing materials. For example, as we have seen in section 1.3.1, azopolymer brushes possess the same capability of being patterned at the microscale using interference lithography, bringing also an increased stability due to covalent attachment to substrate. However, up to date, no reports on their application in cell culture are present in the literature.

1.4.2 Single laser beam topographies

The actual step towards a real-time control of the topographical changes of the cell environment implies the use of materials, which can be precisely manipulated in physiological conditions reproduced *in vitro*. This could be possible coupling a visible light-responsive material, as a lot of azobenzene-based materials are, with a fast photolithographic technique in a temperature-

and pH-controlled environment. One possibility regards the induction of spontaneous patterning of a one laser beam with controlled polarization in a one-step irradiation process. This method has been proposed by Barillé et al. in 2011.[80] In that paper the formation of a sort of irregular SRG as a spontaneous arrangement of the material in response to linearly polarized light is shown. The inscription of such a pattern *in vitro* is proposed, directly while the sample is placed in a petri dish and immersed in a phosphate buffered saline (PBS) solution (Figure 9A). The feature dimension can be reduced by changing the liquid height above the sample, but this in turn changed the irradiation time needed for patterning. Anyway, even if PC12 neuronal cells could grow on those substrates, they could not align to the pattern direction.

The second possibility for a real-time control of material patterning is represented by the use of a focused laser beam and a relative movement between the laser and the sample. As we remember from previous section, a single laser beam scanned over the surface of an azopolymer leads to the inscription of grooves and valleys over the surface depending on the power regime and the polarization state of the laser. For this purpose, in a previously published work of our group the use of the focused laser beam of a confocal microscope is proposed in order to pattern an azobenzene material in presence of living cells (Figure 9B).[55] In fact, it was shown how the process is not harmful for cells, which can be imaged after pattern inscription using the same setup. Moreover, this technique was found not to be limited to two topographies to be presented to the cells, but just by designing different regions-of-interest (ROIs) it was possible to choose the pattern geometry, also in a multiplexing way at a single-cell level. Finally the reversibility of the embossed patterns was shown by using an incoherent light source after cell medium removal for about 30 seconds, in timing that are in line with normal laboratory practice (e.g. medium change). This writing–erasure–rewriting cycle did not have any

constraint on the initial and final inscribed topography. As a future perspective, with this tool many biological questions could be answered such as, for example, how the cell accommodates to the dynamically changing topographic signals and in which time window.

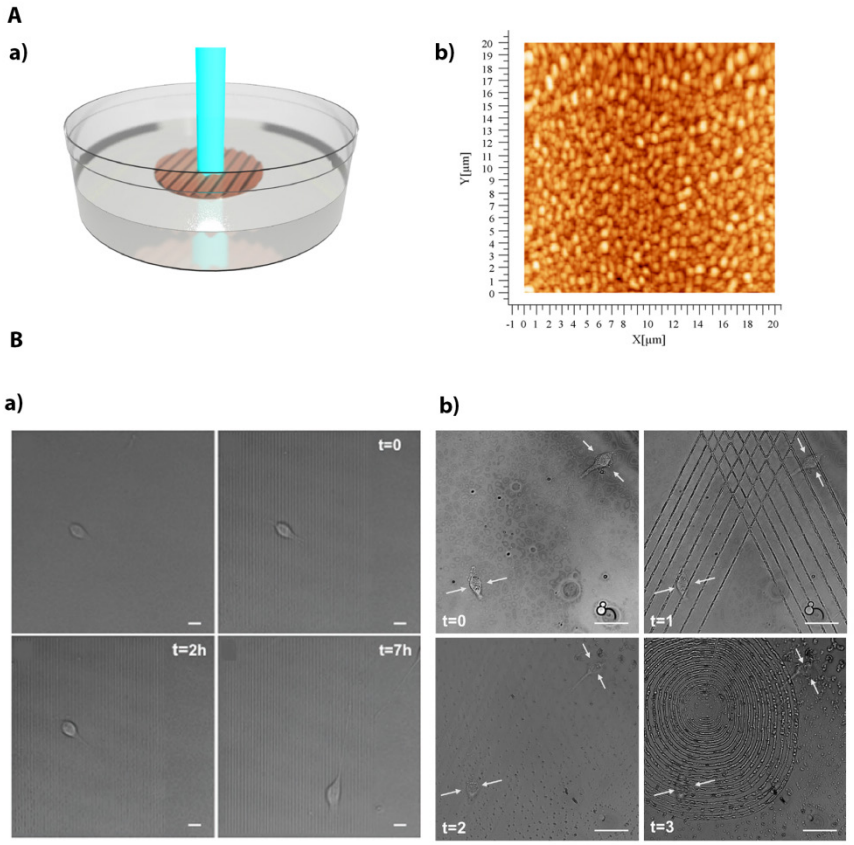

Figure 9. A) a) Graphical representation of the in vitro inscription of SRG on azopolymer with b) AFM analysis.[80] B) a) NIH-3T3 alignment on micropatterned azopolymer from the patterning to 7 hours. b) Writing and erasure process. Scale bars are 20 µm.[55]

1.4.3 Stimuli-responsive LCEs and hydrogel-based actuators as CIMs

As it is explained in section 1.2.3, liquid crystalline elastomers (LCEs) are broadly implemented as actuators and sensors.[32] These materials are stimuli-responsive polymer networks exhibiting reversible large-amplitude shape changes in response to cyclic stimuli. Through the alignment into liquid

crystalline order, they amplify volume changes when there is a transition between liquid crystalline phases. Various stimuli can be used in order to trigger a shape changing transition, but heat is generally used. The nematic-to-isotropic transition temperature of LCEs is typically much higher than room temperature, so their implementation as biomaterials has been limited. However, there is accumulating evidence that in the near future their application in biology and, in particular, as cell-instructive materials, will drive forward the research in the field.[83-87] Another improvement, instead, might be obtained using photoactuating hydrogel systems.[38, 40] As a first example, an azobenzene-containing crosslinker has been used in a PEG-based hydrogel for dynamically change the mechanical properties of the material in a three-dimensional cell culture system.[88]

1.5 Aim and Outline of the Thesis

The main aim of this thesis is to design functional photoresponsive biomaterials exploiting the photoinduced shape changes of azobenzene-containing materials. In fact, one of the major challenges nowadays is the *in vitro* reproduction of the dynamic interplay between cells and the ECM. In particular, surface topography has been demonstrated to play an important role in affecting cell functions and fate.[3] "Smart" biomaterials are indeed required for a dynamic control of cell behavior *in vitro*, simulating the complexity of natural ECM signaling.[2] In this respect, photoresponsive polymeric biointerfaces are attracting attention, because they are capable of many changes in their properties upon the application of light. Here, different photosensitive azobenzene-based materials are designed, in order to exploit their shape changes in response to light for cell culture applications, either in 2D or in 3D. Moreover, in each Chapter an original biological application is proposed, where the azopolymer photostimulation leads to topographical or mechanical changes, sometimes

even in real-time. Throughout this thesis biological studies both at a single- and multiple-cell level are proposed. The rationale of this work stays behind the fact that the development of functional applications for *in vitro* cell culture studies starts from the single-cell behavior, in order to establish both the technique and biological knowledge in the new experimental conditions. After that, the developed techniques can be applied to more complex biological systems, where the intercellular interaction plays an active role in determining the overall cell behavior. Following this idea, this thesis aims to develop functional applications for the established photopatterning techniques on azobenzene-based thin films in multicellular processes. At the same time, new photosensitive materials are proposed and evaluated for smart single-cell culture. In particular, the work described here covers the synthesis of some azobenzene monomers and polymers with the realization of suitable structures for cell culture purposes. Following, the outline of the thesis is reported with a brief description of each Chapter.

The **Chapter 1** of this thesis presents an introduction on azobenzene-containing materials with an overview of the existing photopatterning techniques. Then, the recent use of these photoresponsive materials as cell culture substrates is presented. Finally, the potential application of these materials in cell biology is highlighted. In **Chapter 2** patterned azopolymer brushes are used as cell instructive supports. In particular, synthesized with a controlled radical polymerization technique, these azopolymer brushes have been patterned at the microscale using a Lloyd's mirror interference lithography configuration. Human umbilical vein endothelial cells (HUVECs) seeded on this patterned substrate oriented in the pattern direction. Finally, pattern reversibility by means of ultrasonication is shown. In **Chapter 3** azobenzene-containing thin films patterned in real-time are used to influence the remodeling of sprouting angiogenesis from HUVEC spheroid models. This patterning has been carried

out using the focused laser beam of a confocal microscope. In **Chapter 4**, instead, the photoinduced mass migration of an azobenzene molecular glass has been used in order to influence the behavior of Madin-Darby canine kidney (MDCK) cells, either as static patterns, or in real-time. In particular, an application of static topographies in wound healing is proposed, while cell signaling through cytosolic Ca^{2+} concentration in real-time is investigated. In **Chapter 5** the realization of an azobenzene-based photoresist is shown, together with the microfabrication of 3D photoresponsive structures by means of two-photon lithography**.** Finally, the interaction of NIH-3T3 fibroblasts with these structures upon photostimulation is reported. In **Conclusion and Future Perspectives** a summary about the main results achieved in this thesis is presented and future applications are proposed.

1.6 References

1. Ventre, M.; Netti, P. A., Engineering cell instructive materials to control cell fate and functions through material cues and surface patterning. *ACS applied materials & interfaces* **2016,** *8* (24), 14896-14908.
2. Lutolf, M.; Hubbell, J., Synthetic biomaterials as instructive extracellular microenvironments for morphogenesis in tissue engineering. *Nature biotechnology* **2005,** *23* (1), 47-55.
3. Bettinger, C. J.; Langer, R.; Borenstein, J. T., Engineering substrate topography at the micro-and nanoscale to control cell function. *Angew. Chem., Int. Ed.* **2009,** *48* (30), 5406-5415.
4. Flemming, R.; Murphy, C. J.; Abrams, G.; Goodman, S.; Nealey, P., Effects of synthetic micro-and nano-structured surfaces on cell behavior. *Biomaterials* **1999,** *20* (6), 573-588.
5. Ventre, M.; Causa, F.; Netti, P. A., Determinants of cell–material crosstalk at the interface: towards engineering of cell instructive materials. *Journal of the Royal Society Interface* **2012,** *9* (74), 2017.
6. Gooding, J. J.; Parker, S. G.; Lu, Y.; Gaus, K., Molecularly engineered surfaces for cell biology: From static to dynamic surfaces. *Langmuir* **2013,** *30* (12), 3290-3302.
7. Davis, K. A.; Burke, K. A.; Mather, P. T.; Henderson, J. H., Dynamic cell behavior on shape memory polymer substrates. *Biomaterials* **2011,** *32* (9), 2285-2293.
8. Le, D. M.; Kulangara, K.; Adler, A. F.; Leong, K. W.; Ashby, V. S., Dynamic Topographical Control of Mesenchymal Stem Cells by Culture on Responsive Poly (ϵ-caprolactone) Surfaces. *Adv. Mater.* **2011,** *23* (29), 3278-3283.
9. Xie, T., Tunable polymer multi-shape memory effect. *Nature* **2010,** *464* (7286), 267-270.
10. Xiao, X.; Kong, D.; Qiu, X.; Zhang, W.; Liu, Y.; Zhang, S.; Zhang, F.; Hu, Y.; Leng, J., Shape memory polymers with high and low temperature resistant properties. *Sci. Rep.* **2015,** *5*, 14137.
11. Richards, V., 2016 Nobel Prize in Chemistry: Molecular machines. *Nature Chemistry* **2016,** *8* (12), 1090-1090.
12. Feringa, B. L.; Browne, W. R., *Molecular switches*. Wiley Online Library: 2001; Vol. 42.
13. Hartley, G., The cis-form of azobenzene. *Nature* **1937,** *140*, 281.
14. Rau, H., Photoisomerization of azobenzenes. In *Photochemistry and photophysics*, 1990; Vol. 2, pp 119-141.
15. Mahimwalla, Z.; Yager, K. G.; Mamiya, J.-i.; Shishido, A.; Priimagi, A.; Barrett, C. J., Azobenzene photomechanics: prospects and potential applications. *Polym. Bull.* **2012,** *69* (8), 967-1006.

16. Natansohn, A.; Rochon, P., Photoinduced motions in azo-containing polymers. *Chemical reviews* **2002,** *102* (11), 4139-4176.
17. Bandara, H. D.; Burdette, S. C., Photoisomerization in different classes of azobenzene. *Chemical Society Reviews* **2012,** *41* (5), 1809-1825.
18. Goulet-Hanssens, A.; Barrett, C. J., Photo-control of biological systems with azobenzene polymers. *Journal of Polymer Science Part A: Polymer Chemistry* **2013,** *51* (14), 3058-3070.
19. Lagugné Labarthet, F.; Buffeteau, T.; Sourisseau, C., Analyses of the diffraction efficiencies, birefringence, and surface relief gratings on azobenzene-containing polymer films. *The Journal of Physical Chemistry B* **1998,** *102* (15), 2654-2662.
20. Priimagi, A.; Shevchenko, A., Azopolymer-based micro-and nanopatterning for photonic applications. *Journal of Polymer Science Part B: Polymer Physics* **2014,** *52* (3), 163-182.
21. Gao, J.; He, Y.; Liu, F.; Zhang, X.; Wang, Z.; Wang, X., Azobenzene-containing supramolecular side-chain polymer films for laser-induced surface relief gratings. *Chemistry of materials* **2007,** *19* (16), 3877-3881.
22. Priimagi, A.; Cavallo, G.; Forni, A.; Gorynsztejn–Leben, M.; Kaivola, M.; Metrangolo, P.; Milani, R.; Shishido, A.; Pilati, T.; Resnati, G., Halogen Bonding versus Hydrogen Bonding in Driving Self-Assembly and Performance of Light-Responsive Supramolecular Polymers. *Advanced Functional Materials* **2012,** *22* (12), 2572-2579.
23. Saccone, M.; Dichiarante, V.; Forni, A.; Goulet-Hanssens, A.; Cavallo, G.; Vapaavuori, J.; Terraneo, G.; Barrett, C. J.; Resnati, G.; Metrangolo, P., Supramolecular hierarchy among halogen and hydrogen bond donors in light-induced surface patterning. *Journal of Materials Chemistry C* **2015,** *3* (4), 759-768.
24. Lomadze, N.; Kopyshev, A.; Rühe, J. r.; Santer, S., Light-Induced Chain Scission in Photosensitive Polymer Brushes. *Macromolecules* **2011,** *44* (18), 7372-7377.
25. Schuh, C.; Lomadze, N.; Rühe, J. r.; Kopyshev, A.; Santer, S., Photomechanical degrafting of azo-functionalized poly (methacrylic acid)(PMAA) brushes. *J. Phys. Chem. B* **2011,** *115* (35), 10431-10438.
26. Kopyshev, A.; Lomadze, N.; Feldmann, D.; Genzer, J.; Santer, S., Making polymer brush photosensitive with azobenzene containing surfactants. *Polymer* **2015,** *79*, 65-72.
27. Kopyshev, A.; Galvin, C. J.; Genzer, J.; Lomadze, N.; Santer, S., Opto-mechanical scission of polymer chains in photosensitive diblock-copolymer brushes. *Langmuir* **2013,** *29* (45), 13967-13974.
28. Kirby, R.; Sabat, R. G.; Nunzi, J.-M.; Lebel, O., Disperse and disordered: a mexylaminotriazine-substituted azobenzene derivative with

superior glass and surface relief grating formation. *Journal of Materials Chemistry C* **2014,** *2* (5), 841-847.
29. Nakano, H.; Takahashi, T.; Kadota, T.; Shirota, Y., Formation of a Surface Relief Grating Using a Novel Azobenzene-Based Photochromic Amorphous Molecular Material. *Advanced Materials* **2002,** *14* (16), 1157-1160.
30. Priimagi, A.; Barrett, C. J.; Shishido, A., Recent twists in photoactuation and photoalignment control. *Journal of Materials Chemistry C* **2014,** *2* (35), 7155-7162.
31. Yu, H.; Ikeda, T., Photocontrollable Liquid-Crystalline Actuators. *Advanced Materials* **2011,** *23* (19), 2149-2180.
32. Ohm, C.; Brehmer, M.; Zentel, R., Liquid crystalline elastomers as actuators and sensors. *Advanced Materials* **2010,** *22* (31), 3366-3387.
33. White, T. J.; Broer, D. J., Programmable and adaptive mechanics with liquid crystal polymer networks and elastomers. *Nature materials* **2015,** *14* (11), 1087-1098.
34. Katz, J. S.; Burdick, J. A., Light-Responsive Biomaterials: Development and Applications. *Macromolecular bioscience* **2010,** *10* (4), 339-348.
35. Gupta, P.; Vermani, K.; Garg, S., Hydrogels: from controlled release to pH-responsive drug delivery. *Drug discovery today* **2002,** *7* (10), 569-579.
36. Tibbitt, M. W.; Anseth, K. S., Hydrogels as extracellular matrix mimics for 3D cell culture. *Biotechnology and bioengineering* **2009,** *103* (4), 655-663.
37. Hoffman, A. S., Hydrogels for biomedical applications. *Advanced drug delivery reviews* **2012,** *64*, 18-23.
38. Tomatsu, I.; Peng, K.; Kros, A., Photoresponsive hydrogels for biomedical applications. *Advanced drug delivery reviews* **2011,** *63* (14), 1257-1266.
39. Zhao, Y.-L.; Stoddart, J. F., Azobenzene-based light-responsive hydrogel system. *Langmuir* **2009,** *25* (15), 8442-8446.
40. Peng, K.; Tomatsu, I.; Kros, A., Light controlled protein release from a supramolecular hydrogel. *Chemical communications* **2010,** *46* (23), 4094-4096.
41. Rochon, P.; Batalla, E.; Natansohn, A., Optically induced surface gratings on azoaromatic polymer films. *Applied Physics Letters* **1995,** *66* (2), 136-138.
42. Kim, D.; Tripathy, S.; Li, L.; Kumar, J., Laser-induced holographic surface relief gratings on nonlinear optical polymer films. *Applied Physics Letters* **1995,** *66* (10), 1166-1168.
43. Yadavalli, N. S.; Loebner, S.; Papke, T.; Sava, E.; Hurduc, N.; Santer, S., A comparative study of photoinduced deformation in azobenzene containing polymer films. *Soft matter* **2016,** *12* (9), 2593-2603.
44. Yager, K. G.; Barrett, C. J., Light-induced nanostructure formation using azobenzene polymers. In *Polymeric Nanostructures and Their Applications*, 2006; pp 1-38.

45. Karageorgiev, P.; Neher, D.; Schulz, B.; Stiller, B.; Pietsch, U.; Giersig, M.; Brehmer, L., From anisotropic photo-fluidity towards nanomanipulation in the optical near-field. *Nature Materials* **2005,** *4* (9), 699-703.
46. Yadavalli, N. S.; Santer, S., In-situ atomic force microscopy study of the mechanism of surface relief grating formation in photosensitive polymer films. *Journal of Applied Physics* **2013,** *113* (22), 224304.
47. Yager, K. G.; Barrett, C. J., Novel photo-switching using azobenzene functional materials. *Journal of Photochemistry and Photobiology A: Chemistry* **2006,** *182* (3), 250-261.
48. Priimagi, A.; Kaivola, M.; Virkki, M.; Rodriguez, F. J.; Kauranen, M., Suppression of chromophore aggregation in amorphous polymeric materials: towards more efficient photoresponsive behavior. *Journal of Nonlinear Optical Physics & Materials* **2010,** *19* (01), 57-73.
49. Yadavalli, N. S.; Saphiannikova, M.; Santer, S., Photosensitive response of azobenzene containing films towards pure intensity or polarization interference patterns. *Applied Physics Letters* **2014,** *105* (5), 051601.
50. Viswanathan, N.; Kim, D.; Tripathy, S., Surface relief structures on azo polymer films. *Journal of Materials Chemistry* **1999,** *9* (9), 1941-1955.
51. Kim, M. J.; Kumar, J.; Kim, D. Y., Photofabrication of Superhelix-Like Patterns on Azobenzene Polymer Films. *Advanced Materials* **2003,** *15* (23), 2005-2008.
52. Bian, S.; Li, L.; Kumar, J.; Kim, D.; Williams, J.; Tripathy, S., Single laser beam-induced surface deformation on azobenzene polymer films. *Applied physics letters* **1998,** *73* (13), 1817-1819.
53. Bian, S.; Williams, J. M.; Kim, D. Y.; Li, L.; Balasubramanian, S.; Kumar, J.; Tripathy, S., Photoinduced surface deformations on azobenzene polymer films. *Journal of Applied Physics* **1999,** *86* (8), 4498-4508.
54. Ambrosio, A.; Camposeo, A.; Carella, A.; Borbone, F.; Pisignano, D.; Roviello, A.; Maddalena, P., Realization of submicrometer structures by a confocal system on azopolymer films containing photoluminescent chromophores. *Journal of Applied Physics* **2010,** *107* (8), 083110.
55. Rianna, C.; Rossano, L.; Kollarigowda, R. H.; Formiggini, F.; Cavalli, S.; Ventre, M.; Netti, P. A., Spatio-Temporal Control of Dynamic Topographic Patterns on Azopolymers for Cell Culture Applications. *Adv. Funct. Mater.* **2016,** *26* (42), 7572-7580.
56. Tuma, J.; Lyutakov, O.; Huttel, I.; Slepicka, P.; Svorcik, V., Reversible patterning of poly (methylmethacrylate) doped with disperse Red 1 by laser scanning. *Journal of Applied Physics* **2013,** *114* (9), 093104.
57. Hubert, C.; Fiorini-Debuisschert, C.; Maurin, I.; Nunzi, J.-M.; Raimond, P., Spontaneous patterning of hexagonal structures in an azo-polymer using light-controlled mass transport. *Advanced Materials* **2002,** *14* (10), 729.

58. Turing, A. M., The chemical basis of morphogenesis. *Philosophical Transactions of the Royal Society of London B: Biological Sciences* **1952,** *237* (641), 37-72.
59. Galinski, H.; Ambrosio, A.; Maddalena, P.; Schenker, I.; Spolenak, R.; Capasso, F., Instability-induced pattern formation of photoactivated functional polymers. *Proceedings of the National Academy of Sciences* **2014,** *111* (48), 17017-17022.
60. Noga, J.; Sobolewska, A.; Bartkiewicz, S.; Virkki, M.; Priimagi, A., Periodic Surface Structures Induced by a Single Laser Beam Irradiation. *Macromolecular Materials and Engineering* **2017,** *302* (2).
61. Xia, Y.; Whitesides, G. M., Soft lithography. *Annual review of materials science* **1998,** *28* (1), 153-184.
62. Kang, H. S.; Lee, S.; Park, J. K., Monolithic, Hierarchical Surface Reliefs by Holographic Photofluidization of Azopolymer Arrays: Direct Visualization of Polymeric Flows. *Advanced Functional Materials* **2011,** *21* (23), 4412-4422.
63. Lee, S.; Kang, H. S.; Ambrosio, A.; Park, J.-K.; Marrucci, L., Directional Superficial Photofluidization for Deterministic Shaping of Complex 3D Architectures. *ACS applied materials & interfaces* **2015,** *7* (15), 8209-8217.
64. Pirani, F.; Angelini, A.; Frascella, F.; Rizzo, R.; Ricciardi, S.; Descrovi, E., Light-Driven Reversible Shaping of Individual Azopolymeric Micro-Pillars. *Scientific reports* **2016,** *6*, 31702.
65. Li, Y.; Deng, Y.; He, Y.; Tong, X.; Wang, X., Amphiphilic azo polymer spheres, colloidal monolayers, and photoinduced chromophore orientation. *Langmuir* **2005,** *21* (14), 6567-6571.
66. Lambeth, R. H.; Park, J.; Liao, H.; Shir, D. J.; Jeon, S.; Rogers, J. A.; Moore, J. S., Proximity field nanopatterning of azopolymer thin films. *Nanotechnology* **2010,** *21* (16), 165301.
67. Sánchez, C.; Alcalá, R.; Hvilsted, S.; Ramanujam, P., Biphotonic holographic gratings in azobenzene polyesters: surface relief phenomena and polarization effects. *Applied Physics Letters* **2000,** *77* (10), 1440-1442.
68. Likodimos, V.; Labardi, M.; Pardi, L.; Allegrini, M.; Giordano, M.; Arena, A.; Patanè, S., Optical nanowriting on azobenzene side-chain polymethacrylate thin films by near-field scanning optical microscopy. *Applied physics letters* **2003,** *82* (19), 3313-3315.
69. Ambrosio, A.; Camposeo, A.; Maddalena, P.; Patanè, S.; Allegrini, M., Real-time monitoring of the surface relief formation on azo-polymer films upon near-field excitation. *Journal of microscopy* **2008,** *229* (2), 307-312.
70. Zeng, H.; Martella, D.; Wasylczyk, P.; Cerretti, G.; Lavocat, J. C. G.; Ho, C. H.; Parmeggiani, C.; Wiersma, D. S., High-resolution 3D direct laser writing for liquid-crystalline elastomer microstructures. *Advanced materials* **2014,** *26* (15), 2319-2322.

71. Sekkat, Z.; Kawata, S., Laser nanofabrication in photoresists and azopolymers. *Laser & Photonics Reviews* **2014,** *8* (1), 1-26.
72. Palagi, S.; Mark, A. G.; Reigh, S. Y.; Melde, K.; Qiu, T.; Zeng, H.; Parmeggiani, C.; Martella, D.; Sanchez-Castillo, A.; Kapernaum, N., Structured light enables biomimetic swimming and versatile locomotion of photoresponsive soft microrobots. *Nature materials* **2016,** *15* (6), 647.
73. Zeng, H.; Wasylczyk, P.; Parmeggiani, C.; Martella, D.; Burresi, M.; Wiersma, D. S., Light-Fueled Microscopic Walkers. *Advanced Materials* **2015,** *27* (26), 3883-3887.
74. Rocha, L.; Păiuş, C.-M.; Luca-Raicu, A.; Resmerita, E.; Rusu, A.; Moleavin, I.-A.; Hamel, M.; Branza-Nichita, N.; Hurduc, N., Azobenzene based polymers as photoactive supports and micellar structures for applications in biology. *J. Photochem. Photobiol., A* **2014,** *291*, 16-25.
75. Beharry, A. A.; Woolley, G. A., Azobenzene photoswitches for biomolecules. *Chemical Society Reviews* **2011,** *40* (8), 4422-4437.
76. Russew, M. M.; Hecht, S., Photoswitches: from molecules to materials. *Advanced Materials* **2010,** *22* (31), 3348-3360.
77. Broichhagen, J.; Frank, J. A.; Trauner, D., A roadmap to success in photopharmacology. *Accounts of chemical research* **2015,** *48* (7), 1947-1960.
78. Borowiak, M.; Nahaboo, W.; Reynders, M.; Nekolla, K.; Jalinot, P.; Hasserodt, J.; Rehberg, M.; Delattre, M.; Zahler, S.; Vollmar, A., Photoswitchable inhibitors of microtubule dynamics optically control mitosis and cell death. *Cell* **2015,** *162* (2), 403-411.
79. Baac, H.; Lee, J.-H.; Seo, J.-M.; Park, T. H.; Chung, H.; Lee, S.-D.; Kim, S. J., Submicron-scale topographical control of cell growth using holographic surface relief grating. *Mater. Sci. Eng. C Mater. Biol. Appl.* **2004,** *24* (1-2), 209-212.
80. Barille, R.; Janik, R.; Kucharskic, S.; Eyer, J.; Letournel, F., Photo-responsive polymer with erasable and reconfigurable micro- and nano-patterns: An in vitro study for neuron guidance. *Colloids Surf., B* **2011,** *88*, 63-71.
81. Rianna, C.; Calabuig, A.; Ventre, M.; Cavalli, S.; Pagliarulo, V.; Grilli, S.; Ferraro, P.; Netti, P. A., Reversible holographic patterns on azopolymers for guiding cell adhesion and orientation. *ACS Appl. Mater. Interfaces* **2015,** *7* (31), 16984-16991.
82. Lendlein, A.; Behl, M.; Hiebl, B.; Wischke, C., Shape-memory polymers as a technology platform for biomedical applications. *Expert Review of Medical Devices* **2010,** *7* (3), 357-379.
83. Woltman, S. J.; Jay, G. D.; Crawford, G. P., Liquid-crystal materials find a new order in biomedical applications. *Nature materials* **2007,** *6* (12), 929-938.
84. Bera, T.; Freeman, E. J.; McDonough, J. A.; Clements, R. J.; Aladlaan, A.; Miller, D. W.; Malcuit, C.; Hegmann, T.; Hegmann, E., Liquid crystal

elastomer microspheres as three-dimensional cell scaffolds supporting the attachment and proliferation of myoblasts. *ACS applied materials & interfaces* **2015,** *7* (26), 14528-14535.
85. Agrawal, A.; Chen, H.; Kim, H.; Zhu, B.; Adetiba, O.; Miranda, A.; Cristian Chipara, A.; Ajayan, P. M.; Jacot, J. G.; Verduzco, R., Electromechanically Responsive Liquid Crystal Elastomer Nanocomposites for Active Cell Culture. *ACS Macro Letters* **2016,** *5*, 1386-1390.
86. Herrera-Posada, S.; Mora-Navarro, C.; Ortiz-Bermudez, P.; Torres-Lugo, M.; McElhinny, K. M.; Evans, P. G.; Calcagno, B. O.; Acevedo, A., Magneto-responsive liquid crystalline elastomer nanocomposites as potential candidates for dynamic cell culture substrates. *Materials Science and Engineering: C* **2016,** *65*, 369-378.
87. Gao, Y.; Mori, T.; Manning, S.; Zhao, Y.; Nielsen, A. d.; Neshat, A.; Sharma, A.; Mahnen, C. J.; Everson, H. R.; Crotty, S., Biocompatible 3D liquid crystal elastomer cell scaffolds and foams with primary and secondary porous architecture. *ACS Macro Letters* **2015,** *5* (1), 4-9.
88. Rosales, A. M.; Mabry, K. M.; Nehls, E. M.; Anseth, K. S., Photoresponsive elastic properties of azobenzene-containing poly (ethylene-glycol)-based hydrogels. *Biomacromolecules* **2015,** *16* (3), 798-806.

Chapter 2

Light-responsive polymer brushes: active topographic cues for cell culture applications*

Abstract. In the call for novel stimuli-responsive biomaterials azobenzene-containing polymer brushes entail a remarkable potential. In fact, their ability to be patterned at the micro- and nanoscale using interference lithography (IL) might be exploited for the realization of cell-instructive materials (CIMs). In this Chapter, Disperse Red 1 (DR1)-based photoresponsive polymer brushes were synthesized using a controlled radical polymerization technique. A sinusoidal pattern was inscribed on the azopolymer brush samples using the Lloyd's IL configuration. Interestingly, we found that seeded human umbilical vein endothelial cells (HUVECs) oriented in the pattern direction. Furthermore, using a non-cytotoxic ultrasonication treatment, pattern erasure was achieved. Hence, we envisage the possibility to use these surfaces as reconfigurable cell-instructive biomaterials for tissue engineering applications.

*The work described in this Chapter is part of a manuscript submitted for publication: R. H. Kollarigowda, C. Fedele, C. Rianna, A. Calabuig, A. C. Manikas, V. Pagliarulo, P. Ferraro, S. Cavalli and P. A. Netti. "Light-Responsive Polymer Brushes: Active Topographic Cues For Cell Culture Applications". (First two authors contributed equally to the entire work).[§]

2.1 Introduction

The field of photoresponsive surfaces has recently emerged as a fascinating research area for the great potential of these materials in biomedical applications. In particular one of the major challenges nowadays is the *in vitro* reproduction of the dynamic interplay between cells and the extracellular matrix (ECM) architecture.

In fact, cell–matrix signaling is influenced by the abundant micro- and sub-micrometer scale structures of the ECM proteins that play a key role in cell growth, orientation and migration processes, through a mechanism defined as "contact guidance".[1] In particular, surface topography has been demonstrated to play an important role in affecting cell functions and fate. Recent developments in advanced micro- and nanofabrication techniques have enabled material scientists to produce *in vitro* substrates that are able to mimic the structure and length scale of natural topography, especially in two-dimensions.[1-2] However, current research is still focused on finding a straightforward process for precise surface engineering, together with the possibility of creating patterned substrates that can be further modified and even erased during cell culture. In fact, the dynamic state of tissue is regulated by a highly complex temporal and spatial coordination of many different cell-matrix and cell-cell interactions. Thus, "smart" biomaterial systems are required to control cell behavior *in vitro*, simulating the complexity of natural ECM signaling.[3] In this respect, stimuli-responsive polymeric biointerfaces have attracted a lot of interest, because they are capable of conformational and chemical changes upon the application of an external signal. More importantly, these changes are often reversible, mimicking the fast signal remodeling that happens in nature.[4] Among several external stimuli, light is one of the most promising, as it can be precisely localized over a substrate, programmed in time, remotely addressable and it allows for the production of complex patterns in one step without any contact

and contamination. Recent research has demonstrated that thin films of azobenzene-based polymers are good light-responsive systems, thus representing an original type of biomaterials for performing photocontrolled cell culture experiments in which dynamic topographic cues are exploited to induce cell response.[5-9] In fact, azopolymers can be patterned at the micro- and nanometer scale using interference lithographic (IL) techniques, such as the Lloyd's mirror configuration. This method leads to the so-called surface relief grating (SRG) formation, which corresponds to a sinusoidal topography modulation created by exposing the material surface to a laser light interference pattern. This effect is due to the fast and cyclical *trans-cis-trans* isomerization process, induced by light, in push-pull azobenzenes.[10-12] Moreover, patterns inscribed on these substrates have also been erased and subsequently different topographic features have been rewritten in the same region.[11]

The main drawback of these films is related to the lack in stability, as well as their failure in many consecutive uses. Very often, due to the formation of cracks, the underlying polymeric layer easily detaches from the substrate during cell culture. For this reason, complex chemical functionalization of the solid support is usually necessary in order to prevent azopolymer film detachment in aqueous media.[6, 13] In the call for more stable biointerfaces, biomaterials with macromolecules covalently immobilized at their surfaces would be desirable as, for example, polymer brushes. They consist of polymeric chains tethered to solid support from one end and forming layers with different grafting density, from mushroom-like conformations to densely packed chains.

Regarding the possibility to inscribe holographic patterns using azobenzene-containing polymer brushes, few example are already known.[14-17] However, there is a lack in the literature for what concerns the application of azopolymer brushes as cell-instructive materials (CIMs), even if their potential as stable patternable interfaces seems to be remarkable.

In this work, we show that IL patterns in azopolymer brushes induce easily cell orientation, coupling the unique photoresponsive properties of azobenzene-based materials together with the stability of a grafted macromolecular layer. Moreover, we show that ultrasonic cavitation can be employed for disrupting the aggregation formed between polymer chains upon photopatterning, thus succeeding in the erasure of the topographic pattern. Firstly, we present the synthesis of azopolymer brushes that was carried out using a controlled radical polymerization technique. Inscription of an interference pattern was achieved by a Lloyd's mirror IL setup. While, human umbilical vein endothelial cells (HUVECs) response to the inscribed linear topography was observed with an optical microscope. Finally, SRG pattern was mechanically erased by ultrasonication, also in the presence of adherent cells.

2.2 Results and discussion

2.2.1 Azo-pb synthesis and characterization

Reversible addition-fragmentation chain transfer (RAFT) radical polymerization in the "grafting from" approach was used to fabricate our photosensitive polymer brushes, starting from an in-house synthesized azomonomer, (DR1-monomer in **Scheme 1**). This compound was prepared from an amine derivative of the commercially available Disperse Red 1 (DR1) according to a previously reported synthesis.[18] RAFT approach is one of the key techniques among controlled radical polymerization methods to get narrow polydispersity index with multifunctional terminated chains, which can be useful for further functionalization. These macromolecules can be grafted on a solid support in layers with fully tunable structural properties, such as grafting density and thickness.[19-21] This synthetic method has been successfully coupled to a wide variety of materials, covering a broad range of applications, from microelectronics to biomaterials, e.g. drug delivery and cell adhesion control.[22]

In this work azopolymer brushes were grown from amino-silanized glass surface through the immobilization of the chain transfer agent (CTA) via the R group.[19-20] The thickness of the obtained polymer brush layer ranged between 150 and 200 nm, as measured by ellipsometry (data not shown). This result was in good agreement with the theoretical predictions of loading monomer units, confirming the efficiency of our polymerization strategy. The chemical structure and a graphical representation of the polymer brushes are shown in **Scheme 1**.

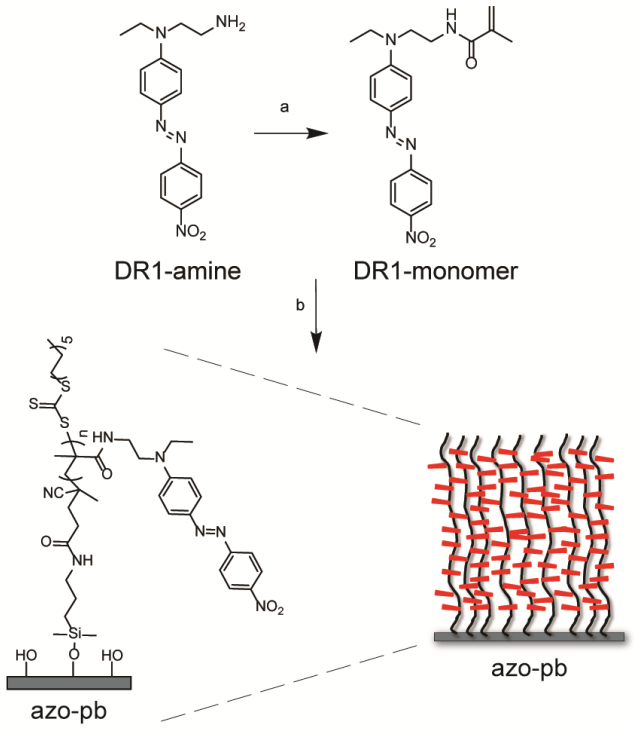

Scheme 1. Synthetic procedure of azo-pb via RAFT technique and azo-pb graphical representation. a) 0.28 mmol of DR1-amine, 1.2 equiv. of methacrylic acid (MA), 1.5 equiv. of EDC·HCl, 1.5 equiv. HOBt·H_2O and 3 equiv. of TEA in 4 ml of DMF for 24 hours at room temperature. b) 1.57 mmol (600 mg) of DR1-monomer, 3.2 µmol (0.79 mg) of initiator, in methanol/1,4-dioxane (1/1, v/v) mixture at 70 °C for 48 hours. The chemical structure and a graphical representation of azopolymer brushes (azo-pb) are depicted, where n stands for

number of repeating units. Polymer backbone is reported in black, while azobenezenes in side chains are colored in red.

Here, the polymeric backbone is depicted in the stretched form, while azobenzene moieties are represented in their preferential orientation on a plane that is parallel to the substrate. In the reported conformation, polymer tails are crowded and forced to stretch away from the surface, along the direction normal to the plane, in order to avoid as much as possible chain overlapping.[23] The chemical characterization of synthesized azopolymer brushes was carried out using two powerful spectroscopic techniques. First of all, we performed an X-Ray Photoelectron Spectroscopy (XPS) analysis to confirm the elemental composition and then Raman spectroscopy.

The topography of dry azopolymer brushes was studied by atomic force microscopy (AFM) as shown in Figure 1A. AFM was also employed to investigate the formation of patterned area on the same sample as well as its erasure.

2.2.2 Azo-pb photopatterning using Lloyd's mirror

In order to obtain linear patterns on azopolymer brushes, the photosensitive property of azobenzene moieties was exploited. In fact, Santer and co-workers have proven that IL can be successfully used to pattern similar azobenzene-containing polymer brushes.[14-15] The probability of light absorption by an azobenzene molecule varies as $\cos^2(\theta)$, where θ is the angle between the light polarization and the azobenzene dipole axis. Thus, azobenzene molecules oriented along the polarization of the laser will absorb, whereas those oriented perpendicular to it will not. This event is able to provoke a movement of the entire polymeric chain and form a surface modulation that resembles the sinusoidal light pattern.[14-15] In this work, we used IL to obtain linear patterns as well. Interference patterns were obtained using a 442 nm He-Cd laser (60 mW power) and we performed a set of experiments with the aim of finding the best

conditions for the realization of holographic patterns, using our synthesized polymer brush samples, in order to perform cell culture studies on these platforms. Therefore, based on earlier achieved information, the pattern pitch was chosen to be 2.5 μm (setting the θ angle between incident beam and mirror to 5°). In fact, we have recently observed that cells cultured on azopolymer SRGs showed a good polarization on this crest-to-crest distance.[8] Furthermore, pattern depth has also been shown to elicit different cell response on different cell lines.[24] For this reason, in order to inscribe a pattern deep enough to be able to influence cell behavior,[1, 24] we tuned laser polarization and beam illumination time. The best results were achieved by exposing the sample to the laser beam with a polarization oriented at 45° that was able to efficiently excite the preponderance of azobenzene moieties in side chain (Figure 1).

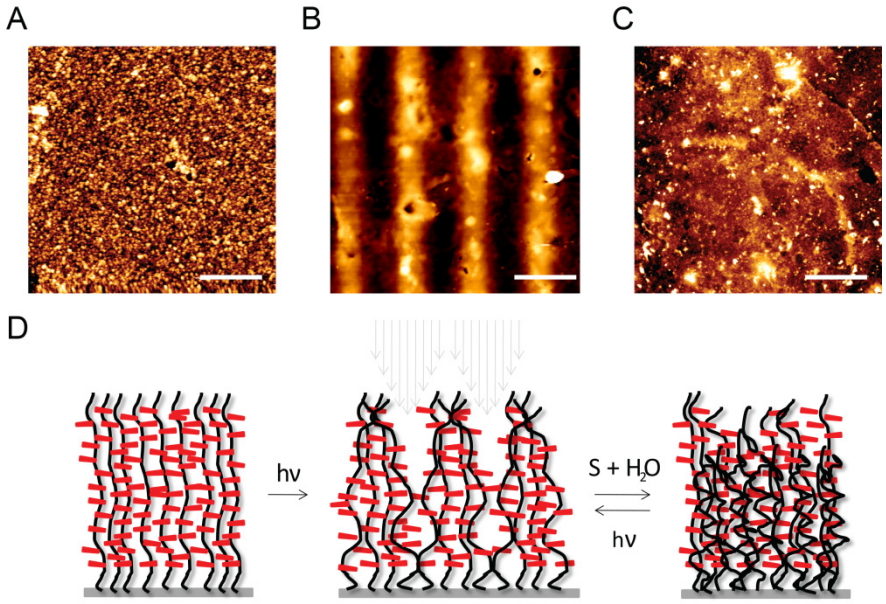

Figure 1. AFM images of A) before and B) after 2 hours of IL exposure with 45° polarization of azo-pb (60 nm pattern height). C) AFM image of erased pattern by sonication with water at room temperature. Micrographs are taken in the same area. Scale bars are 2.5 μm. D) Graphical representation of azo-pb before and after Lloyd's mirror IL exposure and deleted pattern by sonication (S + H_2O means "sonication in water"). This is a simplified representation of the polymer brushes, since currently there is no experimental information on DR1 organization in the brush assembled structures that formed after laser patterning.

In fact, in this situation the intensity interference pattern presents the electric field vector with both non-zero x and y components. This polarization state is thus able to excite the majority of azobenzenes regardless of their orientation in the polymer brush sample.[25] After 1 hour of illumination we obtained a sharp 30 nm-high pattern, while, increasing the illumination time to 2 hours, the height of the pattern raised, reaching in some areas 60 nm (Figure 1B). Further increasing the irradiation time to 3 hours the pattern profile did not change in terms of height (data not shown).

2.3 SRG erasure using ultrasonication

The creation of patterned substrates that can be further modified and even erased during cell culture is an important issue of current research in order to simulate the complexity and remodeling of natural ECM. In this regard, another important characteristic of azopolymer films is that the IL patterns can be erased, either thermally by raising temperature above the polymer glass transition temperature, or optically, using a circularly polarized as well as incoherent and unpolarized light.[26] In our former work, exploiting this azopolymer film property, the topographical pattern was erased with the use of an incoherent and unpolarized light beam of a mercury lamp, while murine fibroblasts were seeded on the polymer. Cells were indeed prone to rearrange their morphology in response to the new topography.[8-9]

Therefore, we tried to modify the pattern also in the case of polymer brushes using the incoherent and unpolarized light of a mercury lamp. However, erasure of SRG patterns with azopolymer brushes resulted more complicated. Neither the use of the focused beam of a confocal microscope in circular polarization was effective in erasing the pattern (data not shown). A possible explanation can be found considering the fact that azobenzene-containing brushes strongly aggregate as reported by Tong et al. in similar polymer systems.[27] Moreover,

we also recently demonstrated aggregation in azobenzene-grafted polymer brushes upon single laser beam exposure.[18] We indeed hypothesize that the strong interaction between azobenzene moieties in this densely packed polymer system increased after the pattern formation and therefore it was difficult to disentangle such network and erase the topographical structures. In fact, as experimentally evidenced by Tong and co-workers, in liquid-crystalline azopolymers different types of aggregation can occur as a consequence of a confinement of the polymer.[27] We can apply these considerations to our case, in which polymer chains are confined over a glass surface. It is known that the laser interference forces the polymer chains to stretch away from bright areas, constraining the backbones to aggregate in a sinusoidal profile.[11] In this way the formation of compact aggregates is highly probable (as schematically shown in Figure 1D). Nevertheless, even if the use of light as stimulus to erase the photoinscribed patterns would be more convenient for biological investigations, we found that ultrasonication (59 kHz) in water at room temperature was an efficient way to disrupt aggregation allowing pattern deletion.

Ultrasounds (US) in a certain medium produce both thermal and mechanical effects. The former are due to absorption of US by the medium, while the latter are usually associated with the acoustic cavitation that is particularly relevant when microbubbles form.[28] During the process energy is transferred from the sound wave to the medium mainly through absorption and scattering processes. Absorption converts acoustic energy irreversibly into heat mainly via viscous friction, even if in water-based media this phenomenon is often negligible. The presence of oscillating microbubbles and the shear force arising during their collapse in the early stage of the ultrasonication process, instead, could be responsible of the disaggregation of polymer brushes by destroying the non-covalent intra- and inter-molecular bonds.[29]

Even though light was not efficient in erasing the pattern in our system, its removal by ultrasonication gave us the possibility to study the reversibility of SRG on the azopolymer brushes without heating the material or using organic solvents. Right after treatment the surface did not recover exactly the initial topography, as shown in the AFM image of Figure 1C. Even though the texture and topography of the polymer brushes were slightly different before and after the sonication process, regeneration with treatment using proper solvent (i.e. DMF) followed by several washing steps with methanol, allowed rewriting of a similar pattern. All AFM images were carried out in the same region of the sample thanks to the use of markers to spot the area of interest. This erasure method was in fact used after each inscription on the same sample in the different illumination conditions. The mechanism by which these patterns form is still not completely elucidated. Santer et al. propose for similar polymer brush systems the occurrence of a chain rupture upon photostimulation with an interference pattern of laser light, which leads to the formation of an irreversible pattern. Moreover, upon a treatment with dimethylformamide (DMF) they show that the pattern depth further increased, owing to the fact that a fraction of the ruptured chains was washed out by solvent treatment. Considering our results in this framework, a possible chain rupture upon IL has to be taken in consideration.[14] Probably, a slight scission indeed occurred, since we noticed a different polymer brush texture after sonication. However, this phenomenon did not limit further patterning cycles (more than 3), which gave patterns of comparable height. Moreover, since a detailed mechanism of SRG formation in azopolymer brush is still not fully understood and our polymer brushes were synthesized in different conditions compared to other similar systems, they might behave in a different manner under external stimuli. However, unraveling the mechanism of pattern formation and investigating on a possible chain rupture were beyond the scope of this thesis work. For our specific purpose, this

patterning/erasure cycle (shown as graphical representation in Figure 1D) was efficient enough to perform biological studies with reconfigurable topography.

2.2.4 Cell culture studies with HUVECs

Our brushes were found biocompatible through a Live/Dead test when seeding HUVECs (Figure 2), which are known to be quite sensitive to surface topography and whose alignment is of particular interest in tissue engineering for achieving functional vascularization.[30-31] This test provides a two-color fluorescence cell viability assay based on the simultaneous visualization of live and dead cells with two probes that measure recognized parameters of cell viability (intracellular esterase activity – Calcein AM) and plasma membrane integrity (ethidium homodimer-1).

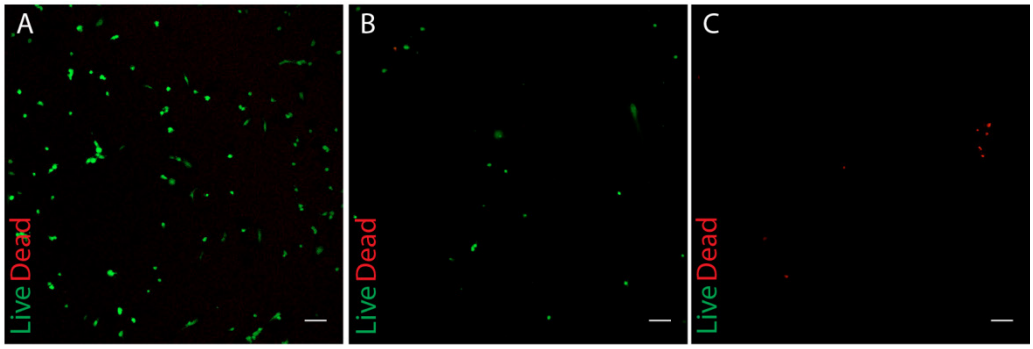

Figure 2. Confocal images of Live/Dead assay on azopolymer brushes. The images represent a merge of the two channels for fluorescent calcein AM (green) and ethidium homodimer-1 (red). A) HUVECs on azopolymer brushes. B) Positive control of live cells on a glass-bottom petri dish, and C) positive control for dead cells after treatment with triton 0.1%. Scale bars are 100 µm.

Interestingly, most of the cells were aligned along the grooves of the patterned area, as can be seen in Figure 3A and B, while they were randomly oriented in non-patterned regions (Figure 3C and D).

We used a qualitative analysis for the evaluation of the cell orientation in order to compare cells on patterned and non-patterned areas using an ImageJ plugin (the procedure is described in details in the experimental section 2.4.5).

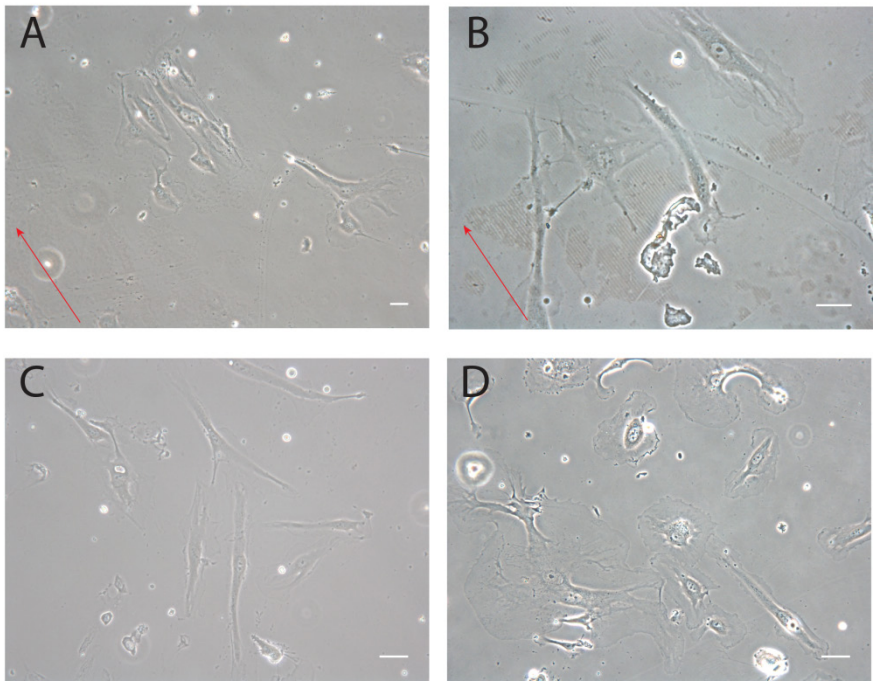

Figure 3. A) and B) represent the phase contrast images of HUVECs on patterned azopolymer brushes after 24 hours of incubation. Red arrows represent pattern direction. C) and D) show cells on non-patterned areas. Scale bars are 30 μm.

Cells on linear patterns displayed a narrower distribution of orientation, whose average values indicated a coalignment with the pattern direction (Figure 4). As expected, cells on non-patterned areas presented a broad distribution, indicating a random orientation.

To test whether our erasure method could be feasible with this cell line, we performed the ultrasonication experiment on a non-patterned sample of azopolymer brushes in the presence of adherent cells. In this case, cell culture medium supplemented with HEPES buffer was used and ultrasonicator bath temperature was set to 37 °C, in order to mimic cell culture conditions. After 1 minute of sonication cells started to detach from the surface, showing a less spread morphology (Figure 5B) until they adopted a round shape after 10 minutes (Figure 5C).

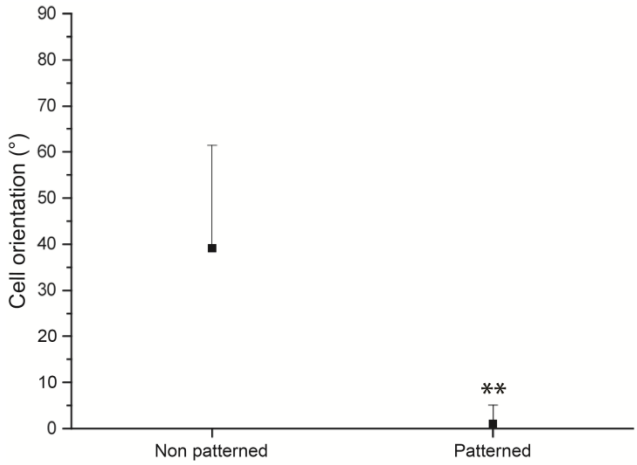

Figure 4. Cell orientation on the SRG pattern in patterned and non-patterned areas. Calculation based on 7-9 cells per area. Cell orientation is evaluated with respect to the pattern direction for cells in the patterned areas, while with respect to the horizontal axis for the non-patterned area. Black squares represent the average value and bars refer to the standard deviation for cell orientation. The asterisks indicates a highly statistical difference between the two cases by performing an Anova test ($p<0.01$).

At the end of the process (10 minutes), cells were completely detached from the substrate (Figure 5C), but, after an overnight incubation, they adhered again to the surface (Figure 5D). This experiment proved that 10 minutes of sonication treatment at 59 kHz at 37 °C (conditions applied also during pattern eresure) was not harmful for cells, which remained viable and adhered again to the polymer brushes. Probably ultrasonication provoked the direct detachment of physisorbed proteins from the surface[32] as protein layer was the sole anchoring element for cells, which minimized cavitation stress just by detaching. While, enzymatic treatments have been found to be highly damaging to cells and ECM even though they are commonly used in every day culture practices.[33] This mechanical pattern erasure method, instead, appeared feasible in presence of living cells.

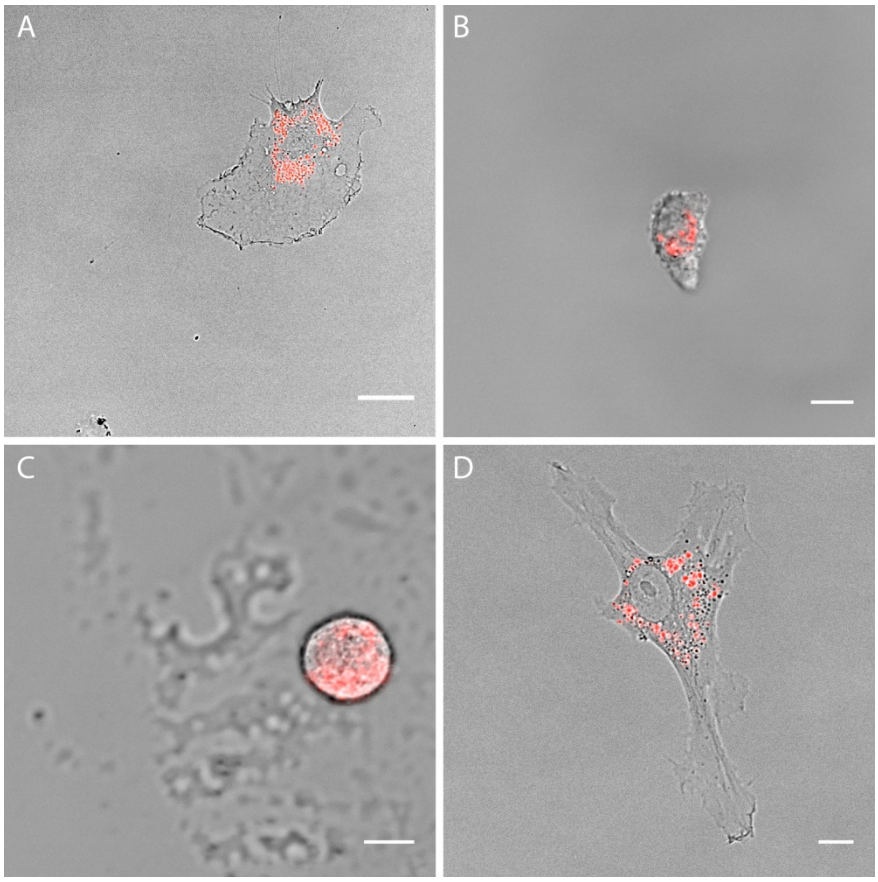

Figure 5. Ultrasonication of non-patterned polymer brushes in presence of cells. A) image of adherent HUVECs on polymer brushes, B) image of a single cell after 1 minute and C) after 10 minutes of sonication at 59 kHz in a sonicating bath set at 37 °C. D) Image of a sonicated cell after an overnight incubation. Cells were stained with vital CellTracker^{TM} CM-Dil. Scale bars are 20, 10, 10 and 30 μm, respectively.

The study of the interaction between cells and their natural microenvironment has been carried out extensively in the last decades.[34-37] The materials used in most of the cases do not allow for a change in their properties, as it happens in nature instead. Therefore, at the moment there is a growing interest in the development of stimuli-responsive biomaterials in order to overcome these limitations. Moreover, the possibility to imprint microfeatures on a substrate, reset the topography with mild conditions and then reconfigure the surface pattern is one of the major goals in microfabrication research related to tissue

engineering. In particular, the methods generally used to obtain a pattern on polymer brush surfaces are still not as straightforward as the photopatterning approach.[38]

In contrast, azobenzene-containing materials are gaining increasing attention for their potential applications in cell culture as dynamically controlled materials. In fact, spin coated azopolymers have recently been used as cell culture supports proving their efficiency in providing different cell response and behavior.[9, 13, 39-40] The use of such polymers may help to gain a deep insight in many biological questions regarding not only tissue engineering and regenerative medicine, but also more basic studies of development and pathogenesis.[3] However the lack in long-term stability of these spin coated polymers could highly reduce their range of applications. For this reason, the use of covalently grafted azopolymer on glass surface, described in this work, might be a real step forward in the realization of stable platforms for the remodeling of topographic signals. Therefore, we are confident that this work will be of interest to the general field of light-stimuli responsive materials.

2.3 Conclusions

In this work, we have shown how SRG inscribed on synthesized azopolymer brushes and mechanically erased by ultrasonication can be exploited as bidimensional reversible surfaces for contact guidance studies through optical inscription and mechanical erasure of micrometer scale topography. Even though, we are still investigating pattern erasure using light sources, since light entails the unique property of a precise spatio-temporal localization, which could enable pattern erasure in a specific part of the surface at will. Nonetheless, the use of ultrasonication allowed cycles of writing/erasure of the pattern. Furthermore, the sonication treatment could be performed even in the presence of cells, without being harmful for them. Moreover, these substrates

were found biocompatible for HUVECs, which were also able to feel the underneath topography by aligning preferentially in the SRG pattern direction or dispose in random direction when seeded on non-patterned brush surface. From these results we envision the possibility to use such polymer brushes as biointerfaces for "on-off" switching topographies allowing the attachment, orientation and detachment of cells using mild conditions. We foresee that such kind of polymeric stimuli-responsive platforms will allow future studies on how remodeling of material topography may influence cell behavior with important impact in the bioengineering research.

2.4 Experimental section

2.4.1 Materials and Methods

All chemicals and solvents were purchased from Sigma-Aldrich at the highest purity available and used without further purification. All the chemical synthesis was carried out under dry nitrogen using standard technique. Human umbilical vein endothelial cells (HUVECs) were purchased from LONZA.

2.4.2 Synthetic procedure for DR1-monomer

0.34 mmol (1.2 equiv., 29.7 mg) methacrylic acid (MA), 0.48 mmol (1.5 equiv., 92 mg of *N*-(3-dimethylaminopropyl)-*N'*-ethylcarbodiimide hydrochloride (EDC·HCl), 0.48 mmol (1.5 equiv., 97.02 mg) 1-hydroxy benzotriazole hydrate (HOBt·H_2O) and 0.96 mmol and (3 equiv., 133 µl) of triethylamine (TEA) were dissolved in 4 ml of *N,N*-dimethylformamide (DMF) in a 25 ml round-bottom flask. 0.28 mmol of an amine-derivative of the commercially available Disperse Red 1 (DR1) (prepared according to our previous work)[18] was added and the reaction was continued for 24 hours at room temperature. The product formation was followed by thin layer chromatography (TLC) and purified by column chromatography with a mixture of methanol/dichloromethane 8/92

(v/v). The product was obtained as red solid with 80% yield. MS for $C_{20}H_{23}N_5O_3$: calculated for $[M+H]^+$ = 382.18 m/z; found (ESI) $[M+H]^+$ = 382.18 m/z. ^{1}H NMR (600 MHz, DMSO-d6): δ ppm 8.37 (d, 2H); 8.14 (t, 1H); 7.94 (d, 2H); 7.85 (d, 2H); 6.97 (d, 2H); 5.66 (s, 1H); 5.35 (s, 1H); 3.55-3.50 (m, 4H), 3.39-3.35 (m, 2H); 1.86 (s, 3H); 1.18 (t, 3H).

2.4.3 Synthetic procedure for azopolymer brush (azo-pb)

The silanization and immobilization of RAFT agent on the glass coverslip have been accomplished following the synthetic procedure already reported by our group.[18] A 25 ml round-bottom flask and a 5 ml vial were washed and dried. All chemicals and dried glass apparatus were placed inside the glove box under nitrogen flow for 30 minutes. 1.57 mmol (600 mg) of DR1-monomer were weighed and transferred into 25 ml round-bottom flask with 10 ml of dry methanol/1,4-dioxane (1/1, v/v) mixture. Then, 3.2 μmol (0.79 mg) of 1,1'-azobis(cyclohexanecarbonitrile) (initiator, I) were weighted and transferred into the 5 ml vial and dissolved in 2 ml of dry methanol/1,4-dioxane (1/1, v/v) mixture. Both monomer and initiator solutions were properly sealed and taken out from the glove box. The monomer solution was degassed by three freeze-thaw cycles for the complete removal of dissolved oxygen from the system. Meanwhile, the initiator solution was degassed by bubbling nitrogen for 30 minutes. After that, monomer and initiator solutions were transferred into the 100 ml corning flask, which contained RAFT-immobilized glass coverslip, under nitrogen atmosphere. The flask was sealed with Teflon tape and heated at 70 °C for 48 hours. The reaction was stopped by exposure to air. The glass substrate was washed with methanol by sonication for 20 minutes at room temperature, the washing process was repeated three times to remove unimmobilized polymer on the glass substrate and finally it was dried in a vacuum oven at 30 °C for 24 hours.

2.4.4 Surface relief grating inscription

A 442 nm He-Cd laser (power of about 60 mW) was used in Lloyd's mirror IL configuration in order to project an interference pattern of light on azopolymer brushes for inducing the formation of SRG. In more details, the azopolymer sample was fixed to one of the mirror edges and the polarized laser beam was reflected on its surface. The pattern pitch was 2.5 μm, given by the equation $2d=\lambda/\sin(\vartheta)$, where λ is the laser wavelength and ϑ is the angle between the incident beam and the mirror. Inscription time was varied from 1 to 2 hours.

2.4.5 Cell culture

HUVECs were cultured in gelatin-coated flasks in an incubator at 37 °C and humidified atmosphere with 5% of CO_2. Cell medium M200 supplemented with LSGS Kit (fetal bovine serum 2% v/v, hydrocortisone 1 μg/ml, human epidermal growth factor 10 ng/ml, basic fibroblast growth factor 3 ng/ml, heparin 10 μg/ml) was used. Cells were detached with trypsin/EDTA (0.25% w/v trypsin/0.02 mM EDTA) and counted with the Neubauer cell counting chamber before seeding on solid substrates. Polymer brushes were sterilized under UV light for 30 minutes prior to cell culture. After 24 hours cells were observed with an Olympus CKX41 microscope and images were taken with a Manta GigE Vision camera (Allied Vision Technologies).

Biompatibility was checked with the LIVE/DEAD® Viability/Cytotoxicity Assay Kit (thermofisher). Calcein AM and ethidium homodimer-1 (EthD-1) have been dissolved in Opti-MEM (Gibco) without FBS at the final concentrations of 2 μM and 4 μM, respectively after the determination of the optimal non-cytotoxic levels for HUVECs. The culture medium was removed, cells were washed twice with PBS and incubated at room temperature for 7 minutes before imaging. The positive control for dead cells was done by treating cells with triton 0.1% for 3 minutes as permeabilizing agent.

Cell orientation on patterns was evaluated with the MomentMacroJ v. 1.3 script (hopkinsmedicine.org/fae/mmacro.htm). Cells were delineated by manually drawing elliptic shapes with fixed aspect ratio. Cell orientation was defined as the angle that the principal axis of inertia (evaluated by the script) formed with a reference axis, i.e. the pattern direction in the case of SRGs and the horizontal axis for flat surfaces.

2.4.6 Ultrasonic cavitation procedure

Azopolymer brush glass substrate was kept in a conical flask with 10 ml of water and sonicated (59 kHz) for 10 minutes at room temperature. Then, the substrate was washed with water and dried in a vacuum oven for 24 hours. After that, the sample topography was characterized by AFM. Since topography was different after water treatement, samples were left overnight in DMF and then washed with methanol by sonication. Subsequently, samples were analyzed again by AFM.

2.4.7 Ultrasonic cavitation in presence of HUVECs

Cells were stained with vital CellTracker™ CM-DiI fluorescent dye before seeding. A staining solution in PBS was made to a final concentration of 2 μg/ml diluting a 2 mg/ml stock solution of dye in DMSO. Cells were covered with 2 ml of the staining solution and incubated first at 37 °C for 5 minutes and then at 4 °C for 15 minutes. After that, cells were washed twice with PBS and finally fresh cell culture medium was added. For imaging during ultrasonication experiment medium was supplemented with 4-(2-hydroxyethyl)piperazine-1-ethanesulfonic acid (HEPES) buffer before the experiment, while ultrasonic cleaner bath was set at 37 °C, in order to reproduce cell culture conditions. Adherent cells were sonicated for 10 minutes at 59 kHz, observed with a TCS SP5 confocal microscope (Leica Microsystems) after 1, 5 and 10 minutes and

incubated overnight at 37 °C in a humidified atmosphere with 5% CO_2 before final observation.

2.5 References

§ Author contributions. In this work Miss Chiara Fedele performed the synthesis of the azobenzene monomer and joined the synthesis of the polymer brush samples. She performed some of the AFM characterizations and assisted during the interference lithography experiments, developing a critical look at the experimental conditions. Finally, she performed all biological experiments.

1. Bettinger, C. J.; Langer, R.; Borenstein, J. T., Engineering substrate topography at the micro-and nanoscale to control cell function. *Angew. Chem., Int. Ed.* **2009,** *48* (30), 5406-5415.
2. Kim, H. N.; Kang, D.-H.; Kim, M. S.; Jiao, A.; Kim, D.-H.; Suh, K.-Y., Patterning methods for polymers in cell and tissue engineering. *Ann. Biomed. Eng.* **2012,** *40* (6), 1339-1355.
3. Lutolf, M.; Hubbell, J., Synthetic biomaterials as instructive extracellular microenvironments for morphogenesis in tissue engineering. *Nat. Biotechnol.* **2005,** *23* (1), 47-55.
4. Stuart, M. A. C.; Huck, W. T.; Genzer, J.; Müller, M.; Ober, C.; Stamm, M.; Sukhorukov, G. B.; Szleifer, I.; Tsukruk, V. V.; Urban, M., Emerging applications of stimuli-responsive polymer materials. *Nat. Mater.* **2010,** *9* (2), 101-113.
5. Baac, H.; Lee, J.-H.; Seo, J.-M.; Park, T. H.; Chung, H.; Lee, S.-D.; Kim, S. J., Submicron-scale topographical control of cell growth using holographic surface relief grating. *Mater. Sci. Eng. C Mater. Biol. Appl.* **2004,** *24* (1-2), 209-212.
6. Barille, R.; Janik, R.; Kucharskic, S.; Eyer, J.; Letournel, F., Photo-responsive polymer with erasable and reconfigurable micro- and nano-patterns: An in vitro study for neuron guidance. *Colloids Surf., B* **2011,** *88*, 63-71.
7. Hurduc, N.; Donose, B. C.; Macovei, A.; Paius, C.; Ibanescu, C.; Scutaru, D.; Hamel, M.; Branza-Nichita, N.; Rocha, L., Direct observation of athermal photofluidisation in azo-polymer films. *Soft matter* **2014,** *10* (26), 4640-4647.
8. Rianna, C.; Calabuig, A.; Ventre, M.; Cavalli, S.; Pagliarulo, V.; Grilli, S.; Ferraro, P.; Netti, P. A., Reversible holographic patterns on azopolymers for guiding cell adhesion and orientation. *ACS Appl. Mater. Interfaces* **2015,** *7* (31), 16984-16991.
9. Rianna, C.; Rossano, L.; Kollarigowda, R. H.; Formiggini, F.; Cavalli, S.; Ventre, M.; Netti, P. A., Spatio-Temporal Control of Dynamic Topographic Patterns on Azopolymers for Cell Culture Applications. *Adv. Funct. Mater.* **2016,** *26* (42), 7572-7580.

10. Frascella, F.; Angelini, A.; Ricciardi, S.; Pirri, F.; Descrovi, E., Surface-relief formation in azo-polyelectrolyte layers with a protective polymer coating. *Opt. Mater. Express* **2016,** *6* (2), 444-450.
11. Priimagi, A.; Shevchenko, A., Azopolymer-Based Micro- and Nanopatterning for Photonic Applications. *J. Polym. Sci. Pol. Phys.* **2013,** *52*, 163–182.
12. Yager, K. G.; Barrett, C. J., All-optical patterning of azo polymer films. *Curr. Opin. Solid State Mater. Sci.* **2001,** *5*, 487-494.
13. Rocha, L.; Păiuş, C.-M.; Luca-Raicu, A.; Resmerita, E.; Rusu, A.; Moleavin, I.-A.; Hamel, M.; Branza-Nichita, N.; Hurduc, N., Azobenzene based polymers as photoactive supports and micellar structures for applications in biology. *J. Photochem. Photobiol., A* **2014,** *291*, 16-25.
14. Lomadze, N.; Kopyshev, A.; Rühe, J. r.; Santer, S., Light-Induced Chain Scission in Photosensitive Polymer Brushes. *Macromolecules* **2011,** *44* (18), 7372-7377.
15. Schuh, C.; Lomadze, N.; Rühe, J. r.; Kopyshev, A.; Santer, S., Photomechanical degrafting of azo-functionalized poly (methacrylic acid)(PMAA) brushes. *J. Phys. Chem. B* **2011,** *115* (35), 10431-10438.
16. Kopyshev, A.; Galvin, C. J.; Genzer, J.; Lomadze, N.; Santer, S., Opto-mechanical scission of polymer chains in photosensitive diblock-copolymer brushes. *Langmuir* **2013,** *29* (45), 13967-13974.
17. Kopyshev, A.; Lomadze, N.; Feldmann, D.; Genzer, J.; Santer, S., Making polymer brush photosensitive with azobenzene containing surfactants. *Polymer* **2015,** *79*, 65-72.
18. Kollarigowda, R.; De Santo, I.; Rianna, C.; Fedele, C.; Manikas, A.; Cavalli, S.; Netti, P., Shedding light on azopolymer brush dynamics by fluorescence correlation spectroscopy. *Soft Matter* **2016,** *12* (34), 7102-7111.
19. Chiefari, J.; Chong, Y.; Ercole, F.; Krstina, J.; Jeffery, J.; Le, T. P.; Mayadunne, R. T.; Meijs, G. F.; Moad, C. L.; Moad, G., Living free-radical polymerization by reversible addition-fragmentation chain transfer: the RAFT process. *Macromolecules* **1998,** *31* (16), 5559-5562.
20. Moad, G.; Chong, Y.; Postma, A.; Rizzardo, E.; Thang, S. H., Advances in RAFT polymerization: the synthesis of polymers with defined end-groups. *Polymer* **2005,** *46* (19), 8458-8468.
21. Willcock, H.; O'Reilly, R. K., End group removal and modification of RAFT polymers. *Polym. Chem.* **2010,** *1* (2), 149-157.
22. Boyer, C.; Bulmus, V.; Davis, T. P.; Ladmiral, V.; Liu, J.; Perrier, S., Bioapplications of RAFT polymerization. *Chem. rev.* **2009,** *109* (11), 5402-5436.
23. Zhao, B.; Brittain, W. J., Polymer brushes: surface-immobilized macromolecules. *Prog. Polym. Sci.* **2000,** *25* (5), 677-710.

24. Loesberg, W.; Te Riet, J.; van Delft, F.; Schön, P.; Figdor, C.; Speller, S.; van Loon, J.; Walboomers, X.; Jansen, J., The threshold at which substrate nanogroove dimensions may influence fibroblast alignment and adhesion. *Biomaterials* **2007,** *28* (27), 3944-3951.
25. Yadavalli, N. S.; Saphiannikova, M.; Santer, S., Photosensitive response of azobenzene containing films towards pure intensity or polarization interference patterns. *Appl. Phys. Lett.* **2014,** *105* (5), 051601.
26. Jiang, X.; Li, L.; Kumar, J.; Kim, D.; Tripathy, S., Unusual polarization dependent optical erasure of surface relief gratings on azobenzene polymer films. *Appl- phys. lett.* **1998,** *72* (20), 2502-2504.
27. Tong, X.; Cui, L.; Zhao, Y., Confinement effects on photoalignment, photochemical phase transition, and thermochromic behavior of liquid crystalline azobenzene-containing diblock copolymers. *Macromolecules* **2004,** *37* (9), 3101-3112.
28. Wu, J.; Nyborg, W. L., Ultrasound, cavitation bubbles and their interaction with cells. *Adv. Drug Delivery Rev.* **2008,** *60* (10), 1103-1116.
29. Gogate, P. R.; Prajapat, A. L., Depolymerization using sonochemical reactors: A critical review. *Ultrason. sonochem.* **2015,** *27*, 480-494.
30. Liliensiek, S. J.; Wood, J. A.; Yong, J.; Auerbach, R.; Nealey, P. F.; Murphy, C. J., Modulation of human vascular endothelial cell behaviors by nanotopographic cues. *Biomaterials* **2010,** *31* (20), 5418-5426.
31. Takahashi, H.; Nakayama, M.; Itoga, K.; Yamato, M.; Okano, T., Micropatterned thermoresponsive polymer brush surfaces for fabricating cell sheets with well-controlled orientational structures. *Biomacromolecules* **2011,** *12* (5), 1414-1418.
32. Agarwal, A.; Jern Ng, W.; Liu, Y., Removal of biofilms by intermittent low-intensity ultrasonication triggered bursting of microbubbles. *Biofouling* **2014,** *30* (3), 359-365.
33. Nash, M. E.; Healy, D.; Carroll, W. M.; Elvira, C.; Rochev, Y. A., Cell and cell sheet recovery from pNIPAm coatings; motivation and history to present day approaches. *J. Mater. Chem.* **2012,** *22* (37), 19376-19389.
34. McNamara, L. E.; McMurray, R. J.; Biggs, M. J.; Kantawong, F.; Oreffo, R. O.; Dalby, M. J., Nanotopographical control of stem cell differentiation. *J. Tissue Eng.* **2010,** *1* (1), 120623.
35. Yeung, T.; Georges, P. C.; Flanagan, L. A.; Marg, B.; Ortiz, M.; Funaki, M.; Zahir, N.; Ming, W.; Weaver, V.; Janmey, P. A., Effects of substrate stiffness on cell morphology, cytoskeletal structure, and adhesion. *Cell motil. cytoskeleton* **2005,** *60* (1), 24-34.
36. Engler, A. J.; Sen, S.; Sweeney, H. L.; Discher, D. E., Matrix elasticity directs stem cell lineage specification. *Cell* **2006,** *126* (4), 677-689.

37. Ventre, M.; Netti, P. A., Engineering Cell Instructive Materials to Control Cell Fate and Functions Through Material Cues and Surface Patterning. *ACS Appl. Mater. Interfaces* **2016,** *8* (24), 14896-14908.
38. Nie, Z.; Kumacheva, E., Patterning surfaces with functional polymers. *Nat. Mater.* **2008,** *7* (4), 277-290.
39. Goulet-Hanssens, A.; Barrett, C. J., Photo-control of biological systems with azobenzene polymers. *J. Polym. Sci., Part A: Polym. Chem.* **2013,** *51* (14), 3058-3070.
40. Rianna, C.; Ventre, M.; Cavalli, S.; Radmacher, M.; Netti, P. A., Micropatterned azopolymer surfaces modulate cell mechanics and cytoskeleton structure. *ACS Appl. Mater. Interfaces* **2015,** *7* (38), 21503-21510.

Chapter 3

Azopolymer photopatterning by confocal microscope for *in vitro* directional sprouting angiogenesis*

Abstract. Angiogenesis requires the temporal and spatial coordination between different cellular events guided by external cues, among which topographical signals play an important role. However, a sound knowledge of the actual influence of dynamic contact guidance in a 3D environment is still lacking. Since a functional vascular network is essential for the fruitful formation of a well-organized tissue, in bioengineering the fine control over the capillaries formation is greatly important. In this chapter we modulate the presentation of topographical cues during sprouting angiogenesis through the real-time photopatterning of a Disperse Red 1-containing polymer (pDR1m) using the focused laser of a confocal microscope with a fine spatio-temporal control. After assessing the effect of a linear static topography in directing the sprouts, we were able to induce a sprouting remodeling by *in situ* azopolymer photopatterning.

*The work described in this Chapter is part of a manuscript in preparation. M. De Gregorio, C. Fedele, S. Cavalli, C. Attanasio, and P. A. Netti, "Azopolymer Photopatterning for Directional Control of Angiogenesis". (First two authors contributed equally to entire work).§

3.1 Introduction

Angiogenesis is the formation of new capillaries from pre-existing blood vessels and requires the temporal and spatial coordination between different cellular processes. It is know that angiogenesis is triggered by external conditions, such as hypoxia and tissue injuries.[1] Up to date, a complete understanding on how endothelial cells (ECs) respond to those complex signals during angiogenesis is still lacking. Thus, tissue engineering is now aiming at implementing biomaterials and finding novel strategies in order to study the dynamical formation of new capillaries *in vitro* for the control over the formation of a functional blood vessel network. To achieve this aim, different methods have been developed. The majority of the approaches reported in the literature is based either on the presence of soluble factors dispersed within the matrix,[2-4] or on the conjugation of pro-angiogenic molecules to engineered scaffolds.[5] Moreover, among different biomolecules, angiogenic inducers, such as VEGF,[4] as well as synthetic peptides,[6] have been extensively exploited. Furthermore, ECs are known to be particularly influenced by topographical cues conferred by the extracellular matrix (ECM) protein architecture.[7] For this reason, natural matrices (e.g. collagen and fibrin) are often used to induce network formation *in vitro*, since they form fibrillar interconnected structures that can be aligned by external stimuli and further remodeled by cells.[8] In the majority of these examples the influence of the contact guidance of the 3D matrix was investigated, but none of those studies was able to address the issue of spatio-temporal presentation of the topographical cues in sprouting angiogenesis, recapitulating the *in vivo* dynamic nature of ECM. In order to fill this lack of knowledge, the use of smart materials, and in particular the use of light-responsive ones, might represent a new way of getting more insights into the angiogenic process. As a matter of fact, the use of azobenzene-based

polymers have recently been presented as a successful approach to change topography in real-time in presence of living cells.[9-10] Poly(Disperse Red 1 methacrylate) (pDR1m) is a well-known azopolymer, which is widely used in photonic applications for its capability of changing its surface profile upon illumination, but recently it has also been used in biological applications.[9-14] When illuminated with the focused laser beam of a confocal microscope, different topographical features can be written in a biocompatible environment. In particular, this technique has been successfully used to induce a response at a single-cell level of NIH-3T3 murine fibroblasts to the dynamic topographic changes in terms of cell adhesion (length and orientation of focal complexes) and shape.[10] In this Chapter an original extension of this method to multicellular processes is shown, in order to study the influence of dynamic contact guidance in more complex biological systems, like sprouting angiogenesis.

3.2 Results and discussion

Since a functional vessel network is essential for the fruitful formation of a well-organized tissue, the fine control over the formation of an efficient vascular system remains one of the greatest challenge to achieve in tissue engineering.[15] Furthermore, the mechanism that leads to the formation of a new capillary from a pre-existing vessel has not yet been completely elucidated.[16] A useful approach for studying this process *in vitro* is represented by the sprouting angiogenesis assay, which allows the study of the formation of new blood vessels testing the effect of different conditions. Among the *in vitro* models, the angiogenic assay with human umbilical vein endothelial cell (HUVEC) spheroids well replicates vessel formation from pre-existent ones.[17] This model allows for the observation of the spheroid characteristics in three dimensions, from cell migration to the distribution of the spheroid mass. Many works have

characterized the influence of soluble factors on the directional movements of endothelial cells (ECs) and some of the biomolecules involved in the angiogenesis process have been identified, but still very little is known about the exact effect of the topographical features of the ECM in the formation of a functional vessel network.

Cells situated at the edge of the sprouts are called “tip” cells for their ability to lead the formation of a new sprout thanks to their long and motile filopodia. These cells are known to be sensitive to pro-angiogenic growth factors and to other guidance cues in order to enable organized vessel growth.[18] Cells forming the sprout, instead, are called “stalk” cells, since they follow the guidance tracks traced by the leading tip cells. This phenotypic specialization in tip and stalk cells is believed to be only transient in early-stage angiogenesis, because the leader cell selection is thought to be the result of a continuous dynamical competition.[19] Moreover, at a single-cell level, tip cells are supposed to move with a persistent polarity, followed by stalk cells, which, on the contrary, prefer to move behind polarized cells.[20] The ability of patterned features to polarize and direct the migration of many cell types has been largely studied.[21] Thus, from this information, we hypothesized that influencing the migration of leading cells during angiogenesis might, in turn, tune tubule orientation, in a cooperative active process with the remodeling of the surrounding collagen fibrils. Moreover, the influence of producing a change in topography during sprout dynamics has not yet been investigated. For this reason, we decided to first assess information on the influence of a static linear topography using HUVEC spheroids as angiogenic model and later, in order to understand the role of the dynamical change of the topographical signal on sprouting angiogenesis, we used a poly(Disperse Red 1 methacrylate) thin film as photoresponsive surface. Thanks to the material patterning at the confocal microscope, we were able to deliver a topographical cue during early-stage

angiogenesis in a spheroid model and then observe the rearrangement of sprouts in real-time.

3.2.1 Effect of static topography on sprouting angiogenesis

First of all, in order to understand how cells respond to static linear topographies in two-dimensions, we used a UV-curable polymer (NOA63, Norland Optical Adhesive), a polyurethane widely used in soft lithography. A NOA63 patterned substrate was obtained by replica molding of a patterned polycarbonate master, followed by UV curing at 365 nm. This method allowed for the fast production of a large uniformly patterned area (~cm^2). After peeling off, the patterned NOA63 membrane was fixed at the bottom of a custom-made single-well plate prepared as described in section 3.4.1. The replica molding gave a linear pattern 150 nm deep and with 2.5 µm pitch, as also revealed by AFM analysis (Figure 1). These pattern features are similar to the typical topographies that can be produced with the focused laser beam scanning technique applied to pDR1m (Figure 4).

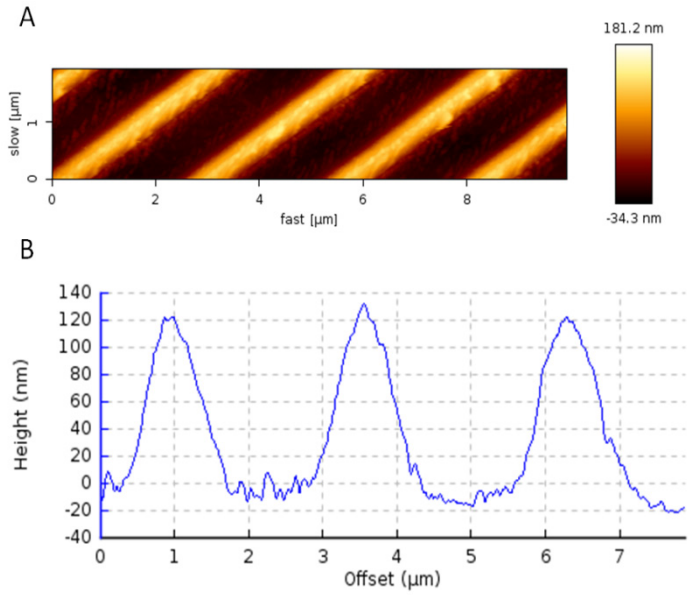

Figure 1. A) AFM analysis of NOA63 patterned substrate and B) cross section.

Subsequently, the substrates were sterilized under UV light in a laminar flow hood and then HUVEC spheroids were seeded on them. After that, samples were incubated in order to allow spheroids to sink to the bottom of the well and therefore let ECs adhere on the patterned material surface. Then a thick layer of collagen was deposited on top of the spheroids, in order to sustain sprouting formation. Fewer studies have investigated the response of ECs to contact guidance if compared to the influence of soluble factors. Some of them have shown that there is a positive correlation between the alignment of endothelial sprouts and the orientation of extracellular matrix fibrillar structure, even if cause and effect of this observation were not established.[22-24] In our experiment, indeed, after 24 hours of incubation the spheroid core acquired a polarized shape and longer sprouts were found in the pattern direction (Figure 2A). As imaged by second harmonic generation (SHG),[25] collagen fibers surrounded each sprout, but, on top of the spheroid core, thicker collagen fibers were localized and disposed in the pattern direction (Figure 2B). This collagen remodeling suggests that cell activity in those regions was more intense. On the contrary, when the spheroid was embedded in the collagen 3D matrix without the presence of the underneath topography, it developed isotropic tubules, while its core maintained a round morphology with collagen fibers disposed all around the spheroid itself (Figure 2C and D). These observations might be an evidence of the fact that a persistent directional migration of the tip cells, caused by the linear topography, was indeed able to orient both the preferential sprouting activity and the collagen fiber remodeling.

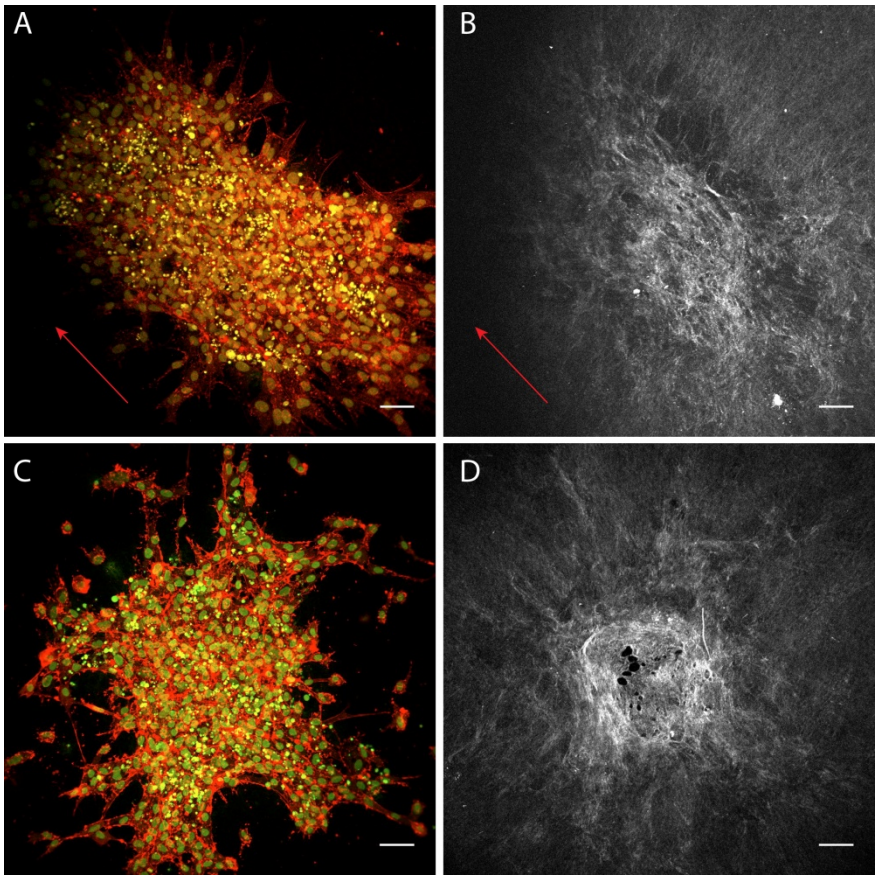

Figure 2. Comparison between HUVEC spheroids in presence of a NOA63 patterned substrate (A and B) and over a flat surface (C and D). A) and C) are z stack maximum projection image of fixed HUVEC spheroids; nuclei are stained in green, while the cytoskeleton is colored in red. B) and D) show collagen organization around the spheroid imaged by second harmonic generation (SHG) using a multiphoton microscope. Red arrows indicate pattern direction.

3.2.2 Effect of pDR1m photopatterning in real-time on sprouting angiogenesis

After assessing that a static topography of the substrate, positioned at the bottom of the well, was able to orient sprouts, we hypothesized that dynamic topographical changes of the substrate could also have an influence on tip cell behavior or in the tip-stalk cell selection, maybe altering sprouting direction in real-time. In order to verity that, glass coverslips were covered with pDR1m by

spin coating and then a custom-made single-well plate was prepared as described in details in section 3.4.1 (Figure 3).

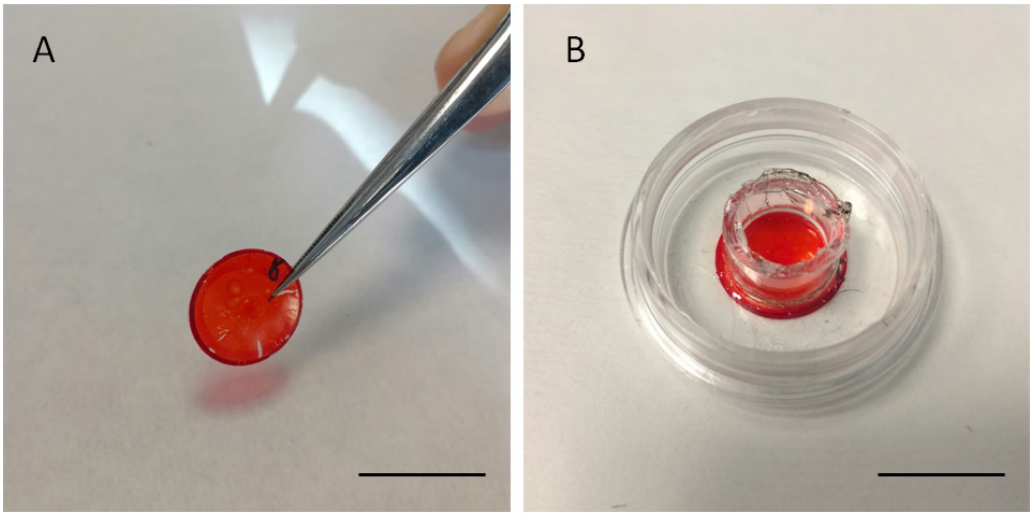

Figure 3. Construction of the custom-made single-well plate for the dynamic patterning. A) pDR1m spin coated glass substrate and B) the final single-well plate. Scale bars are 15 mm.

Later, HUVEC spheroids were seeded as previously described in section 3.2.1 and in the experimental section 3.4.3. After collagen gelation, samples were patterned with the focused single laser beam technique described in the experimental section 3.4.3. Briefly, a 514 nm Argon laser of a confocal microscope is focused at the surface of the photosensitive material with a 25x objective. The confocal software allows to delineate multiple regions-of interest (ROIs) in which the lasers can be selectively tuned. Ideally, there is no limit on pattern shapes that can be inscribed on the pDR1m with this method, but we first decided to draw a set of linear stripes spaced about 3 μm (an example of the inscribed topography is reported in the AFM images in Figure 4). This type of pattern was previously tested in our group with NIH-3T3 murine fibroblasts and it was found able to orient cells along its direction.[10] Furthermore, as described in Chapter 2, a linear pattern produced on azopolymer brushes was also able to induce a preferential orientation of HUVECs at a single-cell level.

Finally, this topography is also similar to the one obtained on NOA63, allowing a comparison with the behavior on static substrates.

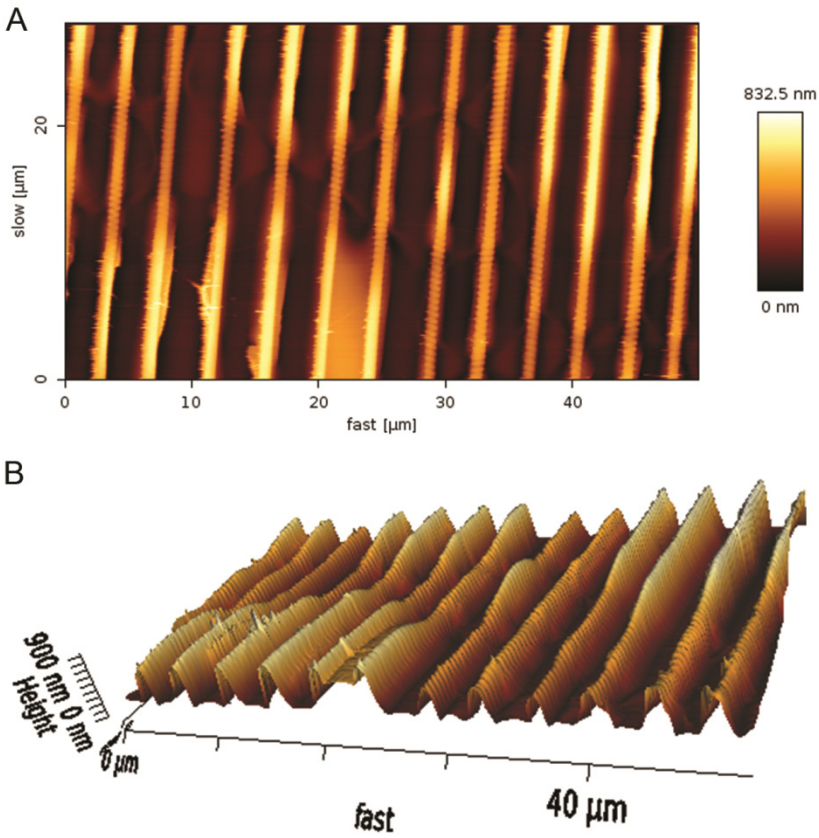

Figure 4. A) AFM analysis of linear topography inscribed by the confocal microscope single laser beam technique in presence of wet collagen and B) its 3D projection.

This topography was inscribed in presence of a thick hydrated collagen layer above the surface and, as we can see from the AFM analysis, this coating did not hinder the mass migration of the azopolymer at the interface. As described in the thesis introduction (Chapter 1) and in a work previously published by our group,[10] the use of the focused single laser beam of the confocal microscope allowed the real-time patterning of the material in presence of living cells. In general, this technique is a versatile tool for real-time biological investigations. During photopatterning, indeed, the laser spot is precisely localized at the

polymer surface, avoiding phototoxic effects. In addition, very often confocal microscopes are equipped with a temperature-controlled chamber so that the biological environment can be easily preserved. Thus, these conditions allowed the observation of cell behavior over several hours after light exposure, following the sprouting remodeling in time. In fact, we performed time lapse imaging also at the confocal microscope after patterning. From these image stacks we were able to notice an intense cell activity after patterning. In particular, we inscribed the pattern when the sprouting activity was already started (Figure 5A). Acting on the temporal presentation of the topographical cue, we noticed a change in the direction of cell sprouts occurred during the first 2 hours, leading to a sprout more aligned to the pattern direction (Figure 5).

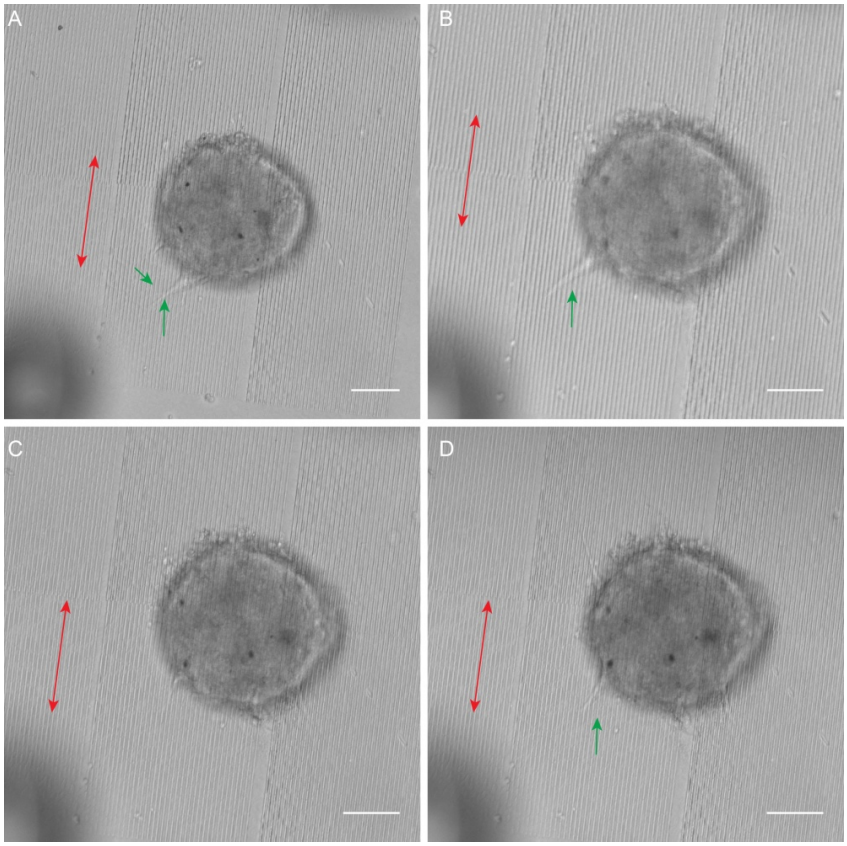

Figure 5. Time lapse imaging of a HUVEC spheroid seeded on pDR1m. A) Image right after pattern formation, and spheroid B) after 98 minute, C) after 114 minutes, and D) after 132

minutes. Red arrows indicate the pattern direction, while green arrows indicate the changing position of the sprout in response to the pattern inscription. Scale bars are 50 µm.

Usually, after patterning eventually followed by time lapse imaging for about 3 hours, cells were placed in the incubator overnight and then fixed, stained and imaged (Figure 6) as previously described.

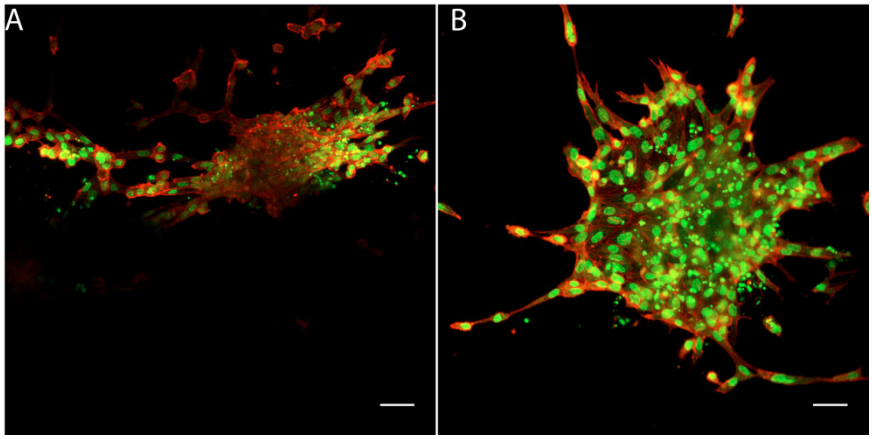

Figure 6. Confocal microscope images of spheroids 24 h after seeding. Representative images of A) HUVEC spheroids cultured on patterned pDR1m and B) control ones on bare glass. The yellow arrow indicates the pattern direction. Scale bars are 20 µm.

As we can clearly see by comparing these images, the final shape of the spheroid, together with its sprouting activity, are completely different between a spheroid interested by the pattern inscription (Figure 6A) and a control one (Figure 6B). In fact, the sprouting activity in the spheroid shown in Figure 6A is greatly anisotropic and long sprouts formed in the pattern direction. In order to evaluate the directionality of the sprouting activity, we used a method previously described by Borselli et al., in which the spheroid image was divided into 8 sectors and the number of sprouts in each sector was quantified. In the samples interested by photopatterning, the pattern was conventionally placed in sectors 1, 4, 5, 8 (Figure 7A), and the same division was kept for the control group (Figure 7B). Sprouts falling in each sector were counted and averaged within the triplicate. Two groups were compared: “Sectors 1, 4, 5, 8” and

“Sectors 2, 3, 6, 7”, as reported in the histograms of Figure 7. As we see from Figure 7C, in the group of patterned samples, 78% of the sprouts were found in the 4 sectors related to the patterned area (sectors 1,4,5,8) and the difference with the average number of sprouts in the non patterned area is statistically significant ($p<0,05$). In contrast, in the flat control group of spheroids (Figure 7D) there was no significant difference between the average number of sprouts in the two types of sectors. The reported data confirm that the *in situ* pattern inscription in early-stage angiogenesis leads to a significant directional sprouting. In this case, we were not able to image collagen fiber arrangement by SHG, because the azopolymer is too sensitive in the SHG excitation conditions, resulting in a damaged surface.

Even in case of fused spheroids we observed a similar behavior. In fact, we inscribed the patterns in different directions and the sprouts clearly followed those directions (Figure 8A). In spite of this behavior, fused spheroids in the control sample assumed a roundish core shape with isotropically protruding sprouts (Figure 8B).

Unfortunately, the pattern reproducibility was not always the same. First of all, from previous studies of our group at a single-cell level, we know that a precise focusing is fundamental for a good patterning. In fact, if this step of the process is not accomplished with high accuracy, the resulting pattern resolution and quality is poor. In the case of multicellular system, the obtainment of a precise focusing is complicated by the presence of the big cell aggregate. Furthermore, a liquid medium above the surface has also been found disturbing in confocal pattern manipulation.[9] Sometimes, indeed, a side topography formed, that could also be due to some scattering events occurring at the collagen-pDR1m interface.

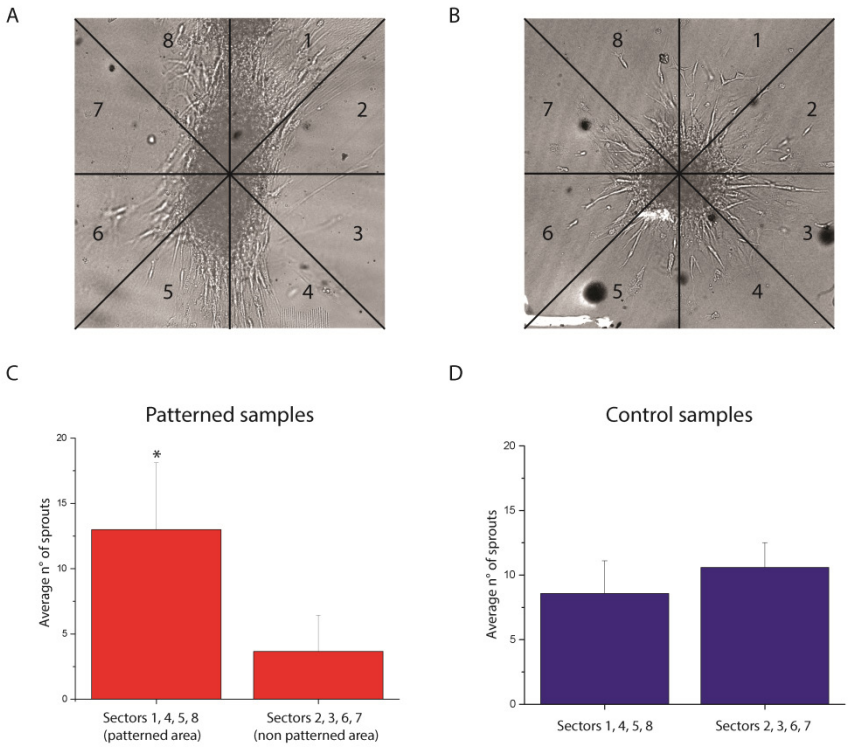

Figure 7. Effect of the pattern on angiogenesis modulation. Images A) and B) show the methodology used for sprouting quantification in the case of patterned and control samples, respectively. Histograms represent the average number of sprouts originated by three spheroids in three different experiments C) exposed to the pattern, or D) to a flat surface ($p < 0.05$).

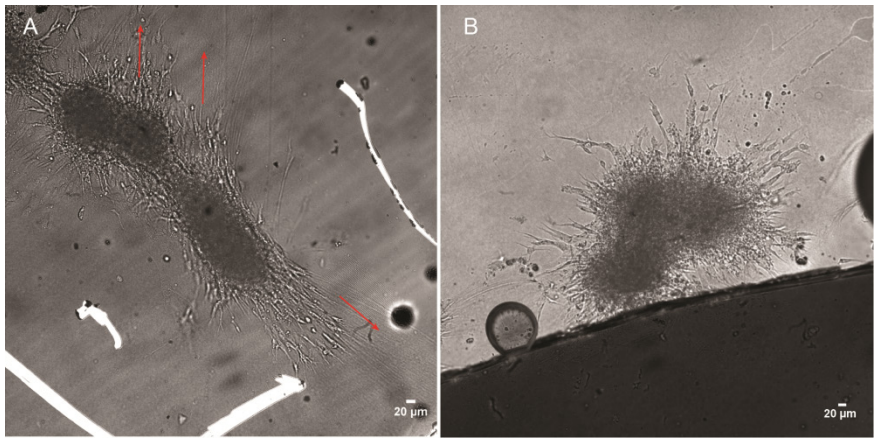

Figure 8. Bright field images of A) fused spheroids forming sprouts in the directions of the different patterns wrote underneath each spheroid by the single laser beam technique as

indicated by the red arrows. B) Fused spheroids displaying a roundish core shape and isotropic sprouting in the control sample.

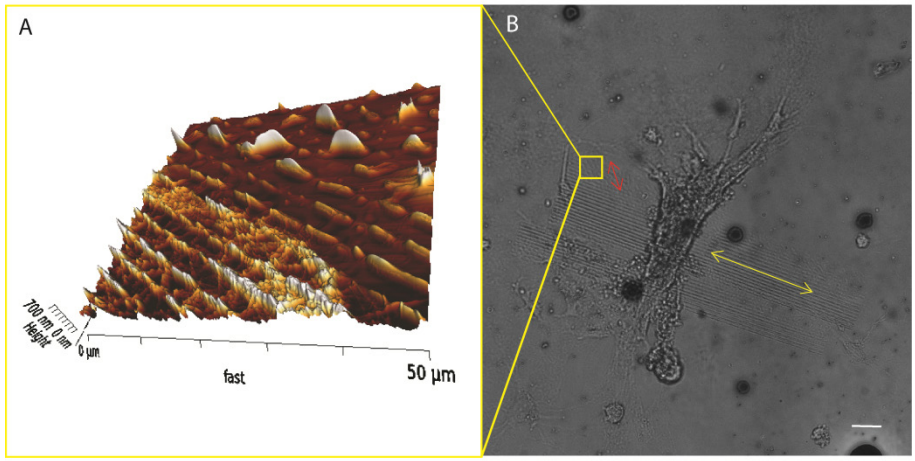

Figure 9. A) AFM image of the side topography at the boundary of the linear one. B) Spheroid showing sprouts not aligned to the linear pattern direction but following the side topography. Scale bar is 20 µm.

In Figure 9 an example of a secondary pattern is shown. In this case, the uncontrolled light stimulus provoked the formation of higher crests, which pointed in a different direction with respect to the rectangular ROIs. Clearly, the side topography effect on HUVEC behavior was dominant, leading to the polarization of the spheroid in the direction opposite to the pattern through sprout advancement in the crests direction. On the other hand, this observation validates the hypothesis that contact guidance plays a major role during sprouting process.

3.3 Conclusions

In tissue engineering, the generation of a functional blood vessel network is essential for the fruitful formation of well-organized tissue. For this reason, the spatial and temporal control over the vascular network formation *in vitro* is of great importance. In the call for novel smart biomaterials and devices, which

could help in giving more insights in the dynamic interplay between cells and the surrounding environment, azopolymers emerge as ideal candidate for this purpose. In fact, taking advantage of our previous experience about the ability of the photoinduced mass migration in such thin films to generate cell-instructive structures in real-time, in the work presented here, this methodology was extended to a more complex multicellular system that is a spheroid of endothelial cells employed for an *in vitro* sprouting angiogenesis assay. The polarized shape of spheroids imaged after 24 hours demonstrated that topographic signals play a major role in directing new sprouts, probably due to contact guidance of leader cells. After assessing the effect of a static linear patterned 2D surface on directional sprouting, the use of single laser beam of a confocal microscope as photopatterning method was successfully implemented to elicit a contact guidance sprout directionality, with the possibility to follow up remodeling of sprouts direction in real-time. Future developments will include an investigation of different topographies that could maximize the directional sprouting response.

3.4 Experimental section

3.4.1 Sample preparation

For the realization of the static topography, NOA63 (Norland Optical Adhesive) was patterned by replica molding from a patterned polyurethane master and polymerized under UV light exposure for 20 minutes. While, for the realization of the dynamic substrate, poly(Disperse Red 1 methacrylate) (pDR1m), purchased from Sigma-Aldrich, was dissolved in chloroform (5% w/v) and then spin coated onto a glass coverslip (15 mm diameter). A custom-made single-well plate was built, in which patterned NOA63 or pDR1m thin film was at the bottom of each well and a polystyrene hollow cylinder (10 mm

internal diameter) was glued on each well using polymerized NOA63 after UV light exposure.

3.4.2 Cell culture and generation of endothelial spheroids

Human Umbilical Vein Endothelial Cells (HUVECs) (Lonza) were grown in Medium 200 (M200) supplemented with LSGS kit (Life-Technologies) at 37 °C in 5% CO_2 and 100% relative humidity. After 3-4 days of culture, confluent HUVEC monolayer (II-IV passage) was trypsinized and 800 cells per spheroid were suspended in culture medium containing 0.25 mg/ml (w/v) carboxymethylcellulose (Sigma), seeded into ultra-low-attachment u-bottom 96-well plates (Costar) and cultured as described above to allow spheroids formation.

3.4.3 In vitro sprouting angiogenesis assay

After 24 hours, spheroids were harvested and centrifuged at 900 rpm for 15 min. Then 1-2 spheroids were seeded in the custom-made single-well plates. Few minutes later spheroids were coated by 1.2 mg/ml bovine skin collagen and then collagen gelation was induced in an incubator for 45 minutes. Subsequently, complete M200 culture medium, supplemented with HEPES (Sigma) (25 ul/ml), was added. Regarding the experiments with NOA63, the samples were left in the incubator overnight and then fixed. Concerning the experiment with pDR1m, instead, after the seeding procedure polymer surface was photopatterned by a confocal microscope (TCS SP5 STED, Leica Microsystems) using an Argon laser at 514 nm, applying a methodology previously reported by our laboratory.[10] Briefly, rectangular regions-of-interest (ROIs) were drawn, spaced 3 μm, directly underneath spheroid border. Samples, prepared in triplicates, were left in the incubator overnight and then fixed in 4% paraformaldehyde. Control samples (spheroids seeded on flat azopolymer thin film as well as on plain glass) were seeded following a

standard procedure, which involves spheroid embedding in the collagen matrix before seeding.

3.4.4 Imaging

Samples were fixed with 4% paraformaldehyde, stained with sytox green (nuclei) and rhodamine phalloidin (cytoskeleton) for the confocal microscope imaging. Collagen fibers were imaged through second harmonic generation (SHG) using a multiphoton microscope (TCP SP5 multiphoton, Leica Microsystems).

3.5 References

§ Author contributions. Miss Chiara Fedele fabricated all the substrates and performed the patterns photoinscription, taking care of the imaging (through AFM and confocal microscopy). She assisted during spheroid model assay. Finally, the candidate strongly contributed in the project elaboration.

1. Martín-Saavedra, F. M.; Wilson, C. G.; Voellmy, R.; Vilaboa, N.; Franceschi, R. T., Spatiotemporal control of vascular endothelial growth factor expression using a heat-shock-activated, rapamycin-dependent gene switch. *Human gene therapy methods* **2013,** *24* (3), 160-170.
2. Tabata, Y.; Miyao, M.; Yamamoto, M.; Ikada, Y., Vascularization into a porous sponge by sustained release of basic fibroblast growth factor. *Journal of Biomaterials Science, Polymer Edition* **1999,** *10* (9), 957-968.
3. King, T. W.; Patrick, C. W., Development and in vitro characterization of vascular endothelial growth factor (VEGF)-loaded poly (DL-lactic-co-glycolic acid)/poly (ethylene glycol) microspheres using a solid encapsulation/single emulsion/solvent extraction technique. *Journal of biomedical materials research* **2000,** *51* (3), 383-390.
4. Richardson, T. P.; Peters, M. C.; Ennett, A. B.; Mooney, D. J., Polymeric system for dual growth factor delivery. *Nature biotechnology* **2001,** *19* (11), 1029-1034.
5. Zisch, A. H.; Lutolf, M. P.; Ehrbar, M.; Raeber, G. P.; Rizzi, S. C.; Davies, N.; Schmökel, H.; Bezuidenhout, D.; Djonov, V.; Zilla, P., Cell-demanded release of VEGF from synthetic, biointeractive cell ingrowth matrices for vascularized tissue growth. *The FASEB journal* **2003,** *17* (15), 2260-2262.
6. Carmeliet, P.; Conway, E. M., Growing better blood vessels. *Nature biotechnology* **2001,** *19* (11), 1019-1021.
7. Gasiorowski, J. Z.; Liliensiek, S. J.; Russell, P.; Stephan, D. A.; Nealey, P. F.; Murphy, C. J., Alterations in gene expression of human vascular endothelial cells associated with nanotopographic cues. *Biomaterials* **2010,** *31* (34), 8882-8888.
8. Koike, N.; Fukumura, D.; Gralla, O.; Au, P.; Schechner, J. S.; Jain, R. K., Tissue engineering: creation of long-lasting blood vessels. *Nature* **2004,** *428* (6979), 138-139.
9. Rianna, C.; Calabuig, A.; Ventre, M.; Cavalli, S.; Pagliarulo, V.; Grilli, S.; Ferraro, P.; Netti, P. A., Reversible holographic patterns on azopolymers for guiding cell adhesion and orientation. *ACS Appl. Mater. Interfaces* **2015,** *7* (31), 16984-16991.

10. Rianna, C.; Rossano, L.; Kollarigowda, R. H.; Formiggini, F.; Cavalli, S.; Ventre, M.; Netti, P. A., Spatio-Temporal Control of Dynamic Topographic Patterns on Azopolymers for Cell Culture Applications. *Adv. Funct. Mater.* **2016,** *26* (42), 7572-7580.
11. Barille, R.; Janik, R.; Kucharskic, S.; Eyer, J.; Letournel, F., Photo-responsive polymer with erasable and reconfigurable micro- and nano-patterns: An in vitro study for neuron guidance. *Colloids Surf., B* **2011,** *88*, 63-71.
12. Baac, H.; Lee, J.-H.; Seo, J.-M.; Park, T. H.; Chung, H.; Lee, S.-D.; Kim, S. J., Submicron-scale topographical control of cell growth using holographic surface relief grating. *Mater. Sci. Eng. C Mater. Biol. Appl.* **2004,** *24* (1-2), 209-212.
13. Hurduc, N.; Donose, B. C.; Macovei, A.; Paius, C.; Ibanescu, C.; Scutaru, D.; Hamel, M.; Branza-Nichita, N.; Rocha, L., Direct observation of athermal photofluidisation in azo-polymer films. *Soft matter* **2014,** *10* (26), 4640-4647.
14. Rocha, L.; Păiuş, C.-M.; Luca-Raicu, A.; Resmerita, E.; Rusu, A.; Moleavin, I.-A.; Hamel, M.; Branza-Nichita, N.; Hurduc, N., Azobenzene based polymers as photoactive supports and micellar structures for applications in biology. *J. Photochem. Photobiol., A* **2014,** *291*, 16-25.
15. Wood, J. A.; Liliensiek, S. J.; Russell, P.; Nealey, P. F.; Murphy, C. J., Biophysical cueing and vascular endothelial cell behavior. *Materials* **2010,** *3* (3), 1620-1639.
16. Morin, K. T.; Smith, A. O.; Davis, G. E.; Tranquillo, R. T., Aligned human microvessels formed in 3D fibrin gel by constraint of gel contraction. *Microvasc. Res.* **2013,** *90*, 12-22.
17. Korff, T.; Augustin, H. G., Integration of endothelial cells in multicellular spheroids prevents apoptosis and induces differentiation. *The Journal of cell biology* **1998,** *143* (5), 1341-1352.
18. Gerhardt, H.; Golding, M.; Fruttiger, M.; Ruhrberg, C.; Lundkvist, A.; Abramsson, A.; Jeltsch, M.; Mitchell, C.; Alitalo, K.; Shima, D., VEGF guides angiogenic sprouting utilizing endothelial tip cell filopodia. *J. Cell Biol.* **2003,** *161* (6), 1163-1177.
19. Eilken, H. M.; Adams, R. H., Dynamics of endothelial cell behavior in sprouting angiogenesis. *Curr. Opin. Cell Biol.* **2010,** *22* (5), 617-625.
20. Szabo, A.; Perryn, E. D.; Czirok, A., Network formation of tissue cells via preferential attraction to elongated structures. *Phys. Rev. Lett.* **2007,** *98* (3), 038102.
21. Liliensiek, S. J.; Wood, J. A.; Yong, J.; Auerbach, R.; Nealey, P. F.; Murphy, C. J., Modulation of human vascular endothelial cell behaviors by nanotopographic cues. *Biomaterials* **2010,** *31* (20), 5418-5426.
22. Lee, P.; Lin, R.; Moon, J.; Lee, L. P., Microfluidic alignment of collagen fibers for in vitro cell culture. *Biomed. Microdevices* **2006,** *8* (1), 35-41.

23. Heath, D. E.; Lannutti, J. J.; Cooper, S. L., Electrospun scaffold topography affects endothelial cell proliferation, metabolic activity, and morphology. *J. Biomed. Mater. Res., Part A* **2010,** *94* (4), 1195-1204.
24. Krishnan, L.; Underwood, C. J.; Maas, S.; Ellis, B. J.; Kode, T. C.; Hoying, J. B.; Weiss, J. A., Effect of mechanical boundary conditions on orientation of angiogenic microvessels. *Cardiovasc. Res.* **2008,** *78* (2), 324-332.
25. Roth, S.; Freund, I., Second harmonic generation in collagen. *The Journal of chemical physics* **1979,** *70* (4), 1637-1643.
26. Borselli, C.; Oliviero, O.; Battista, S.; Ambrosio, L.; Netti, P. A., Induction of directional sprouting angiogenesis by matrix gradients. *J. Biomed. Mater. Res., Part A* **2007,** *80* (2), 297-305.

Chapter 4

Effect of surface topography on epithelial cell migration and signaling*

Abstract. Cell migration plays a crucial role in many biological processes, such as in wound healing and cancer metastasis, regulating in a collective fashion cell displacements. Recently, understanding the effect of topographical signals in these processes is gaining increasing attention, together with the investigation of the dynamic interaction with the extracellular matrix using novel intelligent materials. In this Chapter surface relief gratings (SRGs) on an azobenzene molecular glass are implemented as contact guidance platforms in wound healing assay. Furthermore, a preliminary study on the influence of real-time photopatterning on cell collective response is reported, even in terms of Ca^{2+} signaling.

The project was developed in the group Prof. Arri Priimägi, Tampere University of Technology (Finland). Biological experiments have been performed at the Institute for Biosciences and Biomedical Technology (BioMediTech) in Tampere under the supervision of Dr. Soile Nymark and Dr. Teemu Ihalainen.

*The work described in this Chapter is part of a manuscript in preparation. C. Fedele, T. O. Ihalainen, S. Nymark, S. Cavalli, P. A. Netti and A. Priimägi, "Effect of surface topography on epithelial cell migration in wound healing assay"

4.1 Introduction

Cell migration plays a crucial role in regulating many biological processes in physiological as well as pathological conditions.[1] In several situations, cells need to migrate persistently in a specific direction over long distances and in a collectively and coordinated way, such as epithelial cells in wound healing and embryo development. To date, the role of chemical cues in guiding epithelial cell migration has been extensively studied, whereas the exact function of physical signals coming from the extracellular matrix (ECM) in collective cell migration has only recently gained attention.[1-3]

At the wound boundary, many cells appear much more elongated than the others behind, acquiring a kind of mesenchymal phenotype. The so-called epithelial-mesenchymal transition (EMT) is a physiological process that causes an epithelial cell to assume mesenchymal cell properties through multiple biochemical changes.[4] Among others, this transition includes enhanced migratory capacity and invasiveness, resembling the process by which non-invasive tumor cells turn into metastatic ones. Thus, the influence of physical cues on epithelial cell behavior and the identification of the signaling pathways which lead, for example, to EMT might not only increase knowledge on epithelium mechanotransduction (i.e. the ability of cells to translate external mechanical stimuli into a biochemical response), but it might also provide new insights into the plasticity of cellular phenotypes for possible future therapeutic interventions.[5]

The study of the influence of topographical and mechanical signals on cell migration has been carried out extensively at a single-cell level, but recent studies are now approaching to the multicellular level using many microfabrication techniques.[1, 6] Soft lithography has represented a versatile tool for the cell-material manipulation at the micro-scale, e.g. through removable microstencils or 3D microwell fabrication.[7] However, the materials that are

usually implemented for this purpose are not able to reproduce *in vitro* the dynamic interplay existing *in vivo* between cells and ECM. As we have seen in previous chapters, the use of azobenzene-containing materials represents a step beyond these limitations, since azomaterials are able to modify their shape in response to external light stimuli.[8] This approach has recently been successfully implemented in cell culture applications, also in a reversible manner.[9-12]

In this Chapter, an azobenzene-functionalized molecular glass has been patterned on a large area by interference lithography in Lloyd's mirror configuration (see Chapter 1 and 2) in order to obtain a sinusoidal modulation of the material surface. This substrate has been used for studying the influence of a static regular topography on the collective migration of Madin-Darby canine kidney (MDCK) epithelial cells during wound healing. Later, a tentative identification of possible involved signaling pathways was carried out through the use of pharmacological inhibitors.

Finally, a preliminary study on the mechanotransduction and cell-cell communication via calcium signaling in MDCK cells through real-time patterning of the azomaterial has been performed.

4.2 Results and discussion.

For the study of collective migration in epithelial cells, many recent works used microfabricated substrates in order to confine cells in certain geometries and then model their behavior accordingly.[1, 7] For example, particle image velocimetry (PIV) analysis revealed that MDCK epithelial cell confluent monolayer used to migrate in a vortex-like manner, moving in circles of typically 100–150 μm in diameter, which is the natural correlation length of these cells. When MDCK cells were confined in smaller geometries, like micro-channels, such behavior disappeared.[13] Thus, from these experiments we can say that topographic cues play an important role in the collective organization

of epithelial cell migration. However, to our knowledge, the influence of focal adhesions confinement (which is known to direct cell migration at a single-cell level in many cell lines)[14-15] on epithelial cell migration in collective processes like wound healing has never been studied. Our approach aimed to fill this gap through the use of sinusoidal regular patterns on an azomaterial in an *in vitro* wound healing model. Moreover, the photoinduced mass transport, which characterizes this material, was used to give some insights into the mechanobiology of MDCK epithelial cells and their intercellular communication.

4.2.1 Samples preparation

In order to obtain linear patterns with tunable spacing and modulation depth in a highly reproducible manner, we chose a Disperse Red 1 molecular glass (DR1-glass), a recently synthesized molecule (Figure 1B).[16-17] This molecule has glass forming properties and, bearing a push/pull azobenzene on it (DR1), it allows for photoinduced mass migration at the surface by using a laser source. The light-induced mass transport phenomenon is discussed in more details in Chapter 1. This monodisperse material has photoinduced motions, which do not depend on the polydispersity of the system (differently from azopolymers), allowing for a high reproducibility of the photomechanical behavior.

As we have seen in Chapter 1 and 2, one of the optical methods to obtain large area (~cm^2) sinusoidal patterns on the surface of an azomaterial is interference lithography. In particular, when used in Lloyd's mirror configuration, it allows for the fast inscription (~ minutes) of intensity patterns.[18] This method results in the formation of a half circle of patterned area, where the pattern spacing (and consequently the modulation depth) can be easily tuned by changing the angle between the mirror and the incoming laser. In Figure 1A and C an AFM analysis of a typically inscribed pattern is reported.

In our study we needed first to understand which pattern had the greatest influence on MDCK cell behavior. So, we inscribed three patterns with different pitch: 500 nm, 1 µm and 2.8 µm, corresponding to different angles between the laser and the mirror (28°, 14° and 5°, respectively).

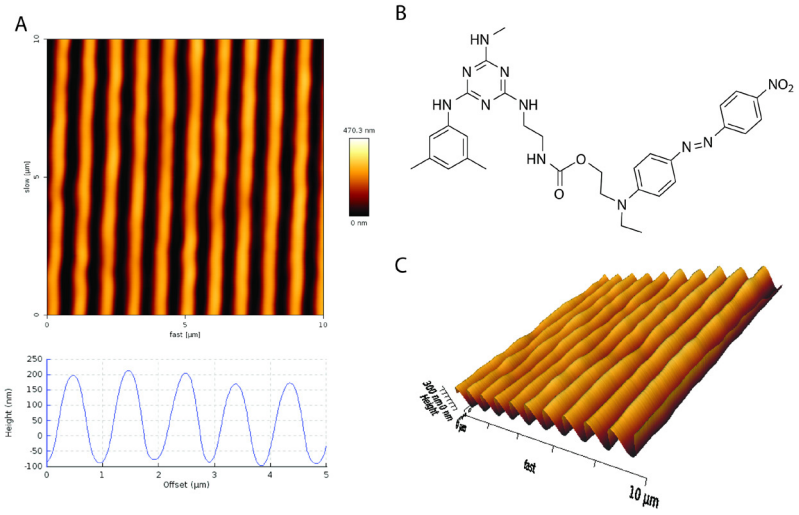

Figure 1. A) AFM analysis of the SRG topography with 1 µm pitch and its cross section. B) DR1-glass chemical structure. C) AFM micrograph 3D projection.

4.2.2 MDCK cells response to static Surface Relief Grating (SRG) topography at a single-cell level and in wound healing assay

After sterilization and collagen I coating, MDCK cells were seeded on all different samples and put inside the BioStation incubator for the migration experiment for 5 days. When epithelial cells are cultured at a single-cell level, they behave like mesenchymal cells, due to the so-called epithelial-mesenchymal transition (EMT). In this state they are more sensitive to the typical cues that influence cells during migration. In Figure 2 cell behavior after 24 hours of migration is shown. At his time point, cells were organized in isles, whose shape differed from a sample to another. In fact, it is known that the transition to a collective migration in epithelial cells depends on the density of cells.[1] This means that cell-cell contacts play a key role in collective behavior

of cells, providing a strong “mechanical coupling” and allowing biochemical signaling between neighboring cells. In Figure 2B, the influence of the 1 µm pattern on cell behavior was more visible, as cell islands acquired a more pronounced elongated shape in the pattern direction. The 2.8 µm pattern was able to induce cell orientation as well, even if in a less evident way (Figure 2C). Moreover, the migration of the cells was different. Usually, epithelial cell migration is described, adopting the physics of fluids, as a turbulent flow, where cells move in circle.[1, 7] On the patterns, as it happens at a single-cell level and in other cell lines like fibroblasts,[6, 19-20] epithelial cells were able to move along the pattern direction even in a collective directional flow, until they reached a certain cell density threshold.

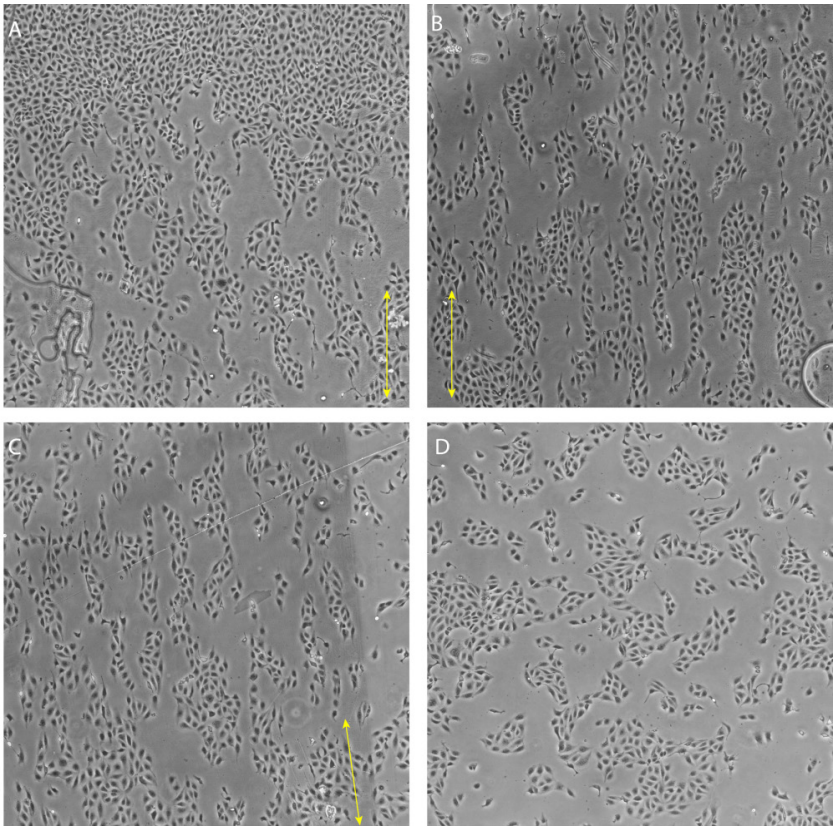

Figure 2. Bright field 4x images of MDCK during migration on patterns with different pitch. A) 500 nm, B) 1 µm, C) 2.8 µm and D) flat, respectively. Images were taken after 24 hours of migration. Yellow arrows indicate pattern direction.

After that, an *in vitro* wound healing assay was performed. Among the *in vitro* models for wound healing, the most reliable one has been introduced by Poujade et al..[21] This method used freestanding PDMS membranes with rectangular through holes (stencils). Cells were seeded in these confining wells where they reached confluence. PDMS membranes were subsequently peeled off, allowing cell monolayer to migrate in a collective fashion toward the gap. We used the described technique using PDMS slices instead of stencils in order to confine cells around the slice and create a boundary. Our set of samples was made up of three configurations: one with the slice placed along the pattern stripes (from now on it will be referred to as "parallel sample"), the second where the slice was placed orthogonally to the stripes (called "orthogonal sample") and a flat control sample (the two configurations of the patterned samples are sketched in Figure 3). After cells reached confluence, we peeled off the PDMS, thus generating a model wound *in vitro*. First, we performed a test with 2.8 μm-patterned substrates fixing them at different time points, so that we could monitor cytoskeletal organization and cell-cell junctions with high resolution. As we can clearly see from Figure 3A and B, at time zero, that is right after PDMS peeling off, both the wound boundaries of the parallel and orthogonal samples were perfectly flat, while, looking at Figure 3C and D, after 24 hours the situation changed. In fact, a great difference was visible between the parallel sample and the orthogonal one. In the former, after 24 hours the boundary was still flat, while in the latter cells at the boundary acquired a different shape, protruding lamellipodia rich of actin fibers in the pattern direction, in order to migrate along it and close the wound. This happened also to the flat control and in the flat areas of the other samples (data not shown). This observation is in agreement with the normal behavior of epithelial cells, which are able to change phenotype (EMT process) in response to a tissue injury and start migrating in order to heal.[21]

The same experiment was performed in the BioStation incubator with the 1 μm-sample, in order to follow cell migration for 6 days (Figure 4). Since the very beginning, we observed that the two patterned samples (parallel and orthogonal) were behaving in a completely different way. In fact, the migration in the parallel sample was evidently slowed down by the pattern (also if compared to the flat sample), since cells at the leading edge preferentially migrated along it, rather than across it.

On the contrary, cells on the orthogonal sample were faster and their migration was more persistent. This behavior was similar to the one observed in the flat sample, but after 6 days, the orthogonal sample presented a healed region regarding only cells above the pattern, showing that, in the exactly same conditions, the pattern speeded up the migration, or, more probably, it increased the persistency of the migration, speeding up the overall healing process. A quantification of the behavior on different patterns through PIV is ongoing.

Finally, in order to understand the signaling pathways involved in the migration aided by the topographical cues, we tested different inhibitor drugs in the migration experiment on the 1 μm sample.[2, 5] It is well-established that the cell cytoskeleton is responsible for cell stiffness level through the increased polymerization of actin fibers due to myosin activity.[22] Myosin is regulated by the phosphorylation of the myosin light chain (MLC) by the MLC kinase (MLCK), whose activity is triggered by elevated activation of the small GTPase RhoA, causing, in turn, upregulation of the activity of the RhoA-dependent kinase (ROCK).[23-24] RhoA activity can be increased by an higher engagement of integrin receptors by the formation of bigger adhesion complexes. Another signaling pathway, instead, is naturally able to counterbalance the RhoA-ROCK pathway. This pathway is generally accompanied by elevated activity of phosphatidylinositol-3-kinase (PI(3)K).

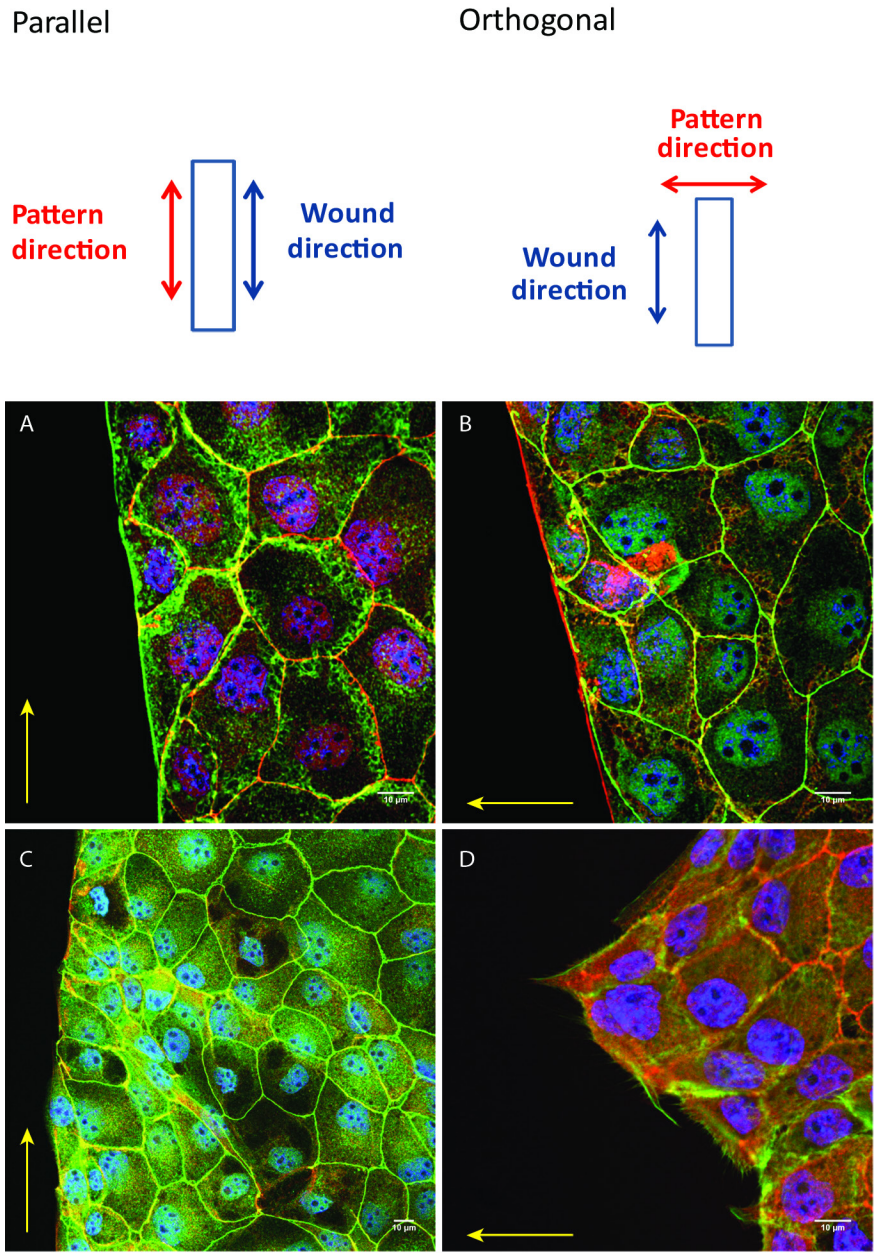

Figure 3. Confocal images of immunolabeled MDCK cells at the boundary of the wound on patterned samples (2.8 µm pitch). Tight junctions are stained in green, cytoskeleton in red, while nucleus is colored in blue. A) and C) are parallel samples, while B) and D) represent the orthogonal samples. Samples were fixed at different time points, respectively, A) and B) represent the samples right after PDMS peeling off, while C) and D) were fixed after 24 hours. Yellow arrows indicate the pattern direction. Scale bars are 10 µm.

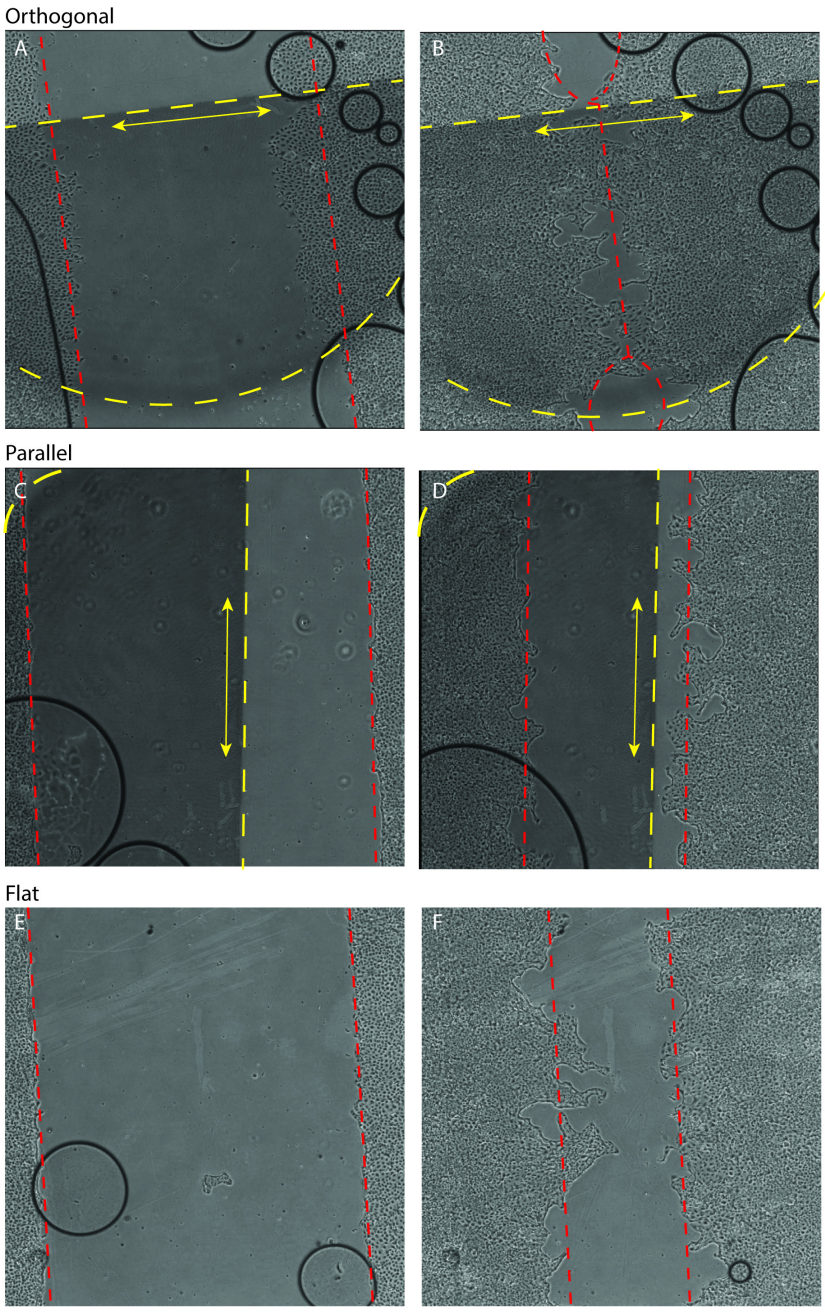

Figure 4. Bright field images (2x) of in vitro wound healing during migration on the three samples: A) and B) orthogonal, C) and D) parallel and E) and F) flat. In particular, A), C) and E) represent the in vitro wound right after PDMS slice peeling off, while B), D) and F)

represent the situation after 6 days. Yellow dashed lines delimitate the patterned area and yellow arrows highlight the pattern direction, while red dashed lines indicate qualitatively the wound boundaries.

A well-known antagonist of PI(3)K activity is PTEN (phosphatase and tensin homolog), also known for being a tumor suppressor.[25] We selectively inhibited these different pathways using Y27632, a ROCK inhibitor (Figure 5A), LY294002, a PI(3)K inhibitor (Figure 5B), and bpV(HOpic), a PTEN inhibitor (Figure 5C). Introducing in the culture medium Y27632 ROCK inhibitor, we reduced the cellular contractility. In fact, together with other molecules of this type (e.g. blebbistatin), Y27632 selectively abrogates intercellular forces leading to the impossibility of the force transmission between a cell and its neighbors. As we can see from Figure 5A, after 24 hours of migration cell isles are not elongated in the pattern direction, as it happens instead in the patterned control (Figure 5D). This behavior is even more evident if we compare Figure 5A with Figure 5B.

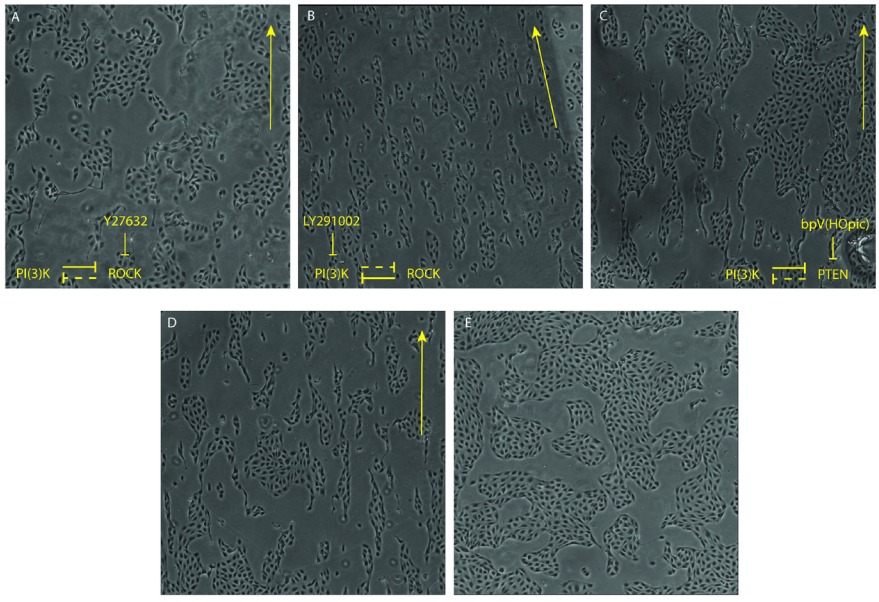

Figure 5. Bright field images (4x) of MDCK during migration on patterns with 1 μm pitch in presence of different drugs. Respectively, A) Y27632, B) LY294002, C) bpV(HOpic), D)

control sample without any drug and E) flat control sample with 1.5 µl of DMSO. The images are taken after 24 hours of migration. Yellow arrows indicate the pattern direction. Yellow lines represent the active signaling pathway, while dashed lines represent the pharmacologically inhibited pathway.

The latter represents the 24 h image of the LY294002 inhibited PI(3)K pathway. Here, an enhancement of ROCK activity occurred, resembling the single-cell behavior of MDCK cells, which prefer to individually follow the pattern. Furthermore, in this sample a decrease in cell proliferation has been detected. This observation was in good agreement with a previous report on the implication of PI(3)K signaling pathway in the control over cell proliferation.[26] Finally, knowing that PTEN is an antagonist of PI(3)K, the use of the drug bpV(HOpic) (which pharmacologically suppresses PTEN) is expected to enhance PI(3)K activity and, potentially, downregulate ROCK activity. In fact, it has been reported that ROCK is able to regulate PTEN to control cell migration.[27] ROCK downregulation by PTEN inhibition has been recently demonstrated in non-invasive melanoma cells, which have a higher basal level of PTEN with respect to invasive melanoma cells.[2] Effectively, also in MDCK cell type the pharmacological inhibition of PTEN level was able to partially suppress ROCK pathway, thus leading to a less evident capacity by the cells of following the pattern (Figure 5C).

All these observations taken together give us the evidence of a strong implication, as expected, of the ROCK signaling pathway in the mechanism of MDCK epithelial cells in EMT to sense micrometric topographical cues. In fact, on microscale topography a focal adhesion confinement is provoked.[15] Presumably, this geometrical control over adhesion complexes increased ROCK activity, upregulating the RhoA-ROCK pathway. In other words, this activity most probably increased cell stiffness through ROCK triggered actin polymerization, leading to a less compliant membrane. This behavior has been referred to as topotaxis, the mechanism by which stiffer cells (whose membrane

is less compliant) are able to adhere only on the topography ridges, while softer cells are able to isotropically spread between interstitial parts of the topography through membrane protrusions. In this way, stiffer cells are able to feel the anisotropy of the underneath topography, while softer cells perceive a patterned substrate as a flat surface, losing the contact guidance information.[2]

4.2.3 Real-time response of MDCK monolayer to topography changes

After assessing the influence of microtopography on MDCK cell migration, we wanted to understand the influence of the dynamic change in the topography over the behavior of a confluent MDCK cell monolayer. At the molecular level, the entire process of cell migration is the result of a complex dynamical equilibrium. For this reason, the real-time patterning might allow the understanding of many still unraveled aspects of the cell-ECM interaction. In fact, we exploited the photoinduced motions of DR1-glass, adapting the technique introduced in Chapter 1 and later described in more details in Chapter 3. This approach is based on the use of the focused laser beam of a confocal microscope in order to deform the azobenzene-containing material in contact with cells.[9] This surface mass-transport takes place at the interface between cells and the material, provoking a perturbation of the focal contacts, followed by a sudden reaction of the cell monolayer. In Figure 6 we can see the cell displacement in response to different movements of the laser. In particular, Figure 6 shows the experiment in which circular regions-of-interest (ROIs) were drawn and the laser movement was set to unidirectional (Figure 6A and C) and bidirectional mode (Figure 6B and D). This means that the laser is switched on only when the galvanometric mirrors go from left to right or it switches on in both directions. As we can see from Figure 6C and from the AFM analysis after cell removal (Figure 6E), an uneven distribution of material occurred upon laser scanning in the unidirectional mode, where the material piles up to the left

part of the ROI, going in the opposite direction with respect to the laser movement.

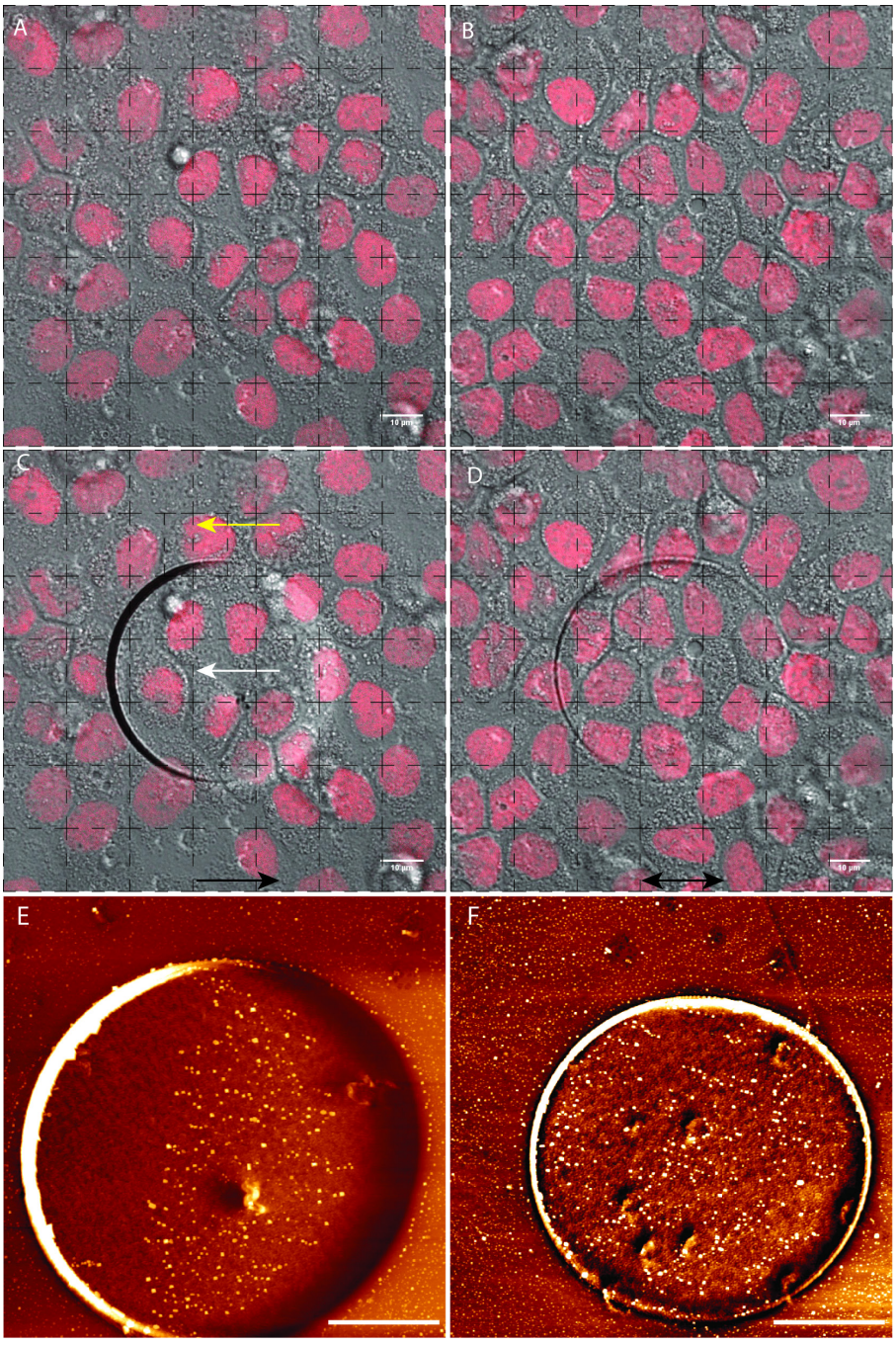

Figure 6. Real-time patterning of DR1-glass by confocal microscope. A) and B) before; C) and D) after, respectively, unidirectional movement of the laser and with a bidirectional movement

of the laser (scale bars are 10 μm). The dashed grid helps in the visualization of cell displacement inside the circular ROI. Yellow arrow shows the material displacement, while the white arrow shows cell displacement. Black arrows show the laser movement, either unidirectional (6C) or bidirectional (6D). E) and F) are the AFM micrographs of the surface after cell removal, respectively, in unidirectional and bidirectional mode.

The cell response to that perturbation was almost immediate. This indicates a fast transmission of forces from a cell to another trough cell-cell contacts. As we can see from the yellow arrows in the Figure 6C, cells moved in the direction of the material, following its displacement. Instead, when the laser movement was symmetric, i.e. the laser was always switched on inside the ROI, the material was pushed in both directions leading to the formation of a circular pile at the boundaries (Figure 6F). As we can see from Figure 6D, neither cells nor the material showed a net displacement. We hypothesized that the real-time patterning of DR1-glass had a direct effect on the focal contacts between cells and the surface with a direct implication of integrin transmembrane receptors as mechanical transducer elements. Integrins have been correlated to elevated levels of cytosolic Ca^{2+}.[28] The exact mechanism behind this feedback interaction has not yet been resolved. However, it is well-established that Ca^{2+} signaling plays an important role in mechanotransduction, either through focal adhesion complexes or by intercellular signaling. For this reason, in order to have a deeper understanding of the communication between cells during real-time patterning, we followed intracellular Ca^{2+} concentration, $[Ca^{2+}]$, with a fluorescent dye. Intercellular calcium waves (ICWs) mediate the transmission of information among cells through an increase in cytoplasmic $[Ca^{2+}]$, which spreads (generally in an isotropic manner) from an initiating or trigger cell to the neighbors.[29] This type of cell-cell communication provides the coordination and synchronization of functions of a large group of cells. ICWs are complex spatio-temporal events that involve active signal transduction within and between cells. For investigating ICWs *in vitro*, a combination of multiple

experimental approaches is needed such as real-time microscopy, molecular biology, pharmacology, and mathematical modeling. However, the relationship between *in vivo* ICWs and regulation of tissue functions is not fully understood. In 1990, a first article on the topic reported the detection of ICWs by airway epithelium in response to mechanical stimulation using an AFM tip on a single cell as a triggering event.[30] After this study, ICWs have been found to be also initiated by various stimuli in many different cell types. It is known that a cell membrane stress triggers the production of inositol 1,4,5-trisphosphate (IP_3), acting as a messenger in intercellular communication through gap junctions, while ATP is the most studied paracrine factor involved in the process. Generally, the mechanical stimulation is locally achieved by the use of a micropipette with or without plasma membrane disruption. The main disadvantage of the used method is the difficulty in the quantification of the mechanical stimulus and the associated intensity-response. Moreover, this stimulation causes tissue damage and is not able to replicate the effects of dynamic cell-ECM interactions In this work, we used the real-time patterning on DR1-glass described above as external stimulation on MDCK cell monolayer (Figure 7). In this experiment, we used wild type MDCK cells and followed intracellular [Ca^{2+}] with a fluorescent dye to study ICW in living cells during pattern inscription. We switched on the 488 nm laser in both unidirectional (Figure 7A and B) and bidirectional mode (Figure 7C and D) in the central region of the sample, drawing a circular ROI. As we described above, the laser movement over the sample from left to right was able to move the material in an uneven way. We indeed observed that in correspondence to the material pile, at a certain moment of the inscription the deformation of the material was able to start an increase in cytosolic Ca^{2+} concentration. Then, as the deformation proceeded, this event triggered the spreading of Ca^{2+} to other

cells in a wave-like manner. Moreover, the wave did not spread isotropically to neighbors, but it was able to selectively extend to cells along the ROI boundary.

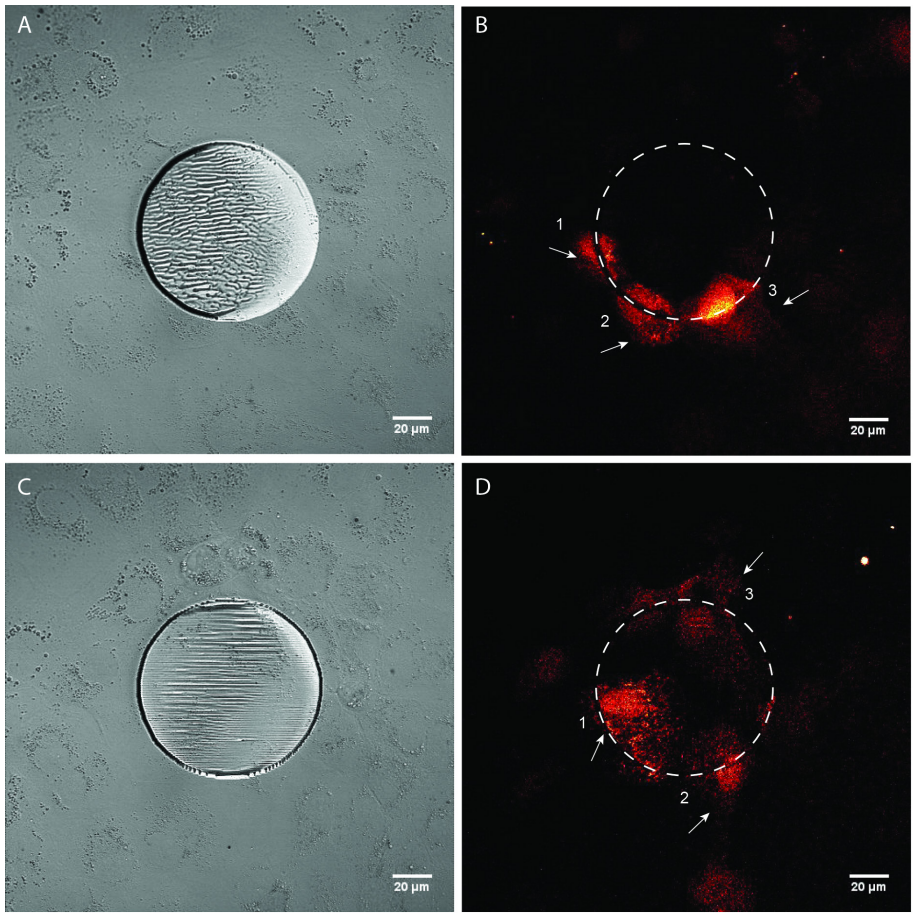

Figure 7. Ca^{2+} activity during real-time patterning visualized using laser scanning confocal microscope. A) and C) are bright field images of the sample after photopatterning, while B) and D) represent changes in cytosolic [Ca^{2+}] during the 10 minutes' time of photopatterning. This indicates the propagating [Ca^{2+}] wave from one cell to the neighbor along the circular border. The white dashed circle represents the ROI, while white numbers and arrows indicate the order of appearance of the fluorescent signal of the Ca^{2+} ions.

This observation could be an evidence of the fact that, in our case, the increase in [Ca^{2+}] was activated by stretch-activated ion channels with integrins acting as mechanotranducers. In fact, intracellular Ca^{2+} levels are frequently elevated by release from intracellular reservoirs via a molecular pathway which involves Phosphatidylinositol 4,5-bisphosphate (PIP_2) hydrolysis and the generation of

IP_3. PIP_2 levels are elevated by adhesion in a Rho-dependent manner, confirming the results shown in the previous section. Furthermore, an IP3 exchange via gap junctions might be involved in the communication mechanism as well.

4.3 Conclusions

In this Chapter we have seen how topographic signals play a major role in epithelial cell mechanotransduction. In particular, in the first part of the work, the use of the static sinusoidal surface modulation of photoinscribed SRG on collective migration of MDCK epithelial cells has been investigated, revealing that the pattern with 1 μm pitch was the most efficient in aligning and directing cell migration until confluence was reached. This means that the topography has a prominent role in defining the migration of MDCK cells when they assume the mesenchymal phenotype due to the EMT. For this reason, in *in vitro* wound healing essay a topography which "links" the wound boundaries (orthogonal sample) is able to speed up the migration process by increasing the persistency of cell trajectories.

In the second part of this Chapter, instead, the photopatterning ability of DR1-glass has been exploited as an original tool for the concurrent induction and observation of MDCK monolayer stress-related responses in terms of displacement and topography-dependent activation of Ca^{2+} signaling in real-time.

4.4 Experimental section

4.4.1 Substrate preparation by spin coating and photopatterning

Square glass coverslips were washed in acetone, isopropyl alcohol and water in an ultrasonicating bath for 10 min each time, and then dried under a fume hood prior to the spin coating process. Disperse Red 1 molecular glass (DR1-glass,

Solaris Chem. Inc.) was dissolved in chloroform at a concentration of 5% (w/v). The solution was spun over the cover glass by using a Laurell spin coater (Laurell Technologies Corp.) at 1500 rpm for 30 seconds. Samples were patterned either with the interference lithography technique, or in real-time using the focused beam of a confocal microscope. An optically pumped semiconductor laser (OPSL) with continuous wave (CW) output of 488 nm with 2 W maximum output power (Coherent Genesis CX488-2000) (working intensity of 93±1 mW/cm^2) was used in a Lloyd's mirror configuration with circular polarization to project an interference pattern of light on the azopolymer films, thus inducing mass migration and SRG formation. In more details, in interference lithography the laser operates with single longitudinal mode (SLM). The azopolymer sample was glued to one of the mirror's edge and the circularly polarized laser beam was reflected on it, thus realizing an interference pattern of light. The pattern pitch was given by $d = \frac{\lambda}{2 \sin \vartheta}$, where λ is the laser wavelength and ϑ is the angle between the incident beam and the mirror. By varying ϑ, patterns with different pitch could be easily prepared. For the real-time patterning an LSM-780 (Carl Zeiss GmbH) was used (60x objective) in bleaching mode using a 488 nm laser line at 100% power to modify the material in the selected regions-of-interest (ROIs). Rectangular ROIs were drawn directly underneath the cell monolayer either in unidirectional or in bidirectional scanning mode.

4.4.2 AFM characterization

A JPK NanoWizard II (JPK Instruments), mounted on the stage of an Axio Observer Z1 microscope (Zeiss), was used to characterize the azopolymer films. For imaging of SRG patterned sample, a silicon nitride tip (MLCT, Bruker) with a spring constant of 0.01 N/m was used in contact mode, in air at room temperature, while, for imaging the sample patterned in real-time after

cell removal by trypsinization we used a PNP DB (Pyrex-nitride probes, Nanotech) with a spring constant of 0.48 N/m in contact mode, in air at room temperature.

4.4.3 Cell culture and immunolabeling

Madin-Darby canine kindney (MDCK) epithelial cells were cultured in MEM GlutaMax® supplemented with 10% FBS and 1% Pen/Strep, while MDCK H2B-mCherry medium was supplemented with 0.5 mg/ml geneticin (G418). They were incubated at 37 °C in a humidified atmosphere of 95% air and 5% CO_2. Prior to cell seeding, DR1-glass substrates were sterilized under UV light for 30 min. and collagen coated with a solution of 50 μg/ml of collagen I in acetic acid 0.02N for 30 minutes. At the end of the experiments, cells were fixed with 4% paraformaldehyde for 15 min, permeabilized with 0.1% Triton X-100 in PBS for 15 min and then immunolabeled with anti-ZO-1 and anti-mouse Alexa-561-linked secondary antibody for the tight junction, Alexa-647-phalloidin for the cytoskeleton and DAPI for nuclei. For wound healing experiments, PDMS slices (1:10 w/w, curing agent: Sylgard 184 pre-polymer) of about 0.3 x 1.5 cm each were cut in sterile conditions and placed on the substrates either along the pattern direction or orthogonally to it (in case of patterned samples).

4.4.4 Migration experiments

MDCK migration experiments were carried out using Nikon BioStation CT. Samples were fixed to the bottom of a 6-well plate by using small 1:20 w/w PDMS drops to avoid sample movement during imaging. In case of wound healing experiments PDMS slices were peeled off under laminar flow and straight after that the 6-well plate was put inside the microscope holder and incubated for 1 hour prior starting the experiment for equilibration. Images were taken every 20 minutes for 5-6 days without medium change.

4.4.5 Drugs inhibition experiment

For the perturbation of the signaling pathway related to cell migration, working concentrations of 5 μM Y27632, 10 μM LY294002 and 100 nM bpV(HOpic) were reached in the culture medium (2 ml) before the migration experiment. Samples were left inside BioStation incubator for 1 hour before starting the experiment for temperature equilibration.

4.4.6 Ca^{2+} staining

In order to follow intracellular fluctuations in calcium concentration, [Ca^{2+}], Rhod-3 Calcium Imaging Kit was used. First, we dissolved the content of one vial of Probenecid in 1 ml of HEPES buffered Hank's Balanced Salt Solution (HBSS) to prepare 250 mM Probenecid stock solution. Then, we prepared the buffers as follows. The loading buffer was made up of HEPES buffered HBSS containing 2.5 mM Probenecid, 20 μl of 100X PowerLoad™, and 10 μM Rhod-3 AM. The incubation buffer was composed by HEPES buffered HBSS containing 2.5 mM Probenecid. HBSS alone was used for washing steps. After medium removal from adherent cells, they were washed twice in HBSS. Then, 1 ml of loading buffer was added to cells and they were incubated in the dark at room temperature for 45 minutes. After incubation, cells were washed twice with HBSS. 1 ml of incubation buffer was added to cells, which were incubated again at room temperature in the dark for 45 minutes. Finally, before live imaging, cells were washed once in HBSS and an imaging buffer was added (HEPES buffered HBSS containing 1% FBS, 1.3 mM $CaCl_2$ and 0.5 mM $MgCl_2$).

4.5 References

1. Vedula, S. R. K.; Ravasio, A.; Lim, C. T.; Ladoux, B., Collective cell migration: a mechanistic perspective. *Physiology* **2013,** *28* (6), 370-379.
2. Park, J.; Kim, D.-H.; Kim, H.-N.; Wang, C. J.; Kwak, M. K.; Hur, E.; Suh, K.-Y.; An, S. S.; Levchenko, A., Directed migration of cancer cells guided by the graded texture of the underlying matrix. *Nature materials* **2016,** *15*, 792-801.
3. Wu, T.-H.; Li, C.-H.; Tang, M.-J.; Liang, J.-I.; Chen, C.-H.; Yeh, M.-L., Migration speed and directionality switch of normal epithelial cells after TGF-β1-induced EMT (tEMT) on micro-structured polydimethylsiloxane (PDMS) substrates with variations in stiffness and topographic patterning. *Cell communication & adhesion* **2013,** *20* (5), 115-126.
4. Kalluri, R.; Weinberg, R. A., The basics of epithelial-mesenchymal transition. *The Journal of clinical investigation* **2009,** *119* (6), 1420-1428.
5. Das, T.; Safferling, K.; Rausch, S.; Grabe, N.; Boehm, H.; Spatz, J. P., A molecular mechanotransduction pathway regulates collective migration of epithelial cells. *Nature cell biology* **2015,** *17* (3), 276-287.
6. Teixeira, A. I.; Abrams, G. A.; Bertics, P. J.; Murphy, C. J.; Nealey, P. F., Epithelial contact guidance on well-defined micro-and nanostructured substrates. *Journal of cell science* **2003,** *116* (10), 1881-1892.
7. Zorn, M. L.; Marel, A.-K.; Segerer, F. J.; Rädler, J. O., Phenomenological approaches to collective behavior in epithelial cell migration. *Biochimica et Biophysica Acta (BBA)-Molecular Cell Research* **2015,** *1853* (11), 3143-3152.
8. Mahimwalla, Z.; Yager, K. G.; Mamiya, J.-i.; Shishido, A.; Priimagi, A.; Barrett, C. J., Azobenzene photomechanics: prospects and potential applications. *Polymer bulletin* **2012,** *69* (8), 967-1006.
9. Rianna, C.; Rossano, L.; Kollarigowda, R. H.; Formiggini, F.; Cavalli, S.; Ventre, M.; Netti, P. A., Spatio-Temporal Control of Dynamic Topographic Patterns on Azopolymers for Cell Culture Applications. *Advanced Functional Materials* **2016,** *26* (42), 7572-7580.
10. Hurduc, N.; Macovei, A.; Paius, C.; Raicu, A.; Moleavin, I.; Branza-Nichita, N.; Hamel, M.; Rocha, L., Azo-polysiloxanes as new supports for cell cultures. *Mater. Sci. Eng., C* **2013,** *33* (4), 2440-2445.
11. Barille, R.; Janik, R.; Kucharskic, S.; Eyer, J.; Letournel, F., Photo-responsive polymer with erasable and reconfigurable micro- and nano-patterns: An in vitro study for neuron guidance. *Colloids Surf., B* **2011,** *88*, 63-71.
12. Baac, H.; Lee, J.-H.; Seo, J.-M.; Park, T. H.; Chung, H.; Lee, S.-D.; Kim, S. J., Submicron-scale topographical control of cell growth using holographic surface relief grating. *Mater. Sci. Eng. C Mater. Biol. Appl.* **2004,** *24* (1-2), 209-212.

13. Vedula, S. R. K.; Leong, M. C.; Lai, T. L.; Hersen, P.; Kabla, A. J.; Lim, C. T.; Ladoux, B., Emerging modes of collective cell migration induced by geometrical constraints. *Proceedings of the National Academy of Sciences* **2012,** *109* (32), 12974-12979.
14. Bettinger, C. J.; Langer, R.; Borenstein, J. T., Engineering substrate topography at the micro-and nanoscale to control cell function. *Angewandte Chemie International Edition* **2009,** *48* (30), 5406-5415.
15. Ventre, M.; Natale, C. F.; Rianna, C.; Netti, P. A., Topographic cell instructive patterns to control cell adhesion, polarization and migration. *Journal of the royal society Interface* **2014,** *11* (100), 20140687.
16. Bennani, O. R.; Al-Hujran, T. A.; Nunzi, J.-M.; Sabat, R. G.; Lebel, O., Surface relief grating growth in thin films of mexylaminotriazine-functionalized glass-forming azobenzene derivatives. *New Journal of Chemistry* **2015,** *39* (12), 9162-9170.
17. Kirby, R.; Sabat, R. G.; Nunzi, J.-M.; Lebel, O., Disperse and disordered: a mexylaminotriazine-substituted azobenzene derivative with superior glass and surface relief grating formation. *Journal of Materials Chemistry C* **2014,** *2* (5), 841-847.
18. Priimagi, A.; Shevchenko, A., Azopolymer-based micro-and nanopatterning for photonic applications. *Journal of Polymer Science Part B: Polymer Physics* **2014,** *52* (3), 163-182.
19. Chun Leong, M.; Sri Ram Krishna, V.; Teck Lim, C.; Ladoux, B., Geometrical constraints and physical crowding direct collective migration of fibroblasts. *Communicative & integrative biology* **2013,** *6* (2), e23197.
20. Flemming, R.; Murphy, C. J.; Abrams, G.; Goodman, S.; Nealey, P., Effects of synthetic micro-and nano-structured surfaces on cell behavior. *Biomaterials* **1999,** *20* (6), 573-588.
21. Poujade, M.; Grasland-Mongrain, E.; Hertzog, A.; Jouanneau, J.; Chavrier, P.; Ladoux, B.; Buguin, A.; Silberzan, P., Collective migration of an epithelial monolayer in response to a model wound. *Proceedings of the National Academy of Sciences* **2007,** *104* (41), 15988-15993.
22. An, S. S.; Laudadio, R. E.; Lai, J.; Rogers, R. A.; Fredberg, J. J., Stiffness changes in cultured airway smooth muscle cells. *American Journal of Physiology-Cell Physiology* **2002,** *283* (3), C792-C801.
23. Wettschureck, N.; Offermanns, S., Rho/Rho-kinase mediated signaling in physiology and pathophysiology. *Journal of molecular medicine* **2002,** *80* (10), 629-638.
24. Riento, K.; Ridley, A. J., Rocks: multifunctional kinases in cell behaviour. *Nature reviews Molecular cell biology* **2003,** *4* (6), 446-456.
25. Hopkin, K., A surprising function for the PTEN tumor suppressor. *Science* **1998,** *282* (5391), 1027-1030.

26. Yang, S.; Kim, H.-M., The RhoA-ROCK-PTEN pathway as a molecular switch for anchorage dependent cell behavior. *Biomaterials* **2012,** *33* (10), 2902-2915.
27. Li, Z.; Dong, X.; Wang, Z.; Liu, W.; Deng, N.; Ding, Y.; Tang, L.; Hla, T.; Zeng, R.; Li, L., Regulation of PTEN by Rho small GTPases. *Nature cell biology* **2005,** *7* (4), 399-404.
28. Pelletier, A.; Bodary, S.; Levinson, A., Signal transduction by the platelet integrin alpha IIb beta 3: induction of calcium oscillations required for protein-tyrosine phosphorylation and ligand-induced spreading of stably transfected cells. *Molecular biology of the cell* **1992,** *3* (9), 989-998.
29. Leybaert, L.; Sanderson, M. J., Intercellular Ca2+ waves: mechanisms and function. *Physiological reviews* **2012,** *92* (3), 1359-1392.
30. Sanderson, M. J.; Charles, A.; Dirksen, E. R., Mechanical stimulation and intercellular communication increases intracellular Ca2+ in epithelial cells. *Cell regulation* **1990,** *1* (8), 585-596.

Chapter 5

Design of azobenzene-containing gelatin photoresist for the realization of photoactuable 3D smart structures for cell culture applications*

Abstract. The ability to trigger morphological and mechanical responses in hydrogel systems implies the spatio-temporal control over material properties at the molecular scale. Using light-responsive reactions in hydrogels, such as azobenzene photoisomerization, represents a smart approach for improving our understanding on how cells interact with a changing microenvironment. In this Chapter, two-photon polymerization was used as microfabrication technique of a custom photoresist made up of a chemically modified gelatin and a synthesized azobenzene crosslinker. This photoswitch conferred to the final hydrogel photoresponsive properties, which were able to produce an in plane deformation of NIH-3T3 cell nuclei. This proof of concept experiment paves the way to future mechanotransduction studies in a 3D environment, going from static to dynamic intelligent materials for cell culture applications.

*The work described in this Chapter is part of a manuscript in preparation. F. A. Pennacchio, C. Fedele, S. Cavalli, R. Vecchione, P. A. Netti. "Design of azobenzene-containing gelatin photoresist for photoactuable 3D smart structures for cell culture". (First two authors contributed equally to the entire work.).[§]

5.1 Introduction

The ideal platform for the *in vitro* study of cellular response to varying physiological-like conditions would include the fabrication of tridimensional structured platforms that are able, at the same time, to deliver biochemical, topographical and mechanical cues with a fine spatio-temporal control.[1-2] In order to unravel the complex mechanisms at the basis of cell-material interaction, many reports in the literature make use of advanced microfabrication techniques to structure both synthetic and nature-derived materials in complex 3D architectures and with "smart" functionalities. In particular, a great attention is taken by hydrogels, three-dimensional polymeric networks with a strong hydrophilicity that are able to mimic the mechanical properties of natural tissues. However, the fabrication of biologically relevant tridimensional structures bearing the necessary chemical cues for cell growth still remains challenging. In this respect, two-photon polymerization (2PP) lithography represents a valid technique for the 3D microfabrication of biocompatible scaffolds taking advantage of photopolymerization and photocrosslinking reactions of many different mixtures (photoresists), leaving the possibility to use functional customized materials widely open. Moreover, to introduce a spatio-temporal control over cell-material interaction, nowadays actuating hydrogels are employed. These systems are able to respond to many different external stimuli, such as pH, temperature,[3] electrical and magnetic fields,[4-5] enzymes[6] and light.[7] The latter can be based either on, for example, light-to-heat conversion,[8-9] or on the isomerization of azobenzene moieties,[10] or, finally, on the presence of photocleavable groups.[11] Recently, 2PP has also been used for the miniaturization of photoactuable liquid crystalline elastomers (LCEs) based on azobenzenes for various technological applications, e.g. soft robotics. This approach resulted in a successful maintenance of the liquid

crystalline order inside the polymerized structures, scaling down to the microscale the photoinduced shape changes of azobenzene-containing LCEs.[12-13] However, this miniaturization in a biocompatible environment still represents a difficult task in the field of photoresponsive hydrogels.

In this work, the combination of the hydrogel chemical and mechanical characteristics with light-responsiveness in 3D complex structures is proposed, through the design of an acrylamide-modified gelatin containing azobenzene-based crosslinkers. This collagen-derived material already includes the biochemical signals for cell recognition as well as the functional groups (acrylamides) for a radical crosslinking polymerization to take place. In fact, 2PP simplifies the processability of this hydrogel, which is characterized by a sol-gel transition in the physiological temperature range. First of all, the chemical modification of gelatin is presented, in order to allow a 2PP processing. Then, the photoresist design is shown, including the synthesis and characterization of an azobenzene-based crosslinker, which provides light-responsive properties to the final material. Finally, the application of an array of simple squared structures in single-cell confinement is proposed, as well as their capability to deform cell nuclei upon light stimulus.

5.2 Results and discussion

5.2.1 Photoresist preparation

Gelatin is a natural material derived from the denaturation of collagen I. This proteic polymer is inherently biocompatible and it already contains the chemical cues necessary for cell recognition and remodeling of the extracellular matrix. This is a great advantage in the general field of biomaterials, as well as in our case, for the construction of cell culture substrates, which need to interact with cells and support their growth.[14] Gelatin hydrogel shows a gel-to-sol transition temperature at 37 °C, which makes it not usable in physiological

conditions and thus it is necessary to crosslink it. Among crosslinking strategies, we chose two-photon polymerization (2PP) for its potential in the fabrication of complex 3D structures. This technique is performed by scanning a focused laser beam into a photopolymerizable mixture, generally from the bottom to the top surface. Inside the focal volume, a photochemical reaction occurs, which converts a liquid into an insoluble polymer or gel. Actually, this technique is still under development; in fact, nowadays it includes many different light-triggered reactions regarding not only polymerization or crosslinking processes, but also, for example, local functionalization and cleavage. A suitable mixture for photopolymerization usually consists of three basic components. First of all, a light-sensitive molecule, the photoinitiator (PI), is needed, which is able to produce active species upon photon absorption at a specific wavelength and initiates the polymerization reaction. Then, the use of functionalized oligomer or pre-polymer backbone is preferred, and, finally, the presence of mono- or multifunctional monomers, which integrate inside the polymer network, is used to contribute to final material properties. In the process of 2PP, PI molecules exposed at a high intensity laser undergo the absorption of two photons (above a certain intensity threshold) mediated by a virtual state that allows the access to an excited triplet state.[15] The absorption of two photons shows a non linear (quadratic) dependence to the intensity, resulting in a highly localized excitation and thus a potentially highly resolved polymerization.[16] The laser is usually in the near infrared region, range in which materials are generally transparent, allowing for a deeper penetration depth with a negligible power loss. These characteristics of 2PP result in the creation of very complex tridimensional structures, just by laser scanning.

Based on the above discussion, we formulated our photoresist mixture as follows: a PI widely used in 2PP (Irgacure 369), a chemically modified gelatin, and, finally, an azobenzene-based bisacrylamide molecule used as crosslinker.

Following an approach recently reported in the literature for gelatin,[17] we modified the amines in side chain of lysine into acrylamide groups in order to obtain a 3D printable material, as confirmed by NMR spectroscopy (Figure 1).

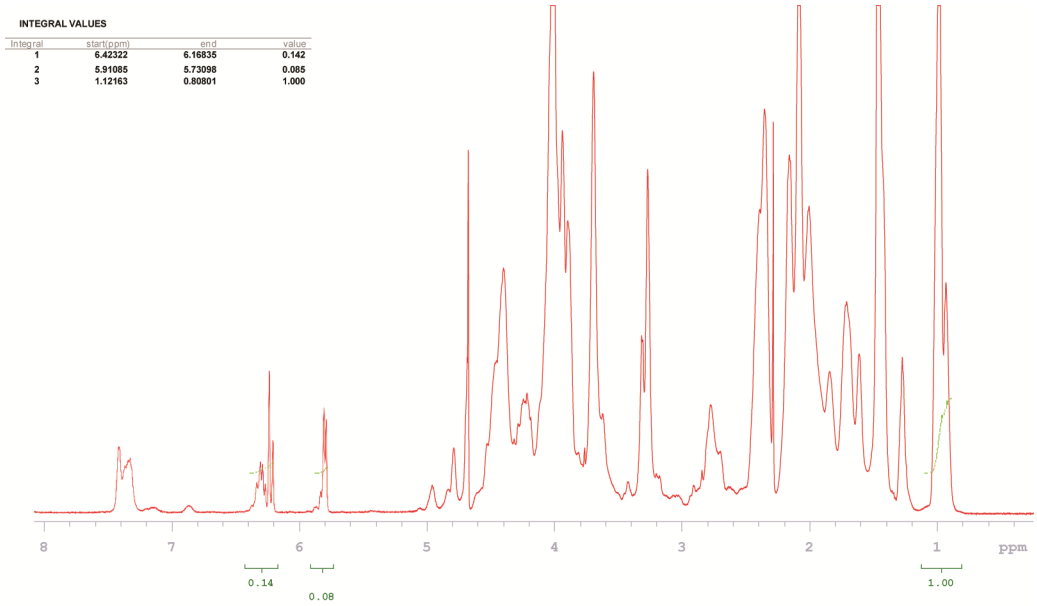

Figure 1. ^{1}H NMR spectrum of modified gelatin.

The presence of two peaks at 5.83 ppm and at 6.25 ppm indicate the success of the reaction since they are relative to the acrylic groups. The methyl signals (at 1.2 ppm) of Val, Ile, and Leu can be used as an internal standard in the ^{1}H NMR spectrum of the gelatin because can be considered chemically inert. This functionalization can be quantified by integrating and dividing the peak at 5.83 ppm with the peak relative to the methyl signals at 1.2 ppm. We optimized the reaction conditions so that this ratio was maximized to the value reported in Figure 1 (0.08). Applying the calculations reported in the literature,[17] we can define a theoretical degree of substitution of free amines as:

$$DS = \frac{0.3699\ mol}{100\ g} * \frac{integration\ at\ 5.83\ ppm}{integration\ at\ 1.12\ ppm} * \frac{100}{0.03798\ mol/100\ g}$$

Where 0.3699 mol is the quantity of Val, Ile, Leu and 0.03798 mol the amount of Lys in 100 g of gelatin as reported in the literature by amino acids analysis.[17]

This calculation gives a theoretical degree of substitution of 83%.

These functionalities allowed for a radical polymerization to take place. In particular, choosing a suitable photoinitiator (Irgacure 369), we were able to start a photopolymerization in the focal volume of the laser of our 2PP system, which works at 780 nm (Photonic professional GT, Nanoscribe).

The azobenzene-based bisacrylamide crosslinker was synthesized as described in Scheme 1A.

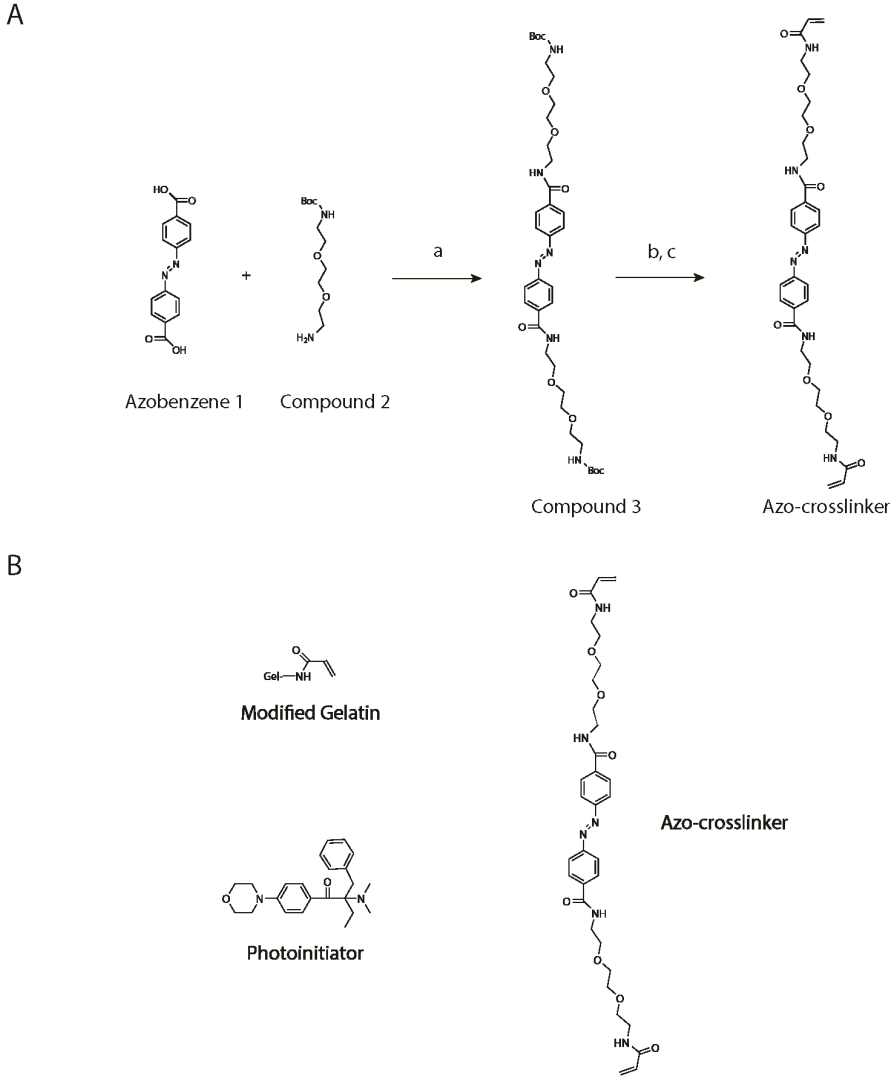

Scheme 1. A) Synthetic scheme of Azo-crosslinker. Reaction conditions: a) 0.111 mmol of azobenzene 1, 4.8 equiv. of TEA, 2.4 equiv. of HOBt·H_2O, 2.4 equiv. EDC·HCl and 2.4 equiv.

of compound 2, overnight at room temperature. b) TFA/CH_2Cl_2 50/50 v/v for 2 hours to remove the Boc protecting group. After the reaction, the product was treated with TEA and co-evaporated with toluene. c) Boc-deprotected compound 3 was reacted with 2.4 equiv. of acrylic acid, 2.4 equiv. of HOBt·H_2O, 2.4 equiv. of EDC·HCl and 4.8 equiv. of TEA overnight at room temperature. B) Chemical structures of the mixture components: acrylamide-modified gelatin, Irgacure 369 as photoinitiator, and in-house synthesized azo-crosslinker.

This short crosslinker gave us the opportunity to add a further functionality to the final structure. In fact, as also reported elsewhere,[18] a photoswitching crosslinker is able to alter the morphological and mechanical properties of the entire polymer matrix through its isomerization upon illumination.[19-20] The choice of an azobenzene-type crosslinker is generally crucial for the stability of the deformations which needs to be compatible with typical timing used in cell culture practices.[18] In fact, we chose a photoswitch, which isomerizes in solution in about 25 minutes of illumination with a UV laboratory lamp (1.2 $mWcm^{-2}$ of diffused light) and in 1 minute by focusing the light of a mercury lamp (filtered for blue light) with a 10x objective. The illuminated mixture was able to back-isomerize in more than three days in the dark. Figure 2 shows the UV/Vis absorption spectra of the azo-crosslinker in solution subjected to a progressive illumination with UV light. Moreover, the UV/Vis spectra show almost zero absorption at the wavelength that is related to the focal volume of the two-photon polymerization system (indicated by the grey dashed arrow in Figure 2) showing the suitability of this crosslinker in our Nanoscribe system.
As also reported in the legend, the black line shows the absorption spectrum of the *trans* isomer, while the other colored lines represent the spectra of the mixture subjected to increasing illumination time with a UV lamp at 356 nm (from 1 minute to 25 minutes in total). As expected, these spectra show a progressive decrease in absorption of the *trans* $\pi \rightarrow \pi^*$ band centered at 331 nm, together with a complementary increase in absorption of the $n \rightarrow \pi^*$ band of the *cis* isomer centered at 420 nm.

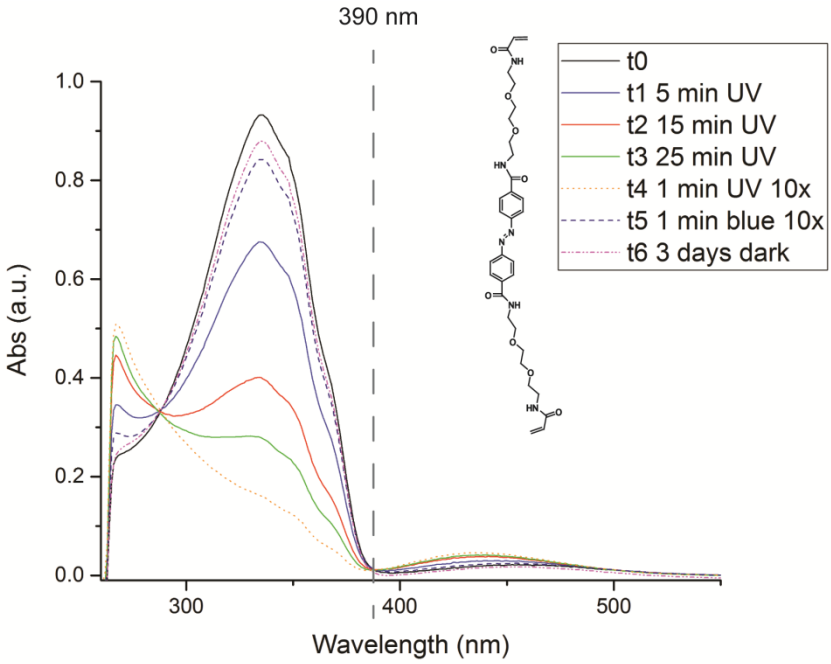

Figure 2. UV/Vis absorption spectra of Azo-crosslinker in DMF in different illumination conditions. The dashed light gray line indicates the molecule absorption at the wavelength (390 nm) of the focal volume of the two-photon polymerization system. In the legend "UV" indicates the diffused light of a laboratory lamp at 365 nm, while "UV 10x" stays for the light of a mercury lamp focused by a 10x objective and filtered in the UV region. Finally, "blue 10x" represents the same light source filtered in the blue region.

The light-induced back-isomerizaton in solution was achieved up to the formation of a photostationary state in 1 minute of photostimulation with a halo lamp filtered for blue light and focused with a 10x objective. However, when incorporated in a polymeric network, the *trans-cis* isomerization kinetics of the material might be different, as well as the *cis-trans* back-isomerization.

5.2.2 Structures characterization

The photoresist mixture was composed by 20% w/v acrylamide-modified gelatin chains, 4% w/w (with respect to gelatin) of the azo-crosslinker and 3% w/w of Irgacure 369 as PI dissolved in a citrate buffer, as we can see in Scheme 1B. These mixture elements were, thus, able to start a radical polymerization

when illuminated with UV light, leading to a final polymer network where the azo-crosslinker integrated in the gelatin matrix. In this way, the mechanical properties of the polymerized material were in the range of typical hydrogels for biological application (elastic modulus of 6.55 ± 0.45 kPa) as confirmed by AFM nanoindentation analysis (Figure 4C).[21] Moreover, an advantage from a microfabricative point of view lies in the fact that the inscription process occurs when the material is in the gel state, eventually allowing for an easier construction of free standing structures. In fact, gelatin is well known to be a difficult material to manipulate, due to its sol-gel properties, which translate into difficult processability with many microfabrication techniques.[22] In our approach, the use of 2PP avoided gelatin processing problems, obtaining the polymerization in complex structures with a good resolution (Figure 3).

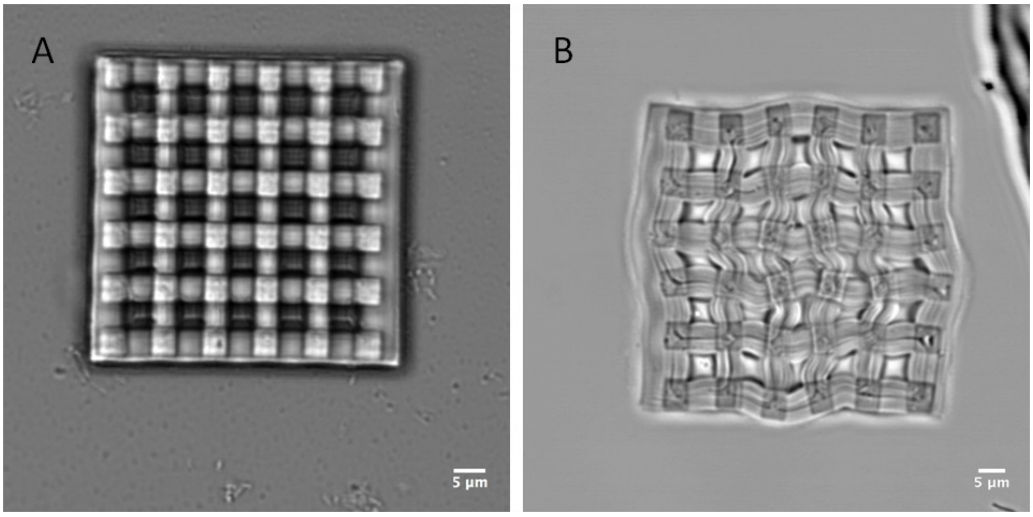

Figure 3. Bright field image of a complex structure obtained with the same writing parameters A) with and B) without azo-crosslinker in the photoresist mixture.

After photopolymerization, the produced gelatin structures could be deformed by the use of a laser light, owing to the presence of the azobenzene. It is already known, in fact, that azobenzenes inside polymeric networks are able to control some mechanical properties, such as the swelling ratio.[18] When isomerizes, the azobenzene molecule undergoes a geometric modification from the linear *trans*

isomer to the bent *cis* one, which affects also its dipole moment.[23-24] Therefore, this conformational change is reasonably supposed to affect gel mechanics and shape. However, the exact prediction of mechanical properties and shape variations that may occur in response to light is not so straightforward. The light-dependent mechanical properties of azopolymer films have been extensively studied, but in the literature only few studies about the characterization of azopolymer hydrogels are present, reporting different photomechanical behaviors. For example, Hosono et al. observed a shrinking accompanied by an increase in storage modulus in an azobenzene-containing poly(amide acid) gel upon light stimulus.[25] Rosales et al., instead, reported on a decrease in elastic modulus upon photostimulation in branched PEG-azobenzene hydrogel.[18] In addition, other studies observed gel−sol transitions upon photostimulation in azobenzene-containing supramolecular systems because photoisomerization was believed to disrupt hydrogen bonds inside the polymeric network.[10] All these reported behaviors strongly depend on the molecular architecture of the material and on the chemical species involved. However, a complete understanding of the hydrogel properties was beyond the scope of this study. Our aim, instead, was the realization of actuating hydrogel structures for the mechanical stimulation of cells at a single cell level, for example, for future advanced studies on the effect of mechanical signals on cell behavior. As proof of concept, we decided to start from simple squared structures (30 x 30 x 10 μm^3) whose photoinduced response was investigated using a multiphoton (MP) laser tuned at 700 nm (in order to excite the azobenzene isomerization at 350 nm). With the use of this source we were able to precisely localize the MP absorption in order to set the experimental conditions for further biological studies. In fact, since UV light is known to be harmful for cells, this method minimized cytotoxic effects, while maximizing the light penetration depth. The photostimulation with MP at a fixed z position

for 10 minutes translated into an expansion of the structures in x and y of about 10%, as shown in Figure 4A and B.

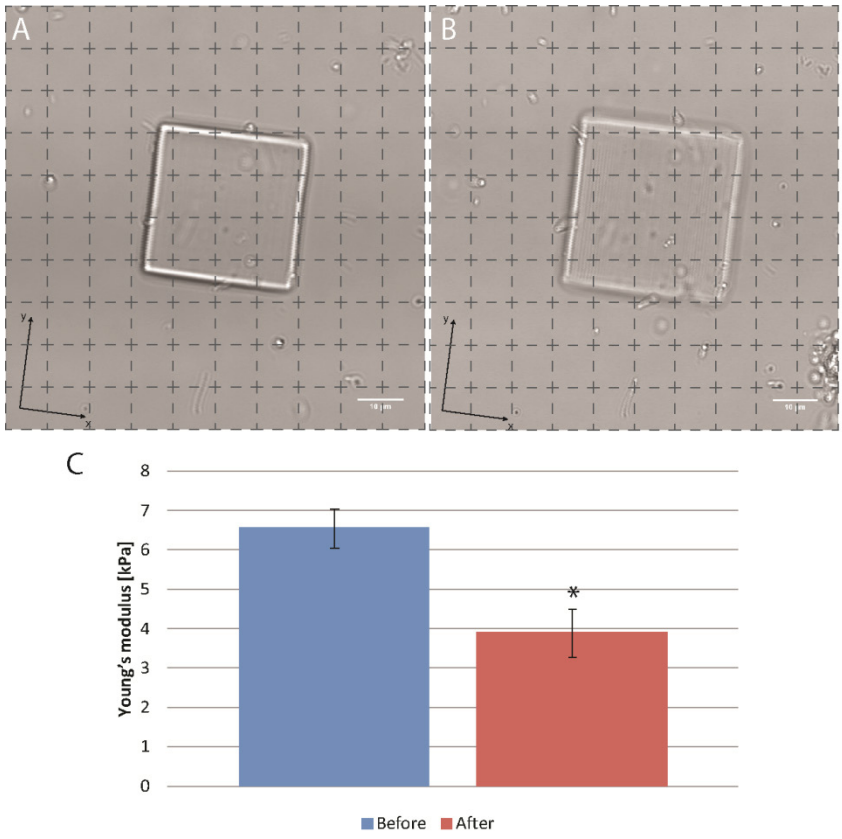

Figure 4. Deformation of the gelatin squared structures upon MP illumination at 700 nm for 10 minutes. A) Before illumination and B) after illumination. As shown in figure, aided by the grid, the illuminated structure increased its x and y dimensions. Scale bars are 10 µm. C) Young's modulus calculated by AFM force mapping on the squared structures before and after illumination at MP. Asterisk indicates statistically significant

Moreover, the shape change under UV light corresponded to a decrease in the elastic modulus (3.89 ± 0.6 kPa) immediately after the stimulation, as detected by AFM force spectroscopy analysis (Figure 4C). As of now, we might speculate that the decrease in elastic modulus was due to an increase of hydrophilicity of the hydrogels upon *trans-cis* isomerization. This shape change was not observed, instead, when the structures were stimulated with other light

sources where the azobenzene has no absorption (633 nm one-photon source or 780 nm two-photon absorption) as visible in Figure 5. Further investigations on the mechanical behavior of the material upon illumination are ongoing.

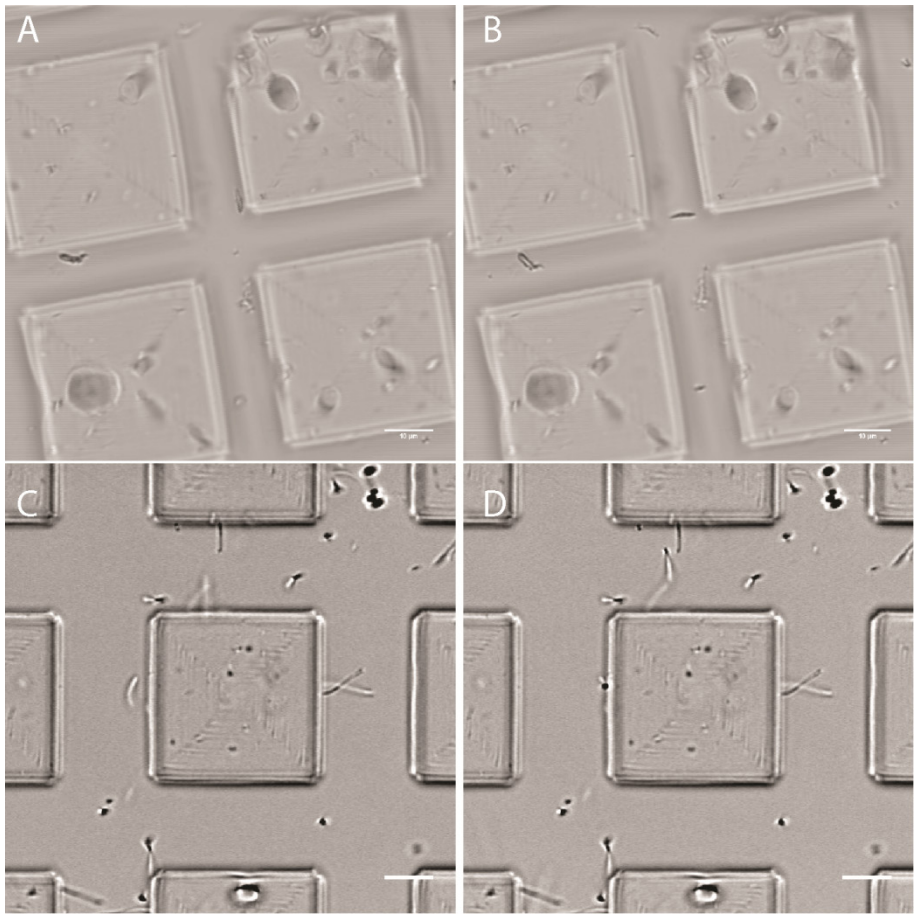

Figure 5. Negative control for photostimulation. Squared structures A) before and B) after a stimulation at 633 nm (100% power). Squared structures C) before and D) after a photostimulation with 780 nm (two-photon absorption). In both cases, as expected, no deformation occurred. Scale bars are 10 μm.

Usually, the deformations induced by azobenezene photoisomerization inside a polymer matrix are fully reversible. Actually, we were not able to induce a shape recovery upon photostimulation in the absorption range of the *cis* isomer, nor waiting for the spontaneous *cis-trans* back-isomerization to take place. This reversibility would be interesting in the field of cell-instructive materials. In

particular, the ability to induce a cyclical mechanical and topographical stimulation, for example, could allow new investigations on cell mechanotransduction.[26] Other reports regarding different photoresponsive systems observed an irreversible swelling upon photostimulation, even when reversible reaction are involved in the photoactuation process (e.g. keto-enol tautomerism).[27] In the reported example a very slow reverse reaction was the cause of the irreversibility in the polymer gel deformations. In our case, the problems in shape recovery of our gelatin hydrogel still need to be addressed. Most probably, the azobenzene increase in dipole moment upon isomerization plays a key role in this process.[24] In fact, once immobilized in a crosslinked polymer matrix, the photoisomerization phenomenon might lead to an increase in the system hydrophilicity causing a water uptake and, consequently, a swelling.[18] Moreover, photothermal effects could also affect the material behavior. In fact, a light to heat conversion might be also involved in the shape change mechanism.

5.2.3 Biological investigation

However, the obtained shape change, even if irreversible, was useful for our biological application, giving an in plane deformation of 10%. For our biological experiments we polymerized the photoresist in a bidimensional large area (~mm^2) array of squared blocks (30 x 30 x 10 μm^3) spaced about 10 μm in a wet environment. Each structure presented a grating (3 μm pitch) on the lateral walls, which allowed for a precise cell confinement in the channels between structures, as we can see in Figure 6.

From the literature, it is known that in presence of microchannels cells tend to position and align inside them in a process sometimes called “gap guidance”.[28] Most probably, as it happens in bidimensional (2D) structures such as linear

surface patterns the topographic cue on the block walls further helped in cell confinement between blocks.[29-30]

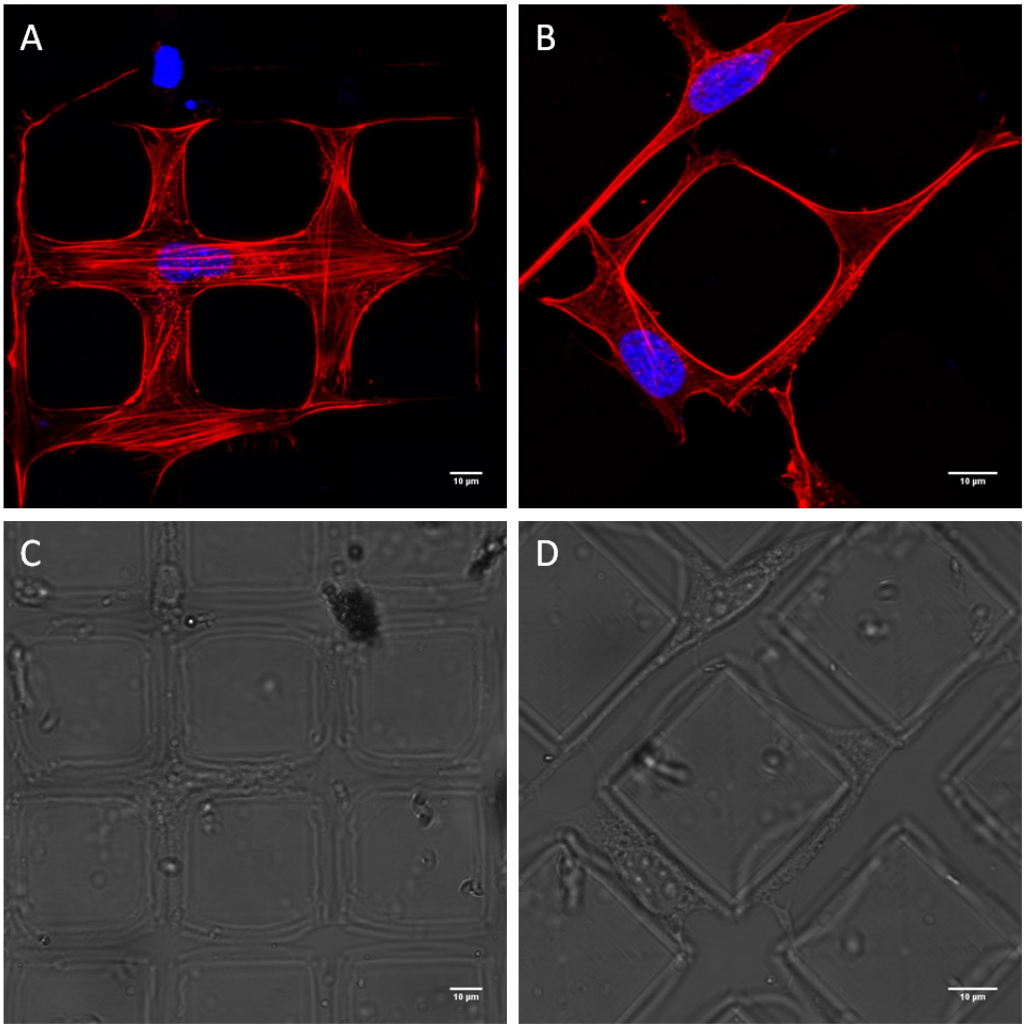

Figure 6. Fixed NIH-3T3 on gelatin structures. A) and B) are z-stacks maximum intensity projection of fixed cells cultured on gelatin structures (nuclei were stained in blue with HOECHST, while the cytoskeleton is colored in red with rhodamin phalloidin). C) and D) are brightfield images of the underneath structures. Scale bars are 10 µm.

Nowadays, the use of 2D structures for the study of the cell-extracellular matrix (ECM) interaction is progressively being substituted by novel 3D cell culturing structures, because they are able to mimic many structural aspects of the *in vivo* ECM.[31-32] In fact, these platforms are able to elicit different cell responses, e.g.

in terms of formation of focal adhesions and cell cytoskeleton structure. In this context, indeed, mechanotransduction (i.e. the ability of cells to translate external mechanical stimuli into a biochemical response) plays a key role.[33-34] In fact, as an example, many research works are evidencing that a change in shape of a cell nucleus (aided by cytoskeletal assembly) is able to alter gene expression through chromatin reassembly.[26] The interaction with the outer environment is able to start a cascade of switch-like events in and between cells, but this way of modeling the cellular responses is not complete enough to understand the time-dependent cell reaction to varying external stimuli, as it happens *in vivo*.[35] Our aim was the obtainment of a cell confining structure for further cell deformation studies in real-time.

Actually, the novelty of our approach lies in the fact that, by engineering the described photopolymerizable material, we were able to locally deliver a mechanical stimulation to the cell nucleus at a single-cell level. Our studies were carried out with NIH-3T3 cells, a model cell line for mechanotransduction studies. Numerous works centered their attention on the effect of a mechanical stimulation on the transcriptional activities of cells, studying the interaction of cytoskeletal tension, nucleous deformation and chromatin reassembly.[31] Our system was able to deform cell nuclei at single cell level, allowing for a high localization of the external light trigger to the material parts. In fact, using a MP laser inside the ROIs (Figure 7), we were able to avoid unwanted interactions between high power laser in the UV spectral region and living cells.

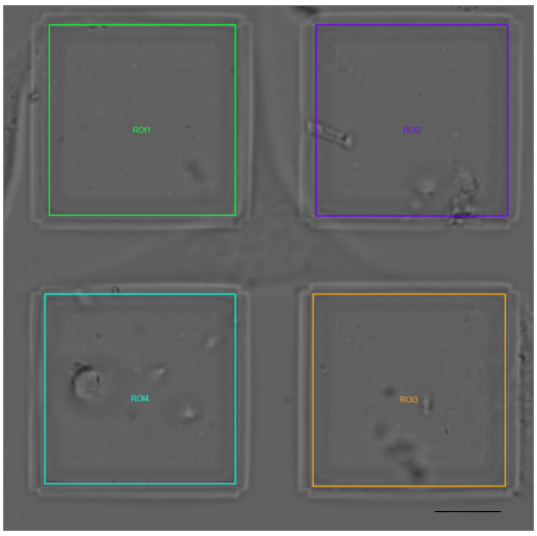

Figure 7 Screenshot from the Leica MP microscope software. The colored squares represent the ROIs corresponding to the gelatin structures to be stimulated. Scale bar is 10 µm.

The deformation took place in 10 minutes of illumination and it allowed for a range of nuclei deformation in x and y of 5-12% (Figure 8 and Table 1).

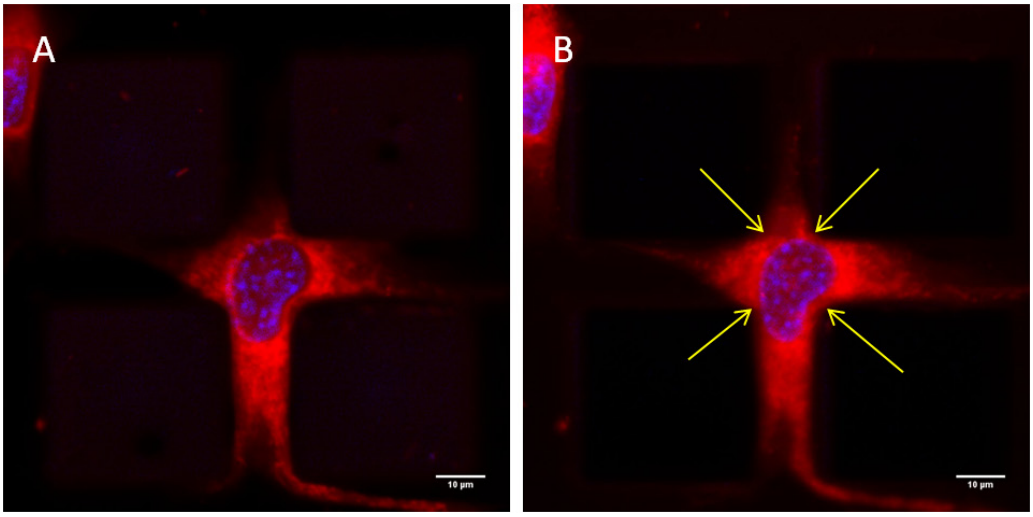

Figure 8. Cell deformation upon gelatin photostimulation. A) Before the light irradiation and B) after 10 minutes of MP stimulation. Yellow arrows indicate the expansion of the stimulated material toward the cell nucleus. The cell is stained with the vital CellTracker Deep Red for the cell body, while HOECHST is used for nucleus staining. Scale bar are 10 µm.

This in plane deformation of the cell nuclei was observed in each stimulated cell, as we can see form the reported data in Table 1.

	Area before stimulation (μm^2)	Area after stimulation (μm^2)	XY Nucleus deformation
1	120.93	106.77	11.7%
2	132.02	120.46	11.6%
3	118.64	110.72	6.7%
4	102.12	97.13	4.5%
5	158.72	145.28	8.4%
6	234.54	222.38	5.2%
7	199.64	160.51	4.6%
8	236.63	269.74	12.3%

Table 1. Evaluation of the in plane deformation of cell nuclei upon gelatin stimulation by comparing the nucleus xy area at a fixed z position before and after structures photostimulation.

The reported deformation range is due to the position of the cell inside the channels and on its adhesion to the structure walls. In particular, cells which were more confined and were situated very close to the structures corners were deformed more efficiently by the structures expansion.

5.3 Conclusions

In this Chapter the realization of a gelatin-based photoresist through a chemical modification of gelatin side chain functions into a photopolymerizable mixture has been shown. In particular, the introduction of an azobenzene-based crosslinker enabled the fabrication of hydrogel structures with high resolution, adding a further functionality to the material. In fact, stimulation with a multiphoton laser in the range of azobenzene isomerization provoked an in plane deformation of the designed structures, with a concomitant change in mechanical properties. These findings demonstrate the applicability of these platforms as versatile, 3D biocompatible cell culturing scaffolds (whose shape can be tailored by two-photon polymerization) while confining cells in 3D

environment. Even if a complete understanding of the light-responsive properties of the materials is still under study, the new gelatin property was exploited as a proof of concept for the deformation of cell nuclei. These preliminary results pave the way to further studies on the effect of these mechanical signals on cell behavior.

5.4 Experimental section

5.4.1 Acrylamide-modified gelatin B synthesis.

Gelatin type B (Bloom strength of 225 g, Sigma) isolated from bovine skin, acrylic acid *N*-hydroxysuccinimide ester (Aldrich) and 4-Methoxyphenol (MeHQ) (Sigma-Aldrich) were used as received. Starting from a protocol reported elsewhere, gelatin was chemically modified with acrylic side groups.[17] After dissolution of 1 g of gelatin in phosphate buffer (pH 7.8) at 40 °C, 0.76 mmol of acrylic acid *N*-hydroxysuccinimide (NHS)-ester (128.5 mg) and 46 ppm of MeHQ were added while vigorously stirring. Briefly, after 1 h, the reaction mixture was diluted and dialyzed for 48 h against distilled water at 40 °C. The reaction product was then freeze-dried leading to a white fluffy solid. The degree of substitution was verified using ^{1}H-NMR spectroscopy at 40 °C and quantified (Figure 1).[36]

5.4.2 Synthesis of azobenzene-based crosslinker (Azo-crosslinker).

Azobenzene 1 was synthesized by an already reported protocol.[37-38] Briefly, azobenzene 1 (30 mg, 0.111 mmol) was dissolved in dichloromethane (CH_2Cl_2) and 74 µl of triehtylamine (TEA) at room temperature. Then 2.4 equiv. of 1-Hydroxybenzotriazole hydrate (HOBt·H_2O), 2.4 equiv. of *N*-(3-dimethylaminopropyl)-*N*′-ethylcarbodiimide hydrochloride (EDC·HCl) and 2.4 equiv. of compound 2 were added and left reacting overnight. The reaction was followed by thin layer chromatography (TLC) and the product was extracted in

dichloromethane. The product was purified by column chromatography. The product formation was confirmed by Mass Spectrometry. MS (ESI): m/z calculated for $C_{36}H_{54}N_6O_{10}$: 731.39 $[M+H]^+$; found: 731.40. After that, compound 3 was treated for 2 hours with a solution of 50/50 v/v trifluoroacetic acid (TFA) in CH_2Cl_2 to remove the Boc protecting group, then co-evaporated with toluene and treated with TEA. Finally, Boc-deprotected compound 3 was reacted with 2.4 equiv. of acrylic acid (197 mmol, 14.2 mg), 2.4 equiv. of HOBt·H_2O, 2.4 equiv. of EDC·HCl and 4.8 equiv. of TEA. The reaction was followed by thin layer chromatography (TLC). The product was purified by column chromatography. The product formation was confirmed by Mass Spectrometry and characterized by UV/Vis spectrophotometry (Figure 2). MS (ESI): m/z calculated for $C_{32}H_{42}N_6O_8$: 639.39 $[M+H]^+$; found: 639.31.

5.4.3 Gelatin photoresist preparation and two-photon polymerization.

Acrylamide-modified gelatin B (20 % w/v) was dissolved in a citrate buffer (pH 3.1) at 40 °C for at least 2 h by gently stirring. When the solution became clear, 4 wt% of azo-crosslinker and 3 wt% of Irgacure 369 were added. The gelatin photoresist was heated above the gelation point at 40 °C and then poured on a round glass slide (30 mm diameter, 0.17 mm thickness) and a PDMS reservoir was placed on it. Then the sample was inserted into a two-photon polymerization system (Photonic Professional GT, Nanoscribe GmbH), which uses a 780 nm Ti-Sapphire laser emitting ≈100 fs pulses at 80 MHz with a maximum output power of 150 mW, equipped with a 63x, 1.4 NA oil immersion objective. The system combines a piezo stage and a high-speed galvo mode for faster structuring. For our purposes, a set of squared blocks (30 x 30 x 10 μm^3) with a lateral grating of 3 μm pitch was fabricated. The used parameters were 7500 μm/s as scan speed, 24 mW as output power. The development was carried out stirring the photoresist in bidistilled hot water (45

°C) for 20 minutes. In this process, the hot water was able to dissolve unreacted material, leaving the structures on the glass. Samples were then left in distilled water until they were used for cell culture.

5.4.5 Cell culture and imaging.

NIH−3T3 fibroblasts were cultured in low glucose DMEM and incubated at 37°C in a humidified atmosphere of 95% air and 5% CO_2. Prior to cell seeding, substrates were sterilized in a solution of Pennicillin-Streptomycin (Pen/Strep) in PBS (Phosphate Buffered Saline) (1:2 v:v) for at least 4 hours. On each sample 40000 cells were seeded and they were left adhering overnight in the incubator. The day after cells were stained with vital CellTracker Deep Red solution (1:1000 in cell culture medium without FBS) for 30 minutes in the incubator and then the nuclei were stained with HOECHST (100 µl of a solution 1:10000 v:v in the culture medium). After that, samples were imaged and stimulated at the A TCS SP5 multiphoton (MP) microscope (Leica Microsystems) (see next section). At the end of the experiment, cells were fixed with 4% paraformaldehyde for 20 min and permeabilized with 0.1% Triton X−100 in PBS for 3 min. Actin filaments were stained with rhodamin−phalloidin. First of all, samples were incubated for 30 min at room temperature in the phalloidin solution (dilution 1:200), and, finally, cells were incubated for 15 min at 37°C in HOECHST solution (dilution 1:1000) to stain cell nuclei. Cells were then imaged at the MP with a 40x water immersion objective 1.1 NA in z-stack mode.

5.4.7 Photostimulation.

The structures (either alone or with seeded cells) were photostimulated using the MP microscope. A 25x water immersion objective was used for the purpose using 6x as zoom factor. The MP pulsed laser was tuned at 700 nm and output power was set at 5% (trans and gain, 13 mW output power), and 42% offset.

Four regions-of-interest (ROIs) were drawn on the squared gelatin structures (Figure 7) in which a MP laser was switched on for 10 minutes at 400 Hz scan speed in bidirectional mode, taking 1 frame per second. The negative controls were performed following the same abovementioned procedure while using both a continuous He-Cd laser of 633 nm at maximum power and a 780 nm MP laser tuned at 13 mW output power.

5.5 References

§ Author contributions. Miss Chiara Fedele strongly contributed in the development of the project idea. She performed the synthetic work and devised the photoresist mixture. The candidate had the chance to participate to the two-photon polymerization processing, in order to learn how to successfully bypass the practical issues during experiments. Moreover, she performed all the biological experiments. Finally, she contributed to the photostimulation experiments.

1. Murphy, W. L.; McDevitt, T. C.; Engler, A. J., Materials as stem cell regulators. *Nature materials* **2014,** *13* (6), 547-557.
2. Lutolf, M. P.; Gilbert, P. M.; Blau, H. M., Designing materials to direct stem-cell fate. *Nature* **2009,** *462* (7272), 433-441.
3. Yamaki, K.; Harada, I.; Goto, M.; Cho, C.-S.; Akaike, T., Regulation of cellular morphology using temperature-responsive hydrogel for integrin-mediated mechanical force stimulation. *Biomaterials* **2009,** *30* (7), 1421-1427.
4. Li, Y.; Huang, G.; Zhang, X.; Li, B.; Chen, Y.; Lu, T.; Lu, T. J.; Xu, F., Magnetic hydrogels and their potential biomedical applications. *Advanced Functional Materials* **2013,** *23* (6), 660-672.
5. Lim, H. L.; Chuang, J. C.; Tran, T.; Aung, A.; Arya, G.; Varghese, S., Dynamic electromechanical hydrogel matrices for stem cell culture. *Advanced functional materials* **2011,** *21* (1), 55-63.
6. Straley, K. S.; Heilshorn, S. C., Dynamic, 3D-Pattern Formation Within Enzyme-Responsive Hydrogels. *Advanced Materials* **2009,** *21* (41), 4148-4152.
7. Tomatsu, I.; Peng, K.; Kros, A., Photoresponsive hydrogels for biomedical applications. *Advanced drug delivery reviews* **2011,** *63* (14), 1257-1266.
8. Ryu, J.; D'Amato, M.; Cui, X.; Long, K. N.; Jerry Qi, H.; Dunn, M. L., Photo-origami—Bending and folding polymers with light. *Applied Physics Letters* **2012,** *100* (16), 161908.
9. Liu, Y.; Boyles, J. K.; Genzer, J.; Dickey, M. D., Self-folding of polymer sheets using local light absorption. *Soft Matter* **2012,** *8* (6), 1764-1769.
10. Peng, K.; Tomatsu, I.; Kros, A., Light controlled protein release from a supramolecular hydrogel. *Chemical communications* **2010,** *46* (23), 4094-4096.
11. Techawanitchai, P.; Ebara, M.; Idota, N.; Asoh, T.-A.; Kikuchi, A.; Aoyagi, T., Photo-switchable control of pH-responsive actuators via pH jump reaction. *Soft Matter* **2012,** *8* (10), 2844-2851.

12. Zeng, H.; Wasylczyk, P.; Parmeggiani, C.; Martella, D.; Burresi, M.; Wiersma, D. S., Light-Fueled Microscopic Walkers. *Advanced Materials* **2015,** *27* (26), 3883-3887.
13. Palagi, S.; Mark, A. G.; Reigh, S. Y.; Melde, K.; Qiu, T.; Zeng, H.; Parmeggiani, C.; Martella, D.; Sanchez-Castillo, A.; Kapernaum, N., Structured light enables biomimetic swimming and versatile locomotion of photoresponsive soft microrobots. *Nature materials* **2016,** *15* (6), 647.
14. Cen, L.; Liu, W.; Cui, L.; Zhang, W.; Cao, Y., Collagen tissue engineering: development of novel biomaterials and applications. *Pediatric research* **2008,** *63* (5), 492-496.
15. Nguyen, L.; Straub, M.; Gu, M., Acrylate-Based Photopolymer for Two-Photon Microfabrication and Photonic Applications. *Advanced Functional Materials* **2005,** *15* (2), 209-216.
16. Sekkat, Z.; Kawata, S., Laser nanofabrication in photoresists and azopolymers. *Laser & Photonics Reviews* **2014,** *8* (1), 1-26.
17. Billiet, T.; Gasse, B. V.; Gevaert, E.; Cornelissen, M.; Martins, J. C.; Dubruel, P., Quantitative Contrasts in the Photopolymerization of Acrylamide and Methacrylamide-Functionalized Gelatin Hydrogel Building Blocks. *Macromolecular bioscience* **2013,** *13* (11), 1531-1545.
18. Rosales, A. M.; Mabry, K. M.; Nehls, E. M.; Anseth, K. S., Photoresponsive elastic properties of azobenzene-containing poly (ethylene-glycol)-based hydrogels. *Biomacromolecules* **2015,** *16* (3), 798-806.
19. Feringa, B. L.; Browne, W. R., *Molecular switches*. Wiley Online Library: 2001; Vol. 42.
20. Russew, M. M.; Hecht, S., Photoswitches: from molecules to materials. *Advanced Materials* **2010,** *22* (31), 3348-3360.
21. Withers, J. R.; Aston, D. E., Nanomechanical measurements with AFM in the elastic limit. *Advances in colloid and interface science* **2006,** *120* (1), 57-67.
22. Cushing, M. C.; Anseth, K. S., Hydrogel cell cultures. *Science* **2007,** *316* (5828), 1133-1134.
23. Klajn, R., Immobilized azobenzenes for the construction of photoresponsive materials. *Pure and Applied Chemistry* **2010,** *82* (12), 2247-2279.
24. Beharry, A. A.; Woolley, G. A., Azobenzene photoswitches for biomolecules. *Chemical Society Reviews* **2011,** *40* (8), 4422-4437.
25. Hosono, N.; Furukawa, H.; Masubuchi, Y.; Watanabe, T.; Horie, K., Photochemical control of network structure in gels and photo-induced changes in their viscoelastic properties. *Colloids and Surfaces B: Biointerfaces* **2007,** *56* (1), 285-289.

26. Tajik, A.; Zhang, Y.; Wei, F.; Sun, J.; Jia, Q.; Zhou, W.; Singh, R.; Khanna, N.; Belmont, A. S.; Wang, N., Transcription upregulation via force-induced direct stretching of chromatin. *Nature materials* **2016,** *15*, 1287-1296.
27. Watanabe, T.; Akiyama, M.; Totani, K.; Kuebler, S. M.; Stellacci, F.; Wenseleers, W.; Braun, K.; Marder, S. R.; Perry, J. W., Photoresponsive hydrogel microstructure fabricated by two-photon initiated polymerization. *Advanced Functional Materials* **2002,** *12* (9), 611-614.
28. Hamilton, D.; Brunette, D., "Gap guidance" of fibroblasts and epithelial cells by discontinuous edged surfaces. *Experimental cell research* **2005,** *309* (2), 429-437.
29. Annabi, N.; Tsang, K.; Mithieux, S. M.; Nikkhah, M.; Ameri, A.; Khademhosseini, A.; Weiss, A. S., Highly elastic micropatterned hydrogel for engineering functional cardiac tissue. *Advanced functional materials* **2013,** *23* (39), 4950-4959.
30. Bettinger, C. J.; Langer, R.; Borenstein, J. T., Engineering substrate topography at the micro-and nanoscale to control cell function. *Angew. Chem., Int. Ed.* **2009,** *48* (30), 5406-5415.
31. Koch, B.; Sanchez, S.; Schmidt, C. K.; Swiersy, A.; Jackson, S. P.; Schmidt, O. G., Confinement and Deformation of Single Cells and Their Nuclei Inside Size-Adapted Microtubes. *Advanced healthcare materials* **2014,** *3* (11), 1753-1758.
32. Vogel, V.; Sheetz, M., Local force and geometry sensing regulate cell functions. *Nature reviews Molecular cell biology* **2006,** *7* (4), 265-275.
33. Ingber, D. E., Cellular mechanotransduction: putting all the pieces together again. *The FASEB journal* **2006,** *20* (7), 811-827.
34. McNamara, L. E.; Burchmore, R.; Riehle, M. O.; Herzyk, P.; Biggs, M. J.; Wilkinson, C. D.; Curtis, A. S.; Dalby, M. J., The role of microtopography in cellular mechanotransduction. *Biomaterials* **2012,** *33* (10), 2835-2847.
35. Hoffman, B. D.; Grashoff, C.; Schwartz, M. A., Dynamic molecular processes mediate cellular mechanotransduction. *Nature* **2011,** *475* (7356), 316-323.
36. Habeeb, A. S. A., Determination of free amino groups in proteins by trinitrobenzenesulfonic acid. *Analytical biochemistry* **1966,** *14* (3), 328-336.
37. Vaselli, E.; Fedele, C.; Cavalli, S.; Netti, P. A., "On–Off" RGD Signaling Using Azobenzene Photoswitch-Modified Surfaces. *ChemPlusChem* **2015,** *80* (10), 1547-1555.
38. Liu, D.; Xie, Y.; Shao, H.; Jiang, X., Using Azobenzene-Embedded Self-Assembled Monolayers To Photochemically Control Cell Adhesion Reversibly. *Angewandte Chemie International Edition* **2009,** *48* (24), 4406-4408.

Conclusions and future perspectives

The work described in this thesis intends to exploit the fascinating photomechanical properties of azobenzene-based materials for the realization of functional photoresponsive cell culture applications.

Up to date, a big variety of photolithographic techniques has been successfully adopted for azopolymer photopatterning and even the possibility of a dynamic modulation of the topographical features of a cell culture substrate appeared to be feasible using these materials. In fact, a great biological interest resides in the dynamic modulation of the cell-material crosstalk, in order to recapitulate *in vitro* the changing interaction between cells and the natural extracellular microenvironment, in terms of biochemical, topographical and mechanical cues. For this purpose, the use of light-responsive materials seems to be powerful, because of the possibility of activating on demand specific material functions. In this thesis work, light-induced topographical and structural modifications of different azobenzene-based materials have been used in many biological applications, either at a single-cell level, or in multicellular systems. In particular, light-based techniques already used for single-cell investigations have been implemented to study more complex biological processes, which involve the cell-cell interactions in their final biological response. At the same time, the realization of novel photoresponsive platforms for dynamic cell culture has been introduced.

In more details, in **Chapter 1** an introduction to the topic is given.

In **Chapter 2**, it is shown how surface relief grating (SRG) inscribed on synthesized azopolymer brushes and mechanically erased by ultrasonication can be exploited as reversible surfaces for contact guidance studies. These substrates were found biocompatible for human umbilical vein endothelial cells (HUVECs), which were also able to feel the underneath topography and align

preferentially in the pattern direction. From these results we envision the possibility to use such polymer brushes as biointerfaces for “on-off” switching topographies.

In **Chapter 3**, the temporal presentation of topographical cues during sprouting angiogenesis is investigated through the real-time photopatterning of Disperse Red 1-containing polymer (pDR1m) using the focused laser of a confocal microscope with a fine spatio-temporal control. After assessing that patterned 2D surfaces with linear grating are able to affect the behavior of cells in sprouting angiogenesis employing a HUVEC spheroid model, this photopatterning method was successfully implemented to elicit a remodeling of sprouting direction in real-time. Further studies will explore the effect of other topographies in order to achieve a full spatio-temporal control of sprouting dynamics.

In **Chapter 4**, photoinscribed topographies on an azobenzene molecular glass (DR1-glass) are implemented as cues for investigations on the contact guidance of Madin-Darby canine kidney (MDCK) epithelial cells. In particular, 1 μm pitch sinusoidal surface modulation most influenced MDCK cells, directing their migration through the activation of the ROCK signaling pathway. For these reasons, an *in vitro* wound healing essay revealed that topographical guidance, which bridged the wound boundaries, was able to speed up the healing process. Finally, preliminary studies on the real-time photopatterning effect on MDCK monolayer were conducted, revealing a topography-dependent activation of Ca^{2+} signaling paving the way to further investigations on the links between epithelial cell mechanobiology and electrophysiology.

Finally, in **Chapter 5** the design of a modified gelatin photoresist containing an azobenzene-based crosslinker enabled the fabrication of hydrogel structures with high resolution, adding a further functionality to the material. In fact, stimulation with a multiphoton laser in the range of azobenzene isomerization

provoked an in plane deformation of the designed structures, with a concomitant change in mechanical properties. Furthermore, preliminary results on the structure stimulation with NIH-3T3 murine fibroblasts pave the way to further studies on the effect of these mechanical signals on cell behavior.

Taken together, these findings add a valuable contribution to the broad field of light-responsive cell-instructive materials and, more specifically, to the actual application of azobenzene-based materials to dynamic cell cultures. Many times in this thesis, we have highlighted the broad potentialities of azobenzene-based materials in providing the ideal tool for the precise spatio-temporal delivery of topographical and mechanical signals to cells. As a matter of fact, owing to the great efficiency in localization of the external trigger and to the tunable photomechanical responses that can be elicited in these materials, also in a reversible manner, they offer the possibility to design a customized dynamic environment for each specific biological application. The reported studies may indeed inspire further applications of these light-responsive materials in order to give new insights into the dynamic cell-material interaction. In fact, many biological issues are still unresolved regarding, for example, how the temporal presentation of cell-instructive cues influences cells in a specific biological process, or in which temporal window the change in physical properties of the material can influence cell fate.